PERFORMANCE OF HIGH RATE SPACE-TIME TRELLIS CODED MODULATION IN FADING CHANNELS

by
Sokoya Oludare Ayodeji
University of KwaZulu-Natal
2005

Submitted in fulfillment of the academic requirement for the degree of MScEng in the School of Electrical, Electronic and Computer Engineering, University of KwaZulu-Natal, 2005

ABSTRACT

Future wireless communication systems promise to offer a variety of multimedia services which require reliable transmission at high data rates over wireless links. Multiple input multiple output (MIMO) systems have received a great deal of attention because they provide very high data rates for such links. Theoretical studies have shown that the quality provided by MIMO systems can be increased by using space-time codes.

Space-time codes combine both space (antenna) and time diversity in the transmitter to increase the efficiency of MIMO system. The three primary approaches, layered space-time architecture, space-time trellis coding (STTC) and space-time block coding (STBC) represent a way to investigate transmitter-based signal processing for diversity exploitation and interference suppression. The advantages of STBC (i.e. low decoding complexity) and STTC (i.e. TCM encoder structure) can be used to design a high rate space-time trellis coded modulation (HR-STTCM).

Most space-time codes designs are based on the assumption of perfect channel state information at the receiver so as to make coherent decoding possible. However, accurate channel estimation requires a long training sequence that lowers spectral efficiency. Part of this dissertation focuses on the performance of HR-STTCM under non-coherent detection where there is imperfect channel state information and also in environment where the channel experiences rapid fading.

Prior work on space-time codes with particular reference to STBC systems in multiuser environment has not adequately addressed the performance of the decoupled user signal-to-noise ratio. Part of this thesis enumerates from a signal-to-noise ratio point of view the

performance of the STBC systems in multiuser environment and also the performance of the HR-STTCM in such environment.

The bit/frame error performance of space-time codes in fading channels can be evaluated using different approaches. The Chernoff upper-bound combined with the pair state generalized transfer function bound approach or the modified state transition diagram transfer function bound approach has been widely used in literature. However, although readily determined, this bound can be too loose over normal signal-to-noise ranges of interest. Other approaches, based on the exact calculation of the pairwise error probabilities, are often too cumbersome. A simple exact numerical technique, for calculating, within any desired degree of accuracy, of the pairwise error probability of the HR-STTCM scheme over Rayleigh fading channel is proposed in this dissertation.

To the Alpha and Omega

Preface

The research work presented in this dissertation was performed by Mr Oludare Ayodeji Sokoya, under the supervision of Professor Fambirai Takawira and Dr Hongjun Xu, at the University of KwaZulu-Natal's school of Electrical, Electronic and Computer Engineering, in the Centre of Radio Access and Rural Technologies. This work was partially sponsored by Alcatel Telecoms and Telkom South Africa Ltd.

Parts of this dissertation have been presented at the Southern African Telecommunication Networks & Application Conference (i.e. SATNAC) 2004 held at the Spier Wine Estate, South Africa and at the SATNAC 2005 held in Central Drakensberg, KZN South Africa.

The entire dissertation, unless specifically indicated, is the author's own original work and has not been submitted in part, or in whole, to any other University for degree purposes.

Acknowledgments

My thanks goes to both of my supervisors, Dr Hongjun Xu and Professor Fambirai Takawira for their inspiration with the topic of this dissertation, careful guidance, constant support and the many encouragements during the past two years.

My parents, Bldr. and Dr (Mrs.) E.O. Sokoya, and brothers especially Dr Gbolahan Sokoya MD, are owed many thanks for their support and their keen interest in my well-being. They have always prayerfully supported me in whatever challenge I have taken up in my life and my MSc was no exception. I would also like to thank my fiancé, Topemi, for all her support and encouragement throughout this dissertation.

Thanks are also owed to Telkom SA Ltd and Alcatel Telecom for their much appreciated and enjoyed financial support and for providing the equipment necessary for completion of my MSc.

Last but definitely not the least I would like to thank all my friends at His People Durban Church and all my postgraduate colleagues for their assistance and for making our time together enjoyable.

I give thanks unto the LORD; for He is good: for His mercy endures for ever.

TABLE OF CONTENT

LIST OF FIGURES

LIST OF TABLES

LIST OF ACRONYMS

1-D	One Dimension
1G	First Generation
2G	Second Generation
3G	Third Generation
AWGN	Additive White Gaussian Noise
BEP	Bit Error Probability
BER	Bit Error Rate
BPSK	Binary Phase Shift Keying
CDMA	Code Division Multiple Access
COD	Complex Orthogonal Design
Db	Decibel
DLST	Diagonally Layered Space-time
FER	Frame Error Rate
HLST	Horizontally Layered Space-time
HR-STTCM	High Rate-Space-time Trellis Coded Modulation
IEEE	Institute of Electrical and Electronic Engineers
KZN	KwaZulu-Natal
LST	Layered Space-time
MANET	Mobile Adhoc Network
Mbps	Mega Bits per Seconds
MIMO	Multiple Input Multiple Output
ML	Maximum Likelihood
MTCM	Multiple Trellis Coded Modulation
PAM	Pulse Amplitude Modulation
PEP	Pairwise Error Probability
PSK	Phase Shift Keying
QAM	Quadrature Amplitude Modulation
QPSK	Quadrature Phase-Shift Keying
Rx	Receiver
SISO	Single Input Single Output

SNR	Signal-to-Noise Ratio
SOSTTC	Super Orthogonal Space-time Trellis Code
STBC	Space-time Block Code
STTC	Space-time Trellis Code
TCM	Trellis Coded Modulation
Tx	Transmitter
UWB	Ultra-Wide-Band
Wi-Fi	Wireless Fidelity Forum
WiMAX	Wireless Interoperability for Microwave Access Forum

LIST OF SYMBOLS

This lists the more common symbols which are used throughout the dissertation.

C	Channel capacity (bits/sec)
h_{ij}	Channel gain from the i^{th} transmit antenna to the j^{th} receive antenna
H	Channel matrix
$\mathrm{H}_m^{(k)}$	Channel matrix from the kth user to the mth receive antenna
R	Transmission Rate (bps/Hz)
R_c	Code Rate
x_t	Valid correct transmitted codeword at time t
$\tilde{x}_t$	Valid incorrect decoded codeword at time t
$\mathrm{x}^{(k)}$	Transmitted Data sequence of the kth user
N	Input frame length in symbols
N_t	Number of transmit antenna
N_r	Number of receive antenna
$P_b(E)$	Average bit error probability
N_c	Encoded data time slots
η^j	AWGN at receiver j
$\frac{N_0}{2}$	Two sided noise power spectral density
E_s	Symbol energy of signal transmitted from antenna i
σ^2	Variance per dimension of h_{ij}
$\mathrm{P}(\mathrm{A} \rightarrow \tilde{\mathrm{A}})$	PEP of transmitting A and incorrectly decoding $\tilde{\mathrm{A}}$
K	Number of users
M	Constellation size (M -PSK)
erfc	Complementary error function
θ	Angular rotation
v_c	Encoder memory
λ_i	Non-zero eigenvalues
u	Redundant bits

CHAPTER 1

CHALLENGES IN WIRELESS COMMUNICATION

1.1 Introduction

Owing to the need to transfer information (voice and data) in a fast, reliable and affordable way, the wireless communication world has been experiencing exponential growth to keep up with today's demand. This is evident in the historical progression growth from the First generation technology (1G) to Second (2G) then to Third generation (3G) and now the much talked about Fourth generation wireless technology. The emerging trend in the wireless communication includes (but not limited to): Wi-Fi, WiMAX, Mobile Adhoc Networks (MANETs), OFDM, UWB, CDMA and many more. The challenges faced in designing robust networks that deliver the performance necessary to support the emerging trend in wireless communication includes

- Traffic patterns, user location, and network conditions are constantly changing.
- Applications are heterogeneous with hard constraints that must be met by the network.
- Energy and delay constraints changes design principles across all layers of the protocol stack.
- Wireless channels are a difficult and capacity limited broadcast communication medium.

As mentioned above, the wireless communication channel is an unpredictable and difficult communication medium as opposed to the wired one. As signals propagate through a wireless channel, they experience random fluctuation and arrive at the destination along a number of different paths, collectively referred to as multipath. These paths arise from scattering, reflection and diffraction of signals propagated by the objects in the environment or refraction in the medium. The fluctuations of signal propagated through the wireless channel result in a signal power drop in the transmitted signal.

The signal power drops due to three main effects:

- *Mean propagation (path) loss*: this comes from inverse power loss, absorption by water, foliage and the effect of ground reflection.
- *Macroscopic fading*: results from a blocking effect by buildings and natural features and is also known as long term fading or shadowing.
- *Microscopic fading*: results from the consecutive and destructive combination of multipaths and is also known as short term fading or fast fading.

Multipath propagation results in the spreading of signal in different dimensions. This spreading includes:

- Delay spread: this is defined as the largest delay amongst various paths. This spread causes frequency-selective fading as the channel acts like a tapped delay line filter. A channel is said to be frequency-selective when the coherence bandwidth is comparable to or less than the signal bandwidth otherwise the channel is said to be non-selective i.e. flat.
- Doppler (or frequency) spread: This spread is caused by time-varying fading that occurs as a result of the relative motion between the transmitter and receiver. This spread is a function of the time-selectivity of the channel. Time selective fading can be characterized by the coherence time of the channel. The coherence time serves as a measure of how fast the channel changes in time– the larger the coherence time, the slower the channel fluctuation.
- Angle spread – This refers to the spread in angle of arrival of the multipath components at the receive antenna array. Angle spread causes space selective fading which means that signal amplitude depends on the spatial location of the antenna. Space selective fading is characterized by the coherence distance

which is inversely proportional to the angle spread – the larger the angle spread, the shorter the coherence distance.

1.2 Diversity

The various challenges of signals in wireless communication channel cause severe attenuation and make it impossible for the receiver to determine the transmitted signals. This phenomenon is called fading. One way to overcome this is to make several replicas of the signal available to the receiver with the hope that at least some of them are not severely attenuated. This technique is called *diversity*. Examples of diversity techniques are:

- Time diversity– the same information is repetitively transmitted at time spacing that exceeds the coherence time of the channel.
- Frequency diversity– the same information is transmitted or received simultaneously on two or more independently fading carrier frequencies.
- Antenna Diversity– is the use of multiple antennas to achieve a level of performance that a single antenna cannot achieve.
    - Spatial Diversity: is the use of multiple antennas to eliminate signal fade from a multipath environment. When multiple antennas are placed at the receive end of a communication system it is called receive diversity while when placed at the transmit end it is called transmit diversity.

      –Receiver Diversity: This is a fairly matured technique and provides better link budget and tolerance to co-channel interference.

      –Transmit Diversity: This is a maturing technique and no added power consumption, complexity or cost to mobiles is needed. The cost of extra transmit antennas is shared amongst all users.
    - Pattern Diversity: This is the use of two or more antennas with minimal overlapping patterns to provide greater overall pattern coverage.
    - Polarization Diversity: This is the use of multiple linearly polarized antennas that are mounted orthogonally to each other.

1.3 Capacity of Multi-Antenna Wireless System in Fading Channel

In this section the basic model of a multi-antenna wireless system and the channel capacity advantage possible in such an environment is presented.

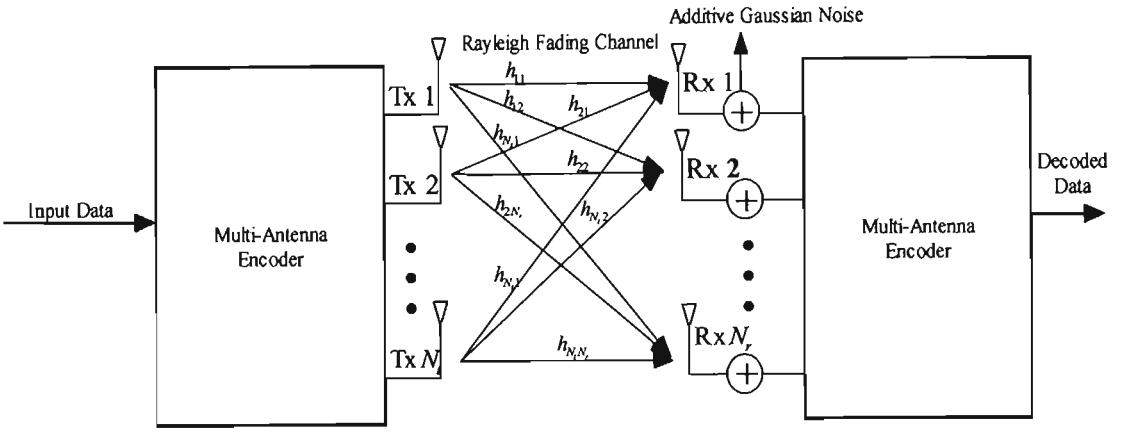

Figure 1.1: Multi-Antenna System

Figure 1.1 shows the block diagram of a multi-antenna wireless system with N_t transmit antennas and N_r receive antennas. The channel for the multi-antenna wireless system can be represented by

$$\mathbf{H} = \begin{bmatrix} h_{11} & \cdots & h_{N_T 1} \\ \vdots & \ddots & \vdots \\ h_{1N_R} & \cdots & h_{N_T N_R} \end{bmatrix} \tag{1.1}$$

where h_{ij} is the complex channel gain between transmitter i and receiver j. The channel gains are assumed to be independent and identically distributed (i.i.d.) zero mean complex Gaussian random variables with unit variance.

Channel capacity can be defined as a measure of the amount of information transmitted and received with a negligible probability of error. Wireless systems require reliable wireless channels with large capacities. Systems which communicate over a Single Input Single Output (SISO) wireless channel have limited capacities in a fading channel when compared to transmission over Multiple input Multiple Output (MIMO) wireless channels. Telatar [1] and Foschini et al [2] have shown that very

high capacities can be obtained by employing multiple antenna elements at both the transmitter and the receiver of a wireless system.

The ergodic (mean) capacity of a SISO system $(N_t = N_r = 1)$ with a random complex channel h is given by [2];

$$C = E\left\{\log_2\left(1 + \mathrm{SNR} \bullet |h|^2\right)\right\} \text{ bits/sec}, \tag{1.2}$$

where SNR is the average signal-to-noise ratio at the receiver branch. If $|h|$ is Rayleigh, $|h|^2$ follows a chi-squared distribution with two degrees of freedom.

For a MIMO channel, the ergodic (mean) capacity can be expressed as (1.3), [1] [2] when the transmitter has no knowledge of the channel but the receiver has perfect channel knowledge and the noise samples are assumed to be uncorrelated

$$C = E\left\{\log_2 \det\left[\mathrm{I}_{N_r} + \left(\frac{\mathrm{SNR}}{N_t}\right) \cdot \mathbf{H}\mathbf{H}^H\right]\right\} \text{ bits/sec}, \tag{1.3}$$

where $\mathbf{H}$ is the MIMO channel matrix of $N_r \times N_t$ dimension given in (1.1) . $(\bullet)^H$ denotes the transpose conjugate of the matrix element, I_{N_r} is the identity matrix of order N_r.

From the law of large numbers, the term $\frac{1}{N_t} \bullet \mathbf{H}\mathbf{H}^H$ tends to $\mathbf{I}_{N_r}$ as N_t gets large and N_r is fixed. Thus;

$$C = E\left\{N_r\left(\log_2\left[1 + \mathrm{SNR}\right]\right)\right\} \text{ bits/sec}. \tag{1.4}$$

It was shown in [30] that the total capacity of MIMO channel is made up by the sum of parallel AWGN SISO sub-channels and that the number of parallel sub-channels is determined by the rank of the channel matrix which is given by $\min(N_t, N_r)$. Further analysis of (1.3) shows that it is possible to decompose $\mathbf{H}\mathbf{H}^H$ as a function of the eigenvalues of the diagonal equivalent matrix of $\mathbf{H}\mathbf{H}^H$ so that (1.3) becomes (1.5), i.e.

$$C = E\left\{\sum_{i=1}^{m}\log_2\left(1+\frac{\mathrm{SNR}}{N_t}\lambda_i\right)\right\} \text{ bits/sec}, \tag{1.5}$$

where m is the number of the non-zero eigenvalues of $\mathbf{H}$.

When the channel is known at the transmitter, the maximum capacity of a MIMO channel can be achieved by using the water filling principle [40] and (1.5) becomes

$$C = E\left\{\sum_{i=1}^{m}\log_2\left(1+\beta_i\frac{\mathrm{SNR}}{N_t}\lambda_i\right)\right\} \text{ bits/sec}, \tag{1.6}$$

where β_i is a scalar, representing the portion of the available transmit power going into the ith sub-channel.

In water-filling, more power is allocated to "better" sub-channels with higher SNR so as to maximize the sum of data rate in all sub-channels.

Figure 1.2 shows the channel capacity plot for a Rayleigh fading SISO channel as calculated by (1.2) and that of a Rayleigh fading MIMO channel (1.3) for various transmit and receive antenna. In general 10,000 channel realizations are used in the capacity plot shown in this section. Note that as the number of antennas is increased that capacity increases significantly.

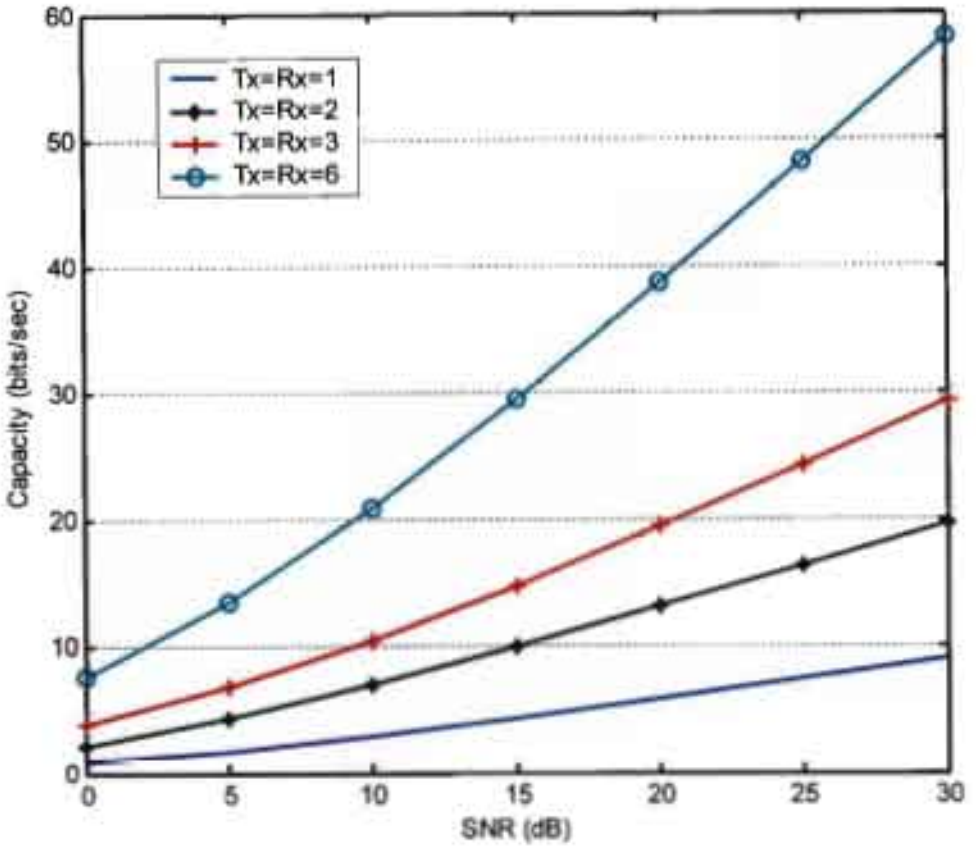

Figure 1.2: Channel Capacity of a SISO channel compared with the ergodic capacity of a Rayleigh fading MIMO channel with diferent number transmit and receive antenna

1.4 Research Motivation

Future wireless local area network (WLAN) services are target specific to 100Mbps at a range of 100m and thus will require a drastic increase in bandwidth efficiency in order to meet with this demand. Current WLAN systems achieve a throughput of up to 54Mbps (IEEE 802.11g) due to channel attenuation, dispersion and sharing of resources between users within a cell.

Multiple antenna transmission boosts significantly the capacities of a wireless network without need to increase bandwidth or transmit power. In fact, multiple antenna systems hold the key to the high-capacity wireless universe because they allow the increase of the rate, improvement of the robustness, and accommodation of more users in a cell. A multiple antenna system can be used to upgrade a link at the

transmitter side, receiver side or both sides. The latter is referred to as Multiple-Input Multiple Output (MIMO).

MIMO systems have received a great deal of attention as a method of increasing the capacity and quality of wireless transmission. Increased capacity can be obtained by using spatial multiplexing at the transmit side while increased quality can be obtained in the wireless transmission by using space-time codes.

By merging the advantages of both space-time trellis coding and space-time block coding, one can construct a high rate space-time trellis coded modulation that provides further performance improvement in a wireless network.

The performance of high rate space-time trellis coded modulation has not been well covered and its performance has only been addressed in a quasi-static fading channel. This research focuses on the performance of high rate space-time trellis coded modulation in both coherent and non-coherent environments. The multiuser behaviours of this code are enumerated. A novel simple numerical technique for analyzing the performance of this code under coherent detection is proposed.

1.5 Thesis Overview

This dissertation is divided into six chapters. Chapter 1 enumerates some of the challenges faced in a wireless communication network. The causes of multipath propagation are discussed and various ways in which the transmitted signals spreads in the multipath environment. Diversity techniques as a means of reducing the effect of multipath propagation, i.e. fading, are also discussed and lastly the capacity advantage that is possible in a multiple antenna system is explained.

Chapter 2 is a literature survey on various types of space-time coding schemes employed in MIMO system. The design and performance criteria of such codes are also enumerated in this chapter. A brief introduction into concatenating channel codes with space-time code, as a way of further improving the performance of space-time codes is also mentioned with particular reference to trellis coded modulation.

Chapter 3 focuses on the performance of high rate space-time coded modulation in a coherent and non-coherent environment. The quasi-static and rapid fading

performance of this code is enumerated in this chapter using coherent detection. A novel idea of applying unitary space-time codes to high rate space-time trellis coded modulation as a means of estimating the channel is also discussed. The results of the performance of this code and other known space-time codes under various fading environments are also discussed in this chapter.

Chapter 4 discusses the multiuser behaviour of both space-time block codes and high rate space-time trellis coded modulation. The Zero-forcing interference cancellation technique is used as a means of decoupling the signal at the receiver end of the system and the signal-to-noise ratio of the desired decoupled signal is derived in this chapter. Various deductions can be drawn from the SNR calculation and also the signal matrix structure for the decoupled signals.

In Chapter 5 a novel mathematical analysis for calculating the performance of high rate space-time trellis coded modulation in quasi-static and rapid Rayleigh fading channels is proposed. This simple numerical technique is useful in observing the asymptotic behaviour of high rate space-time trellis coded modulation at high SNR. The analytical results of this code are compared with the simulated results and various conclusions made depending on the error length and the type of fading channel.

Lastly, chapter 6 presents the conclusions drawn in this dissertation.

1.6 Original Contribution in This Dissertation

The original contributions of this dissertation include:

1. The behaviour of the code presented in [4] under fast Rayleigh fading channel was shown.
2. Performance of the high rate space-time trellis coded modulation using unitary space-time code in estimating the channel for a quasi-static Rayleigh fading was investigated.
3. Analyzing the performance of the high rate space-time trellis coded modulation and standalone space-time block code in a multiuser environment from the signal-to-noise ratio perspective.
4. A simple numerical mathematical analysis for the high rate space-time trellis coded modulation in quasi-static and fast fading channel.

Parts of the work presented in this dissertation have been presented or submitted by the author to this conference:

- Sokoya O.A, Hongjun Xu and Fambirai Takawira, "High Rate Space-time Trellis Coded Modulation with Imperfect Channel estimation," *Proceedings of the South African Telecommunications Networks and Applications Conference (SATNAC 2004),* Spier Wine Estate, Western Cape, South Africa, Sept. 2004

- Sokoya O.A, Hongjun Xu and Fambirai Takawira, "Performance of High rate space-time trellis coded modulation using Gauss Chebyshev Quadrature technique," *Proceedings of the South African Telecommunications Networks and Applications Conference (SATNAC 2005),* Central Drakensberg KZN South Africa Sept. 2005.

- Sokoya O.A, Hongjun Xu and Fambirai Takawira, "Performance Evaluation of High rate space-time trellis coded modulation using Gauss Chebyshev Quadrature technique," *Proceedings of IEE Communication (under review)*

CHAPTER 2

SPACE-TIME CODES

2.1 Introduction

In this chapter, a general introduction to space-time coding is given and the basic space-time coding techniques that are employed in the literature. Also later in this chapter, we expatiate more on the design criteria for most space-time codes and performance of such codes. A brief introduction into concatenation of channel codes and space-time codes as a means of further improving the code performance is also mentioned.

2.2 Space-time Coding

The use of channel code in combination with multiple transmit antenna achieves diversity, but the drawback is loss in bandwidth efficiency. Diversity can be achieved without any sacrifice in bandwidth efficiency if the channel codes are specifically designed for multiple transmit antennas. Space-time coding is a bandwidth and power efficient method of communication over fading channels. It combines the design of channel coding, modulation, transmit diversity, and receive diversity. Space-time codes provide better performance compared to an uncoded system. Some of the basic techniques of space-time codes are reviewed below.

2.3 Layered Space-time Codes.

Layered space-time (LST) codes are channel codes that are designed according to the LST architecture proposed by Foschini in [31]. The construction of the LST codes for an (N_t, N_r) system whose capacity is linearly scaled with N_t is based on an N_t separately coded one-dimensional (1-D) subsystem of equal capacity. The LST architecture demultiplexes a stream of data into N_t layers and each layered data is then 1-D convolutionally encoded by N_t encoders and then transmitted by N_t antennas. The above described layered space-time architecture is formally known as the horizontally layered space-time (HLST) architecture. Data can be rearranged amongst the layers such that the coded data are transmitted by N_t transmit antennas forming a diagonally layered space-time architecture (DLST) [32]. In [32] the performance analysis of both HLST and DLST codes shows that DLST codes achieve better performance when compared with HLST codes.

2.4 Space-time Block Code

Space-time block codes were first presented by Alamouti [3] as a simple transmit diversity technique. Tarokh et al [5], [6] generalized Alamouti's scheme by using the theory of orthogonal design and also extended it to two or more transmit antennas. The orthogonal design allows for the use of a simple maximum-likelihood decoding algorithm based on linear combining at the receiver. There are two classes of space-time block codes generated from orthogonal designs. The first class consists of those from real orthogonal designs for real constellation such as PAM and the second consists of those from complex orthogonal designs for complex constellation such as PSK and QAM.

2.4.1 Real orthogonal design

A real orthogonal design of size n is an $n \times n$ orthogonal matrix whose rows are permutations of real numbers $\pm x_1, ..., \pm x_n$. For example, real orthogonal designs for $n = 2$ and $n = 4$ are:

$$\begin{bmatrix} x_1 & x_2 \\ -x_2 & x_1 \end{bmatrix} \quad \text{and} \quad \begin{bmatrix} x_1 & x_2 & x_3 & x_4 \\ -x_2 & x_1 & -x_4 & x_3 \\ -x_3 & x_4 & x_1 & -x_2 \\ -x_4 & -x_3 & x_2 & x_1 \end{bmatrix},$$

respectively.

The existence of real orthogonal designs for different values of n is known as the Hurwitz-Radon problem in mathematics [35]. From Hurwitz-Radon theory, a full rate real orthogonal design exist only when n=2, 4 or 8.

A set of $n \times n$ real matrices $\{B_1,...,B_k\}$ is called a size k Hurwitz-Radon of matrices if

$$\begin{aligned} & B_i^T B_i = I \\ & B_i^T = -B_i, \quad i = 1,...,k \\ & B_i B_j = -B_j B_i \qquad 1 \le i, j \le k, \end{aligned} \tag{2.1}$$

where $(\bullet)^T$ stands for the transpose of the matrix element.

Let $n = 2^a b$, where b is odd and $a = 4c + d$ with $0 \le d \le 4$ and $0 \le c$. Any Hurwitz-Radon family of $n \times n$ matrices contains strictly less than $\rho(n) = 8c + 2^d$ matrices and $\rho(n) \le n$. From above we can generalize that a Hurwitz-Radon family containing $n-1$ matrices exist if and only if $n = 2$, 4 and 8. Therefore to construct a space-time block code of length p, and using the Hurwitz-Radon family matrices we can construct a set of integer $p \times p$ matrices with $\rho(p)-1$ member's i.e. $\{A_1, A_2..., A_{\rho(p)-1}\}$. Let $A_0 = I$ and $X = (x_1,..., x_p)$, we can construct a $p \times n$ generalized real orthogonal design Φ whose j^{th} column is $A_{j-1}X^T$ for $j = 1, 2, \ldots, n$. It is observed that Φ is full ranked.

2.4.2 Complex orthogonal design

A complex orthogonal design of size n is an orthogonal matrix whose rows are permutations of $\pm x_1,...,\pm x_n$, their conjugates $\pm x_1^*,...,\pm x_n^*$, or multiples of them by i where $i = \sqrt{-1}$. Let v variables $x_1, x_2, \cdots x_v$ represent information symbols from a

signal constellation, such as BPSK or QPSK, to be transmitted through N_t transmit antennas in m time slots. The transmission rate R is given by

$$R = \frac{v}{m}. \tag{2.2}$$

A higher rate means that more information is being carried by the code.

In [3], Alamouti proposed a simple transmit diversity scheme (2.3) which was later shown in [5] as a space-time block code from complex orthogonal design (COD) of rate 1 for $N_t = 2$. [5] also proposed a systematic rate 1/2 COD construction for any number of transmit antenna using rate 1 real orthogonal design. Later works [33], [34] on complex orthogonal design propose STBC codes of different rate and for various transmit antenna but none of this code is full rate. We can therefore generalize that the space-time block code in [3] is a special case of COD with full rate.

$$\mathbf{P}_2 = \begin{bmatrix} x_1 & x_2 \\ -x_2^* & x_1^* \end{bmatrix} \tag{2.3}$$

2.5 Space-time Trellis Code

Space-time trellis coding was introduced by Tarokh et al. [7] as a means of combining signal processing and multiple transmit antennas producing a system with significant gain over the earlier transmit diversity schemes [8, 9]. Baro et al. [12] showed that although the space-time trellis coding presented by Tarokh [7] achieves maximum possible diversity, it does not necessarily provide full coding advantage. Subsequent computer searches in [12] and [36] have yielded new space-time trellis codes with improved coding advantage.

In [37], optimum space-time trellis codes were proposed using generator matrices, which provide maximum diversity and coding gain for various numbers of states and antenna with PSK modulation. It can be shown that the space-time trellis codes presented by Tarokh in [7] provide the best tradeoff between constellation size, data rate, diversity advantage and trellis complexity when compared with other codes [12], [36] and [37].

Space-time trellis codes operates on one input symbol at a time and then produce a sequence of vector symbols whose length represents the number of transmit antennas. To understand the functionality of space-time trellis codes, we look at a simple example of such code using a QPSK signal constellation.

A mobile communication system that is equipped with N_t and N_r transmit and receive antennas respectively is considered. Information data is encoded by the space-time trellis encoder, the encoded data goes through a serial- to-parallel converter, and is divided into N_t streams of data. Each stream of data is used as the input to a transmit antenna. At each time slot t, the output of transmitted signal x_t^i is transmitted using transmit antenna i for $1 \le i \le N_t$. The trellis diagram for a 4-state space-time trellis code is shown in Figure 2.1 below.

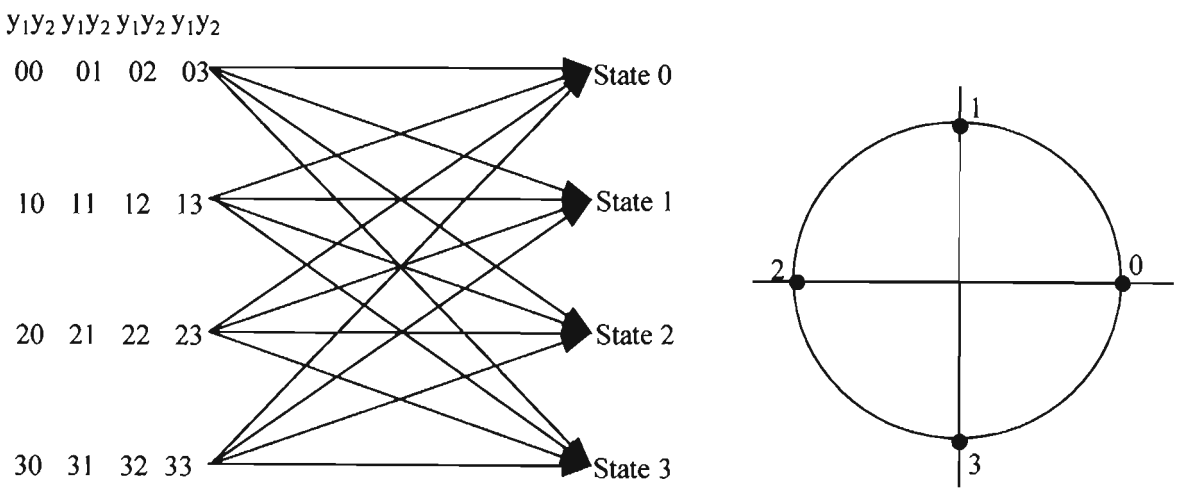

Figure 2.1: 4-State 4-PSK Space-time trellis code

At each time t, the encoder is in a generic state. The input bit stream to the space-time encoder is divided into groups of two bits, $x_1 x_2$. Each group 00, 01, 10 or 11 then selects one of the four branches originating from the corresponding state. The branches are then mapped for every transmit antenna into one of the four constellation points. The edge labels $y_1 y_2$ in the above figure are associated with the four transitions from top to bottom and indicate that symbol y_1 and y_2 are transmitted simultaneously over the first and second antenna respectively. The encoder moves to the next state after transmission of the couple of symbols. At the decoder, the receiver

estimates the transition metric using the Maximum likelihood (ML) method and the Viterbi Algorithm [10] is used to estimate the path with the least metric.

2.6 Code Design and Performance of Space-time Codes

The performance of any space-time code can be expressed in terms of the diversity order and the coding advantage that the code provides. The frame error rate (or bit error rate) versus signal-to-noise rate (SNR) on the log-log scaled curve of a space-time code shows these properties. The shift and slope of the curve corresponds to the coding advantage and diversity advantage respectively. Most designed space-time codes seek to maximize the above measures.

Tarokh et al, in [7] proposed a new criterion for the space-time code design for various fading channels. These criteria were based on the signal matrix over all possible codewords.

For a mobile communication system that is equipped with N_t transmit antennas and N_r receive antennas, the probability of transmitting the codeword $\mathrm{x} = x_1(1),...,x_{N_t}(1),...,x_1(l),...,x_{N_t}(l)$ and deciding erroneously in favour of a different codeword $\tilde{\mathrm{x}} = \tilde{x}_1(1),...,\tilde{x}_{N_t}(1),...,\tilde{x}_1(l),...,\tilde{x}_{N_t}(l)$ is bounded by [7]:

$$\mathrm{P}(\mathrm{x} \to \tilde{\mathrm{x}}) \le \left(\prod_{i=1}^{r} \lambda_i \right)^{-N_r} \left(\frac{E_s}{4N_0} \right)^{-rN_r} \tag{2.4}$$

where r is the rank of the matrix $\mathrm{A}(\mathrm{x},\tilde{\mathrm{x}})$ and λ_i are the non-zero eigenvalues of $\mathrm{A}(\mathrm{x},\tilde{\mathrm{x}})$.

$$\mathrm{A}(\mathrm{x},\tilde{\mathrm{x}}) = \mathrm{B}(\mathrm{x},\tilde{\mathrm{x}}) \bullet \left(\mathrm{B}(\mathrm{x},\tilde{\mathrm{x}})\right)^H$$

$$\mathrm{B}(\mathrm{x},\tilde{\mathrm{x}}) = \begin{bmatrix} x_1(1)-\tilde{x}_1(1) & x_1(2)-\tilde{x}_1(2) & \cdots & x_1(l)-\tilde{x}_1(l) \\ x_2(1)-\tilde{x}_2(1) & x_2(2)-\tilde{x}_2(2) & \cdots & x_2(l)-\tilde{x}_2(l) \\ \vdots & \vdots & \ddots & \vdots \\ x_{n_t}(1)-\tilde{x}_{n_t}(1) & x_{n_t}(2)-\tilde{x}_{n_t}(2) & \cdots & x_{n_t}(l)-\tilde{x}_{n_t}(l) \end{bmatrix}, \tag{2.5}$$

- *Rank Criterion*: In order to achieve the maximum diversity $N_t * N_r$, the codeword matrix $B(x,\tilde{x})$, must be full rank. If the codeword matrix has a minimum rank r over the set of two tuples of distinct codeword, then a diversity of $r * N_t$ is achieved.
- *Coding Advantage Criterion*: The minimum determinant of the codeword matrix, $A(x,\tilde{x})$ taken over all pairs of distinct codewords must be maximized.
- *Orthogonality Criterion:* The transmitted codeword matrix is made orthogonal in order to minimize the decoding complexity as transmit and receive antennas increases. The orthogonality property of the codeword matrix is given by

$$A(x,\tilde{x})=B(x,\tilde{x})*B^{H}(x,\tilde{x})=\left(|B_1|^2+|B_2|^2+...+|B_{N_t}|^2\right)\bullet I_{N_t}, \tag{2.6}$$

where I_{N_t} is an identity matrix of order N_t.

2.7 Concatenated Space-time Codes.

Concatenating channel codes with space-time codes show a considerable increase in the performance of the overall multi-antenna element system [38], [39]. These systems exploit the properties of the channel code to increase either the coding gain or the time-diversity advantage. The channel codes include convolution codes, Trellis coded modulation (TCM) and Turbo coding.

The code construction in this thesis is based on the concatenation of space-time block code and an outer TCM encoder. The standard technique in the design of a TCM (as enumerated in section 2.8) is used to realize a high rate space-time trellis coded modulation with large coding gain when compared with [7].

2.8 Brief Introduction on Trellis Coded Modulation

In trellis coded modulation (TCM), coding and modulation schemes are combined in order to improve the reliability of a digital transmission system without increasing the transmitted power or required bandwidth. A schematic diagram of TCM in an AWGN channel is shown in Figure 2.2 below.

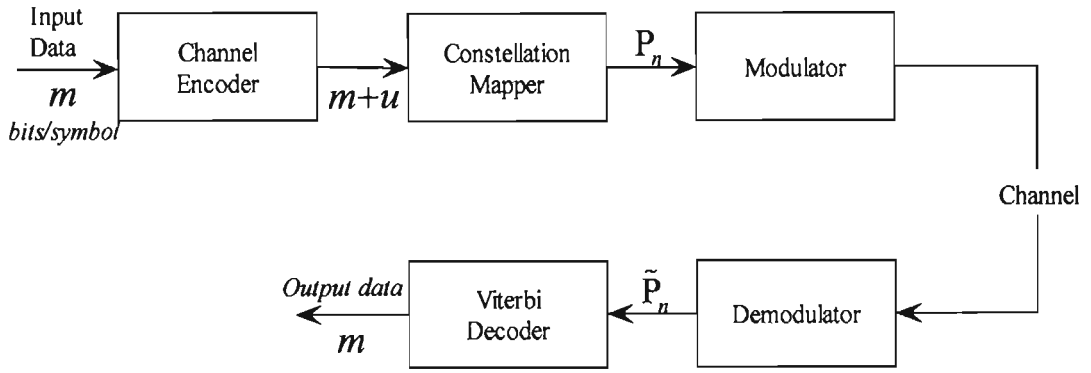

Figure 2.2: Schematic diagram of TCM

The basic idea of TCM combines ordinary rate $R = m/m+u$ binary convolutional codes with an M-ary signal constellation $(M = 2^{m+u} > 2)$ in such a way that coding gain is achieved without increasing the rate at which symbols are transmitted, i.e., without increasing the required bandwidth, compared to uncoded modulation. For example, a rate $R = 2/3$ convolutional code can be combined with 8-PSK modulation by mapping the three encoder output bits in each T-second time interval into on 8-PSK symbol. This TCM scheme can then be compared with uncoded QPSK modulation, since they both have the same spectral efficiency of $\eta = 2$ bits/symbol. The key to the technique is that the redundant bits introduced by coding (i.e. u) are not used to send extra symbols, as in binary modulation, but instead they are used to expand the size of the signal constellation relative to the uncoded system. Thus TCM involves signal set expansion rather than bandwidth expansion.

In a TCM system, if the convolutional codes are chosen according to the usual criterion of maximizing the *minimum free Hamming distance* between codewords and the mapping of the encoder outputs to signal points in the expanded constellation is done independently of the code selection, coding gain is not achieved. However, if the code and signal mapping are designed jointly to maximize the *minimum free*

Euclidean distance between signal sequences, coding gain can be achieved without expanding the bandwidth or increasing the average energy of the signal set. This is accomplished using a technique known as *mapping by set partitioning* [11].

2.9 SUMMARY

In this chapter the channel codes used in MIMO systems are reviewed. The three main primary approaches in space-time coding schemes which are layered space-time codes, space-time block code and space-time trellis code were enumerated in this chapter. Space-time block codes operate on a block of input symbols, producing a matrix output whose columns represent time variation, and rows represent the number of antenna used while space-time trellis codes operate on one input symbol at a time producing a sequence of vector symbols whose length represents antennas.

In space-time block code, the theory of orthogonal design can be used to design both real and complex orthogonal space-time block codes. It can be shown that the simple transmit diversity scheme of Alamouti in [3] is a special case of full rate complex orthogonal space-time block code design.

Space-time trellis codes in [7] fall into the category of space-time codes that offer a good tradeoff between complexity and performance.

The code design criteria and performance of most of the space-time codes were discussed and a brief review of concatenating channel codes with space-time codes as an attempt to further increase the performance of such codes was mentioned in this chapter.

CHAPTER 3

HIGH RATE SPACE-TIME TRELLIS CODED MODULATION

3.1 Introduction

In this chapter a form of space-time trellis coded modulation [4] that utilizes the principle of Ungerboeck [11] in the design of TCM to provide a high rate space-time code will be considered. Since the original space-time trellis coded modulation proposed by Tarokh [7] was handcrafted (i.e. not optimum in design), various research papers [12, 13, 14, 36, 43] have been aimed at constructing space-time codes with the optimum constituent TCM encoder. Most of these papers have been completed with a proposed code construction or systematic search for an optimal constituent TCM encoder with improved worst-case error performance. However, only marginal or moderate gains of average performance over the original space-time trellis code [7] design were obtained from these research efforts.

The construction of the high rate space-time code in this chapter is based on the concatenation of an outer TCM/Multiple TCM with an inner space-time block code. Most of the work in this chapter focus on this transmit coded modulation's scheme design and the comparison of its performance with and without channel estimation at the receiver.

3.1.1 System Model

A communication system equipped with N_t antennas at the transmitter and N_r antennas at the receiver is considered. The transmitter employs a concatenation coding scheme where a Multiple-TCM encoder with multiplicity of N_c is used as an outer code and an $N_c \times N_t$ space-time block code is used as the inner code.

The transmitter encodes k_c information bits into $N_c N_t$ symbols (i.e. $N_c \times N_t$ in matrix dimension) corresponding to the edge in the trellis of the space-time code with 2^{ν_c} states, where ν_c is the memory of the space-time encoder. The encoded symbols are divided into N_t streams, each of which is linearly modulated and simultaneously transmitted via each antenna. The rate of this space-time code is defined as $R_c = k_c / N_c$ bits /symbol. For example let us consider a transmitter that encodes 4 information bits into 4 symbols i.e. $N_t = 2$ and $N_c = 2$. This make $R_c = 2$ bits / symbol which is the rate for a QPSK constellation. This shows that the transmission scheme employed is a full rate or high rate system.

It is assumed that the elements of the signal constellation are chosen so that the average energy of the constellation is one. The channel between the transmit and receive antennas is modelled as frequency non-selective flat Rayleigh fading process. The signal received by the j^{th} receive antenna can be expressed in matrix form as

$$\mathbf{r}^j = \sqrt{\frac{R_c E_b}{N_t}} \bullet \mathbf{H}\ \mathbf{X} + \boldsymbol{\eta}^j, \tag{3.1}$$

where $\mathbf{X}$ is an $N \times N_t$ transmitted codeword matrix of the form given in (3.2),

$$\mathbf{X} = \begin{bmatrix} \mathrm{X}_1(1) & \mathrm{X}_2(1) & \cdots & \mathrm{X}_{N_t}(1) \\ \mathrm{X}_1(2) & \mathrm{X}_2(2) & \cdots & \mathrm{X}_{N_t}(2) \\ \vdots & \vdots & \ddots & \vdots \\ \mathrm{X}_1(N) & \mathrm{X}_2(N) & \cdots & \mathrm{X}_{N_t}(N) \end{bmatrix}, \tag{3.2}$$

with $\mathrm{X}_i(k)$ being the symbol transmitted at the time k by the i^{th} transmit antenna and N being the frame length.

The channel matrix given by $\mathbf{H}$ of dimension $N_t \times 1$ and with elements $h_{i,j}$, $i = 1,2,\cdots N_t, j = 1,2,\cdots N_r$ is the path gain from transmit antenna i to receive antenna j. The channel coefficients are modelled as independent samples of complex Gaussian random variable with zero mean and variance 0.5 per dimension. The noise matrix per j^{th} receive antenna is given by $\boldsymbol{\eta}^j$ and its elements are modelled as independent samples of zero-mean Gaussian random variables with variance $N_0/2$ per dimension.

The construction of the high rate space-time trellis coded modulation (HR-STTCM) [4] is based on expanding the cardinality of an orthogonal space-time signal set before concatenating it with an outer encoder. Once the expanded signal set is formed, the standard set partitioning method can be used to partition codewords in each block-code subset. A simple design rule which is *transition leaving from (and/or merging to) each state are uniquely labelled with codewords from a full rank block code* can be posed on the outer encoder to guarantee that the resulting space-time code achieve full-diversity. To achieve a full rate design, the standard space-time block code [3] is used as a building subset. A distinct block-code subset can be generated from the original signal subset by applying certain unitary transformation, i.e., if $\mathbf{E}(\vec{x})$ is an $N_c \times N_t$ orthogonal block code for an input $\vec{x}$, another orthogonal block code $\tilde{\mathbf{E}}(\vec{x})$ can be formed by

$$\tilde{\mathbf{E}}(\vec{x}) = \mathbf{K} \cdot \mathbf{E}(\vec{x}) \cdot \mathbf{L}, \tag{3.3}$$

where $\mathbf{K}$ and $\mathbf{L}$ are some $N_c \times N_c$ and $N_t \times N_t$ diagonal matrices respectively. This idea is borrowed from the signal expansion used in TCM.

Using the 2×2 Alamouti signals $\mathbf{P}_2$ [3], as the building subset, we can generate additional isolated signal subset. For the QPSK alphabet we can generate the expanded signal subset by using (3.3) with $\mathbf{K}$ being an identity matrix and $\mathbf{L}$ drawn from the following set:

$$\mathbf{L} \in \left\{ \begin{bmatrix} 1 & 0 \\ 0 & \pm 1 \end{bmatrix}, \begin{bmatrix} 1 & 0 \\ 0 & \pm j \end{bmatrix} \right\}. \tag{3.4}$$

The space-time block codes resulting from the four generators i.e. elements of $\mathbf{L}$ shall be denoted correspondingly by

$$\mathbf{A}(x_0, x_1) = \mathbf{P}_2 \times diag[1,1] = \begin{pmatrix} x_0 & x_1 \\ -x_1^* & x_0^* \end{pmatrix} \tag{3.5}$$

$$\mathbf{B}(x_0, x_1) = \mathbf{A}(x_0, x_1) \times diag[1,-1] = \begin{pmatrix} x_0 & -x_1 \\ -x_1^* & -x_0^* \end{pmatrix} \tag{3.6}$$

$$\mathbf{C}(x_0, x_1) = \mathbf{A}(x_0, x_1) \times diag[1, j] = \begin{pmatrix} x_0 & jx_1 \\ -x_1^* & jx_0^* \end{pmatrix} \tag{3.7}$$

$$\mathbf{D}(x_0, x_1) = \mathbf{A}(x_0, x_1) \times diag[1,-j] = \begin{pmatrix} x_0 & -jx_1 \\ -x_1^* & -jx_0^* \end{pmatrix}. \tag{3.8}$$

The expanded signal set matrices above, can be partitioned as shown in Figure 3.1 based on the square Euclidean distance of the input labels. The square Euclidean distance can be calculated for a given pair of signals from each block code:

$\{\mathbf{A}(\alpha_0, \alpha_1), \mathbf{A}(\beta_0, \beta_1)\}, \{\mathbf{B}(\alpha_0, \alpha_1), \mathbf{B}(\beta_0, \beta_1)\}, \{\mathbf{C}(\alpha_0, \alpha_1), \mathbf{C}(\beta_0, \beta_1)\}$ *or* $\{\mathbf{D}(\alpha_0, \alpha_1), \mathbf{D}(\beta_0, \beta_1)\}$

by using

$$d^2(\alpha, \beta) = |\alpha_0 - \beta_0|^2 + |\alpha_1 - \beta_1|^2. \tag{3.9}$$

The classic set partitioning technique [11] was basically provided to do exactly this.

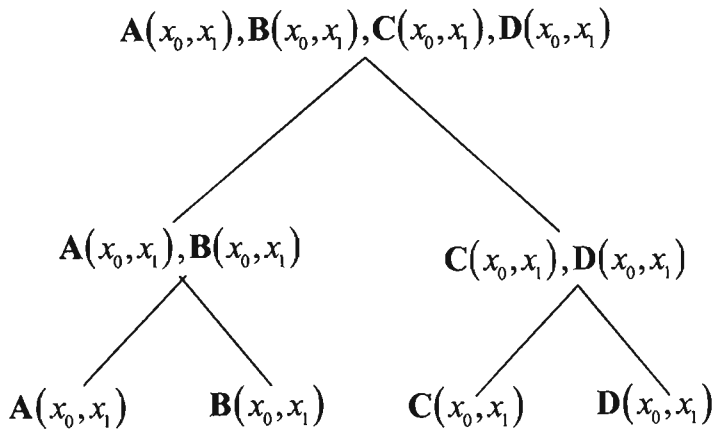

Figure 3.1: Signal Matrix Partition

3.2 Code Performance in Fading Channels

In this section an example of the high rate space-time trellis coded modulation scheme for a system with two transmit antennas in fading channels is introduced. In this case a multiple trellis code modulation (MTCM) encoder with multiplicity of 2 is used as an outer encoder and a 2×2 space–time block code as the inner encoder. For the QPSK example of the HR-STTCM, the encoded bits are naturally mapped to a point on the QPSK constellation, resulting in QPSK symbols that are fed into the space-time block code (inner encoder). Since an MTCM with a multiplicity of 2 is used as the outer encoder, there are $2^4 = 16$ incoming and outgoing transitions needed at each state to achieve the desired code rate of 2bits/symbol. The MTCM encoder will thus have 8 possible parallel transition branches. The standard method [44] of dividing each of the four block code subsets into 2 partitions, as shown in (3.10), based on the square Euclidean is used.

$$\begin{aligned} A_0 &\equiv \{\mathbf{A}(\pm 1,\pm 1),\mathbf{A}(\pm j,\pm j)\} \\ A_1 &\equiv \{\mathbf{A}(\pm 1,\pm j),\mathbf{A}(\pm j,\pm 1)\} \\ B_0 &\equiv \{\mathbf{B}(\pm 1,\pm 1),\mathbf{B}(\pm j,\pm j)\} \\ B_1 &\equiv \{\mathbf{B}(\pm 1,\pm j),\mathbf{B}(\pm j,\pm 1)\} \end{aligned} \tag{3.10}$$

and similarly for C_0, C_1, D_0, and D_1.

The trellis structure for a 2-state and 4- state encoder is shown in Figure 3.2:

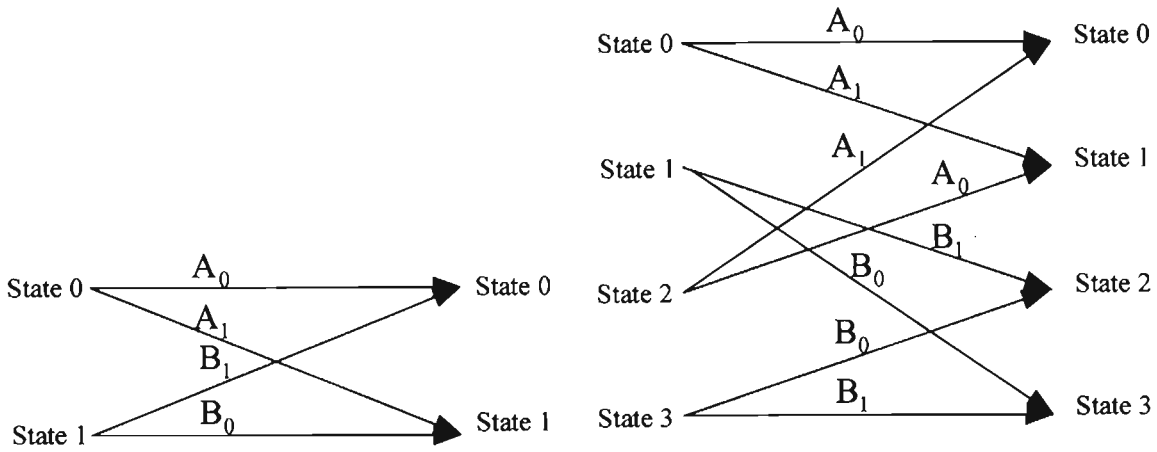

Figure 3.2: 2-State and 4-State 2-bits/symbol HR-STTCM

The decoding complexity of the HR- STTCM construction is made practically low by exploiting signal orthogonality. For a maximum likelihood sequence decoder with perfect channel state information, the branch metric **m**(k) at k^{th} decoding interval (at time $2k$ and $2k$+1) for a transition labelled with transmitted matrix

$$\mathrm{A}_k = \begin{pmatrix} x_1(2k) & x_2(2k) \\ x_1(2k+1) & x_2(2k+1) \end{pmatrix} \tag{3.11}$$

given that the observations at this interval are $r(2k)$ and $r(2k+1)$ and the channel gain $\mathbf{H} = [h(1)\ \ h(2)]^{\mathrm{T}}$ is given as:

$$\mathrm{m}(k) = \sum_{i=2k}^{2k+1} \left| r(i) - \sum_{s=1}^{2} x_s(i) h(s) \right|^2 . \tag{3.12}$$

Once the minimum branch metric per transition is computed, the Viterbi Algorithm [10] is applied to search for the path with the lowest accumulated metric.

When the channel between transmit and receive antenna is constant over a frame length i.e. quasi-static, the probability that the maximum likelihood detector in (3.12) detects erroneously in favour of codeword matrix sequence $\tilde{\mathbf{A}} = \left(\tilde{\mathbf{A}}_1, \tilde{\mathbf{A}}_2, \tilde{\mathbf{A}}_3, ..., \tilde{\mathbf{A}}_N\right)$

when in fact the codeword matrix sequence $\mathbf{A}=(\mathbf{A}_1,\mathbf{A}_2,\mathbf{A}_3,...,\mathbf{A}_N)$ which was transmitted is given by [20]

$$\Pr\left(\mathbf{A}\rightarrow\tilde{\mathbf{A}}\,|\,\mathbf{H}\right)=Q\left(\sqrt{\frac{\|\mathbf{H}\,(\mathbf{A}-\tilde{\mathbf{A}})\|^2}{2\sigma^2}}\right), \tag{3.13}$$

where $Q(y)=\frac{1}{\sqrt{2\pi}}\int_y^\infty e^{-t^2/2}dt$ and by using the inequality $Q(y)\le\frac{1}{2}e^{-y^2/2}$, $y\ge 0$.

In (3.13) we can further express elements of the Euclidean norm i.e. $\|\bullet\|$ as;

$$\begin{aligned}\|\mathrm{H}(\mathrm{A}-\tilde{\mathrm{A}})\|^2 &= \mathrm{tr}\left(\mathrm{H}\bullet\mathrm{H}^H(\mathrm{A}-\tilde{\mathrm{A}})(\mathrm{A}-\tilde{\mathrm{A}})^H\right)\\ &= \left(\sum_{k\in\gamma}\|x_k-\tilde{x}_k\|^2\right)\mathrm{tr}(\mathrm{H}\bullet\mathrm{H}^H)\end{aligned} \tag{3.14}$$

where γ denotes the set of indices k for which $\mathbf{A}_k\neq\tilde{\mathbf{A}}_k$, $\mathrm{tr}(\bullet)$ denotes the trace operator and

$$(\mathrm{A}-\tilde{\mathrm{A}})(\mathrm{A}-\tilde{\mathrm{A}})^H=\left(\sum_{k\in\gamma}\|x_k-\tilde{x}_k\|^2\right)\bullet\mathrm{I}. \tag{3.15}$$

In (3.14) x_k and $\tilde{x}_k$ represent the symbols from which matrices $\mathbf{A}_k$ and $\tilde{\mathbf{A}}_k$ are constructed from. It follows from (3.15) that

$$\left(\sum_{k\in\gamma}\|x_k-\tilde{x}_k\|^2\right)=\frac{\mathrm{tr}\left((\mathrm{A}-\tilde{\mathrm{A}})(\mathrm{A}-\tilde{\mathrm{A}})^H\right)}{N_t}, \tag{3.16}$$

since the codewords $\mathbf{A}_k$ and $\tilde{\mathbf{A}}_k$ are orthogonal.

Substituting (3.16) back in (3.13) we get

$$\begin{aligned}\Pr\left(\mathrm{A}\rightarrow\tilde{\mathrm{A}}|\mathrm{H}\right) &= Q\left(\sqrt{\frac{\mathrm{tr}\left((\mathrm{A}-\tilde{\mathrm{A}})(\mathrm{A}-\tilde{\mathrm{A}})^H\right)}{N_t}\frac{\mathrm{tr}(\mathrm{H}^H\mathrm{H})}{2\sigma^2}}\right)\\ &\le \exp\left(-\frac{\mathrm{tr}\left((\mathrm{A}-\tilde{\mathrm{A}})(\mathrm{A}-\tilde{\mathrm{A}})^H\right)}{N_t}\frac{\mathrm{tr}(\mathrm{H}^H\mathrm{H})}{4\sigma^2}\right).\end{aligned} \tag{3.17}$$

Averaging (3.17) with respect to the distribution of $\mathrm{tr}\left(\mathbf{H}^H\mathbf{H}\right)$ given in (3.20) [41] we get,

$$E\left(\Pr\left(\mathrm{A}\rightarrow\tilde{\mathrm{A}}|\mathrm{H}\right)\right)\leq\left(1+\frac{\mathrm{tr}\left((\mathrm{A}-\tilde{\mathrm{A}})(\mathrm{A}-\tilde{\mathrm{A}})^H\right)}{4N_t\sigma^2}\right)^{-N_tN_r}. \quad (3.18)$$

It should be noted from (3.18) that the average error probability is inversely proportional to $\mathrm{tr}\left((\mathrm{A}-\tilde{\mathrm{A}})(\mathrm{A}-\tilde{\mathrm{A}})^H\right)$. The bound in (3.18) can be minimized if $\mathrm{tr}\left((\mathrm{A}-\tilde{\mathrm{A}})(\mathrm{A}-\tilde{\mathrm{A}})^H\right)$ is maximized.

Thus in quasi-static fading the code performance is a function of the maximum minimum trace of the error signal difference matrix among all pairs of distinct codewords. It should be noted that the trellis's constructions in Figure 3.2 are designed to do this which corresponds to the coding gain advantage that the scheme provides when compared with other space-time coding schemes (i.e. [7, 12 13])and also maintains appropriate diversity gain i.e. N_tN_r.

For a fast fading channel, the channel coefficients are assumed to remain constant during the transmission of one orthogonal block of $\mathbf{A}_k$ matrix, but change in random manner from one block to another. The upper bound in a fast fading environment can be written as:

$$\Pr\left(\mathrm{A}\rightarrow\tilde{\mathrm{A}}|\mathrm{H}\right)\leq\prod_{k\in\gamma}^{L}\exp\left(-\frac{\mathrm{tr}\left((\mathrm{A}_k-\tilde{\mathrm{A}}_k)(\mathrm{A}_k-\tilde{\mathrm{A}}_k)^H\right)}{N_t}\frac{\mathrm{tr}\left(\mathrm{H}_k{}^H\mathrm{H}_k\right)}{4\sigma^2}\right) \quad (3.19)$$

Let L be the size of γ.Since the coefficients of $\mathbf{H}_k$ are independently identically distributed random variables with a pdf given by (3.20), averaging (3.19) over $\mathbf{H}_k$ gives (3.21).

$$f(x)=\frac{1}{(U-1)!}x^{U-1}e^{-x}g(x) \quad (3.20)$$

where $U=N_tN_r$ and $g(x)$ denotes the step function.

$$E\left(\Pr\left(\mathrm{A}\rightarrow\tilde{\mathrm{A}}|\mathrm{H}\right)\right)\leq\prod_{k\in\gamma}^{L}\left(1+\frac{\mathrm{tr}\left(\left(\mathrm{A}_k-\tilde{\mathrm{A}}_k\right)\left(\mathrm{A}_k-\tilde{\mathrm{A}}_k\right)^H\right)}{4N_t\sigma^2}\right)^{-N_tN_r}$$

$$\approx\left(\frac{1}{4N_t\sigma^2}\right)^{-LN_tN_r}\prod_{k\in\gamma}^{L}\left(\frac{\mathrm{tr}\left(\left(\mathrm{A}_k-\tilde{\mathrm{A}}_k\right)\left(\mathrm{A}_k-\tilde{\mathrm{A}}_k\right)^H\right)}{4N_t\sigma^2}\right)^{-N_tN_r}, \quad (3.21)$$

where the above approximation holds for sufficient high values of SNR. From the above equation we can see that the order of diversity is N_rN_tL where L is the minimum (matrix) symbol, i.e. $\mathbf{A}_k$, Hamming distance between the different codewords.

3.3 HR-STTCM with Channel Estimation.

In practice it is always assumed that the receiver has a perfect knowledge of the channel so as to make coherent decoding possible as explained above. This assumption is inappropriate when simulating a physical system, because in a real system the effect of the channel can never be known exactly. Rather some form of estimation is performed to find an approximation for the channel. One method of finding an estimate for the channel is the use of pilot symbols. In [15] a new class of unitary space-time signal was proposed as a form of a pilot symbol to estimate the channel. Various unitary space-time signal constellations were designed in [16], [17] and [18].The metric for the design of such signal constellations includes the chordal distance [45], diversity product distance, subspace distance and the asymptotic union bound.

The unitary space-time symbols are used to estimate the channel coefficients and then coherent detection can be performed using the obtained channel estimate.

3.3.1 System Model

Again a communication system that employs HR-STTCM with N_t transmit and N_r receive antennas is considered. At the beginning of a frame transmission, we use a

sequence of U_p pilot unitary code sequence which is of the forms $N_t \times U_p$ pilot code matrix given in matrix form by $\mathbf{C}_p$. The pilot code matrix used is of the orthogonal code in [3]. When the pilot code matrix is transmitted, we receive:

$$\mathbf{r}_p = \sqrt{E_s}\mathbf{H}\mathbf{C}_p + \boldsymbol{\eta}_p. \tag{3.22}$$

In (3.22) the elements of $\boldsymbol{\eta}_p$ are independently identically distributed complex Gaussian noise and $\mathbf{H}=\left[h_1 \quad h_2,....,h_{N_t}\right]$ is the channel coefficients which span the pilot transmission and it is a zero-mean complex Gaussian random variable.
From (3.22) we can obtain a least-square estimate of channel matrix which is given by:

$$\tilde{\mathbf{H}} = \frac{1}{\sqrt{E_s}}\mathbf{r}_p\mathbf{C}_p^H\left(\mathbf{C}_p\mathbf{C}_p^H\right)^{-1} \tag{3.23}$$

After the channel has been estimated using (3.23) we can then transmit the HR-STTCM codes. At the decoder coherent decoding is then performed using the estimated channel coefficients in (3.23).

3.4 Simulation Result and Discussions

In this section the simulation results of the high rate space-time trellis coded modulation with and without channel estimation is presented. The simulation results are compared with some of the existing space-time codes. The simulation is done for two transmit and one receive antenna. Each frame consists of 256 bits. Figure 3.3 compares the frame error rate performance of STBC, 4-state STTC, 2-state and 4-state HR-STTCM under quasi-static fading assumption i.e. the channel coefficient is assumed to be constant for the frame duration and varies from frame to frame. The simulation shows that STBC by itself performs slightly better than STTC [7] for one receive antenna under fast fading assumption. This can be explained by the multidimensional structure of STBCs, since each codeword spans two time symbols and average noise over time. The simulation also shows that HR-STTCM outperform both STBC and STTC. The coding gain advantage, i.e. shift in the graph downward,

shown in the result (i.e. Figure 3.3) is as a result of the trace condition as enumerated in the analysis above. The design maximizes the minimum trace of the error signal difference matrix by using parallel path in the set partitioning.

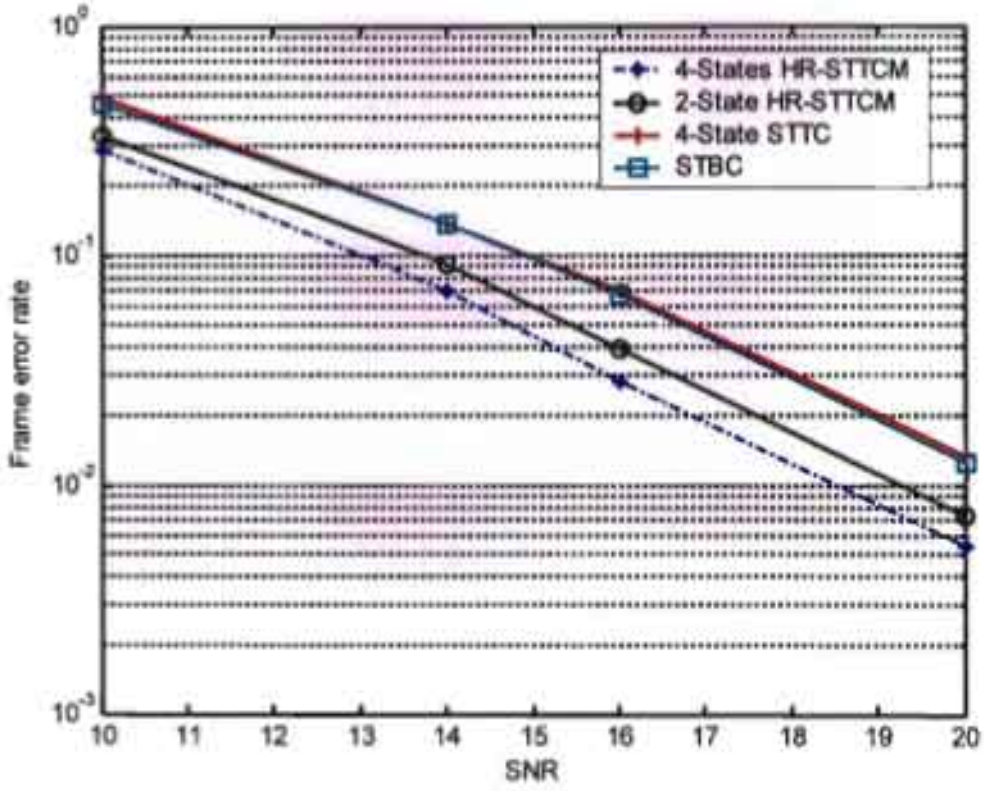

Figure 3.3: Performance of QPSK STBC, STTC and HR-STTCM in quasi-static fading.

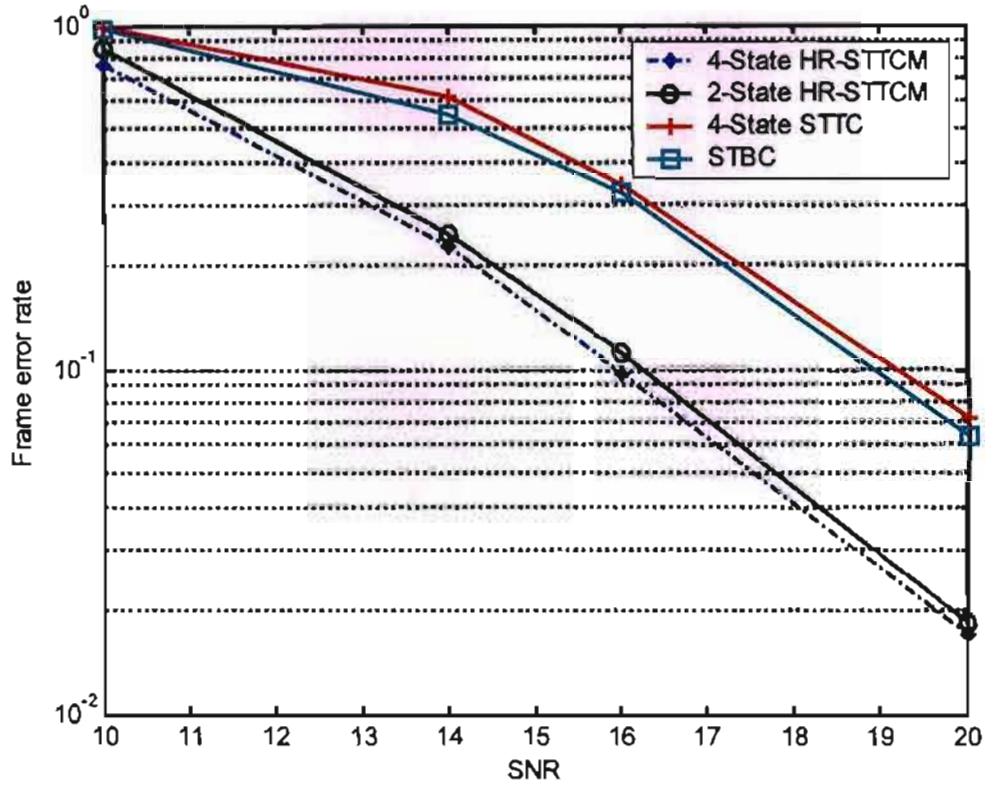

Figure 3.4: Performance of QPSK STBC, STTC and HR-STTCM in fast fading

In Figure 3.4 the frame error rate performance of STBC, 4-state STTC, 2-state and 4-state HR-STTCM under fast fading, i.e. the channel is kept constant for one block of two scalar symbols and then changed from block to block in a random manner, is shown. The result above shows that the HR-STTCM outperforms the STTC and STBC even in fast fading channel. The diversity advantage, i.e. slope of the curve, provided by the HR-STTCM codes in fast fading channel is expected as predicted from the analytical expression above. For quasi-static fading the diversity advantage equal $N_r N_t$ while for fast fading it is $N_r N_t L$.

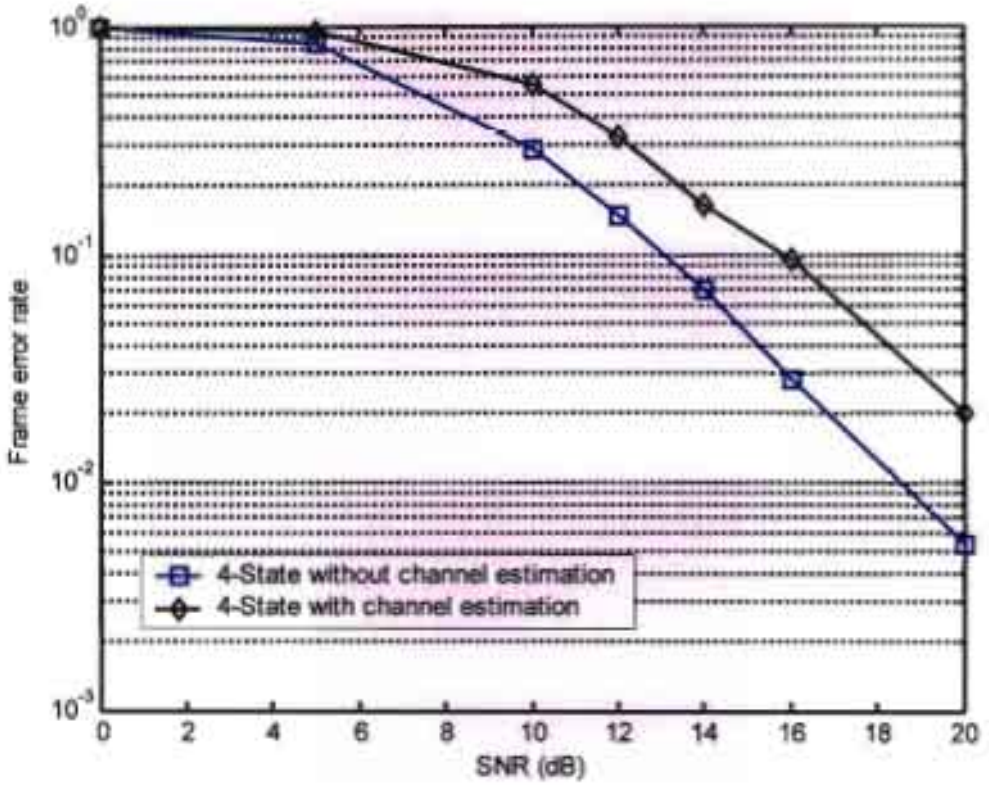

(a)

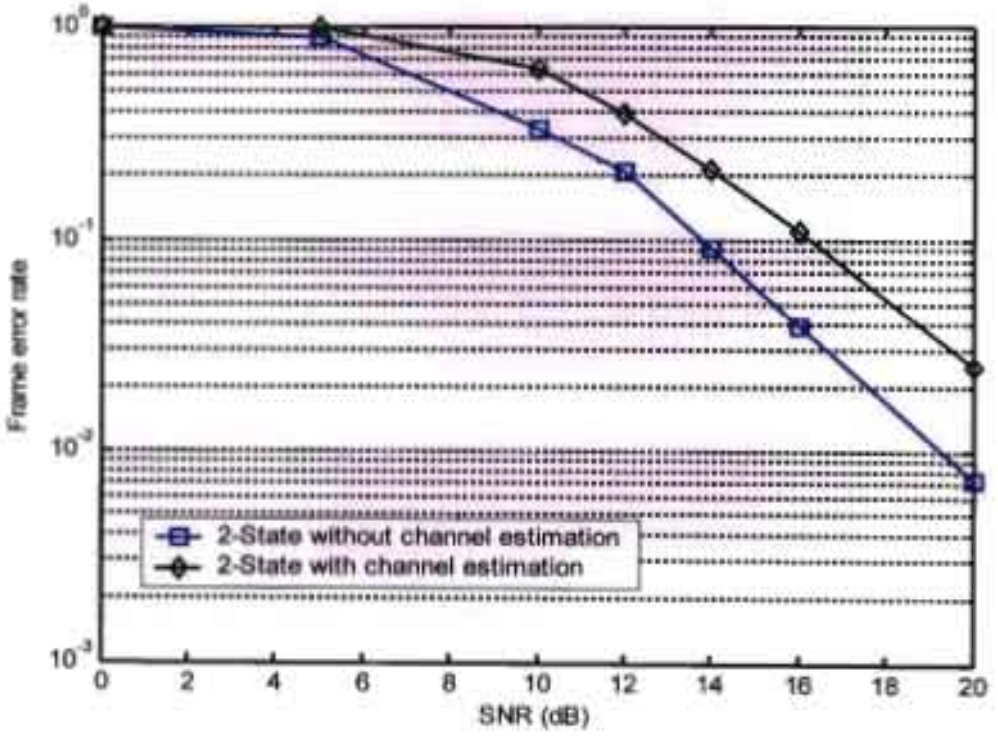

(b)

Figure 3.5: QPSK HR-STTCM schemes with and without channel estimation

Figures 3.5(a) and (b) show the performance of a 4-state and 2-state HR-STTCM schemes with and without channel estimation, respectively. The length of the unitary pilot symbol used in the simulation to estimate the channel is 2. The results show that in both scheme an approximate 3dB penalty is paid by using the unitary pilot symbols to estimate the channel coefficients.

3.5 Summary

In this chapter, the code construction in [4] and the performance of such high rate space-time code with and without channel estimation was reviewed.

The performance of the code in coherent detection, i.e. without channel estimation was enumerated for both quasi-static and fast fading Rayleigh fading channel. The upper bound of the error probability shows that the performance of the code, for a quasi-static fading assumption is a function of the trace of the error signal difference matrix among all pairs of distinct codeword matrix. Maximizing the minimum trace of the error signal difference matrix was accomplished in the construction of the HR-STTCM by using the revolutionary idea in [11] which is signal set partition.

In fast fading channel and at significantly high SNR, the diversity of such space-time code is a function of the minimum (matrix) symbol Hamming distance between the different codewords.

Simulations results show that in both fast and quasi-static fading channel, the HR-STTCM codes outperforms all the existing space-time codes.

The performance of the HR-STTCM in a non-coherent environment was reviewed. The channel coefficient at the receiver was estimated using a unitary space-time orthogonal matrix and simulation result shows that about 3dB was lost due to the imperfect channel estimate.

CHAPTER 4

MULTIUSER SPACE-TIME TRELLIS CODED MODULATION

4.1 Introduction

Space-time block coding is a powerful technique that exploits signal orthogonality at the transmitter and simplified linear decoding at the receiver in order to remove the drawback of space-time trellis codes (i.e. decoding complexity grows exponentially with the number of transmit antennas). The properties of space-time block coding [3, 5] can be used to develop an efficient interference suppression technique that can be used to increase system capacity (in terms of number of users). In a multiuser scenario, with K synchronous co-channel users using space-time block transmission scheme, the behaviour of space-time block coding can be exploited to suppress co-channel interference from the K-1 co-channel space-time user in the desired terminal. Since the construction of the High rate space-time trellis coded modulation (HR-STTCM) is based on the concatenation of outer trellis coded modulation and inner space-time block code, we exploit further the behaviour of the space-time block coding and trellis coded modulation in a multiuser environment.

In this chapter, a standalone space-time block coding scheme in a multiuser environment and the use of an interference suppression technique called zero-forcing to decouple co-channel users is considered. The signal-to-noise ratio (SNR) of a desired decoupled signal is also derived and it is deduced that when zero-forcing is

used in a standalone space-time block code transmission scheme, it completely suppresses co-channel interference.

Later in the chapter the space-time block coding interference suppression technique is applied to HR-STTCM schemes and show from analysis and simulation that although the scheme contains space-time block codes, it is not possible to obtain the single user performance for a decoupled co-channel user as was obtained in the standalone space-time block coding scheme.

4.2 System Model

A multiuser environment with K synchronous co-channel users where each user is equipped with N_t (= 2; full rate complex design) transmit antennas and uses space-time block coding transmission mechanisms is considered. At the receiver of a desired user, there are $K \times N_t$ interfering signals. An interference suppression technique can be used to suppress signals from the $K-1$ co-channel space-time users to achieve the desired diversity order which is N_t. Figure 4.1 below shows the schematic diagram of the STBC in a multiuser environment. The channel coefficients per user $\left(h_{i\in\{1,2\}} = N_c(0,1)\right)$ are assumed to undergo quasi-static and flat Rayleigh fading.

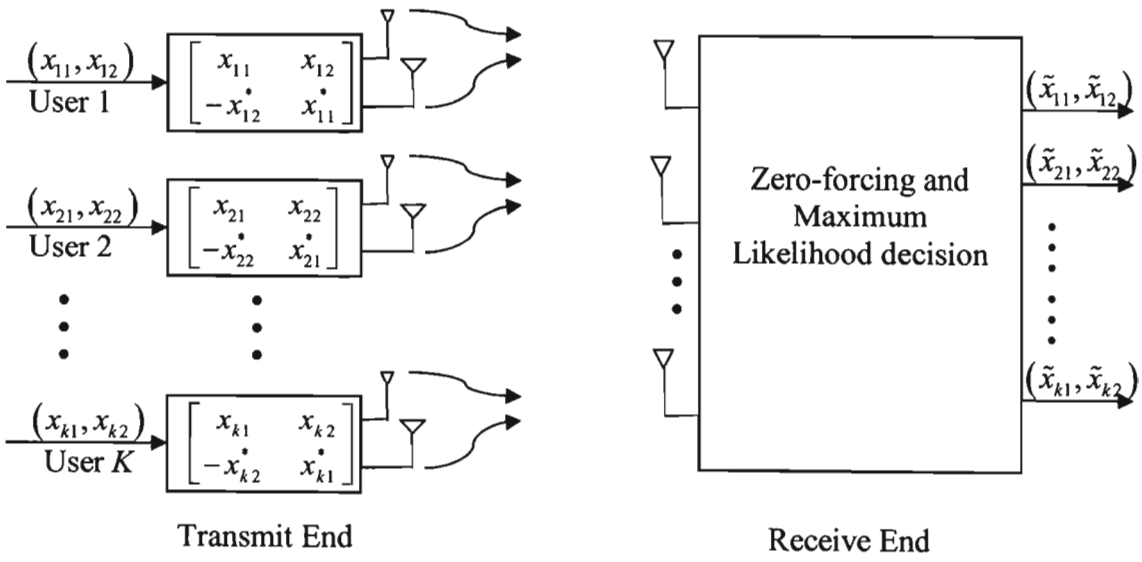

Figure 4.1: Multiuser transmission system with standalone space-time block code

For a single user transmission scenario, that is equipped with N_t(=2) transmit antenna and a single receive antenna, the output at the receiver at two successive time interval i.e. t and t+1 is given by:

$$\begin{aligned} r(t) &= x_1 h_1 + x_2 h_2 + \eta_1 \\ r(t+1) &= -x_2^* h_1 + x_1^* h_2 + \eta_2 \end{aligned} \tag{4.1}$$

where $x_{i\in\{1,2\}} \in \Re$ are the transmitted space-time signals and also elements of a baseband transmission sequence $\Re$ with unit-energy constellation. $\eta_{i\in\{1,2\}}$ are samples of AWGN. The above receiver equation can be written in matrix form as shown below:

$$\begin{bmatrix} r(t) \\ -r^*(t+1) \end{bmatrix} = \begin{bmatrix} h_1 & h_2 \\ -h_2^* & h_1^* \end{bmatrix} \bullet \begin{bmatrix} x_1 \\ x_2 \end{bmatrix} + \begin{bmatrix} \eta_1 \\ -\eta_2^* \end{bmatrix} \tag{4.2}$$

$$\mathbf{r} = \mathbf{H} \bullet \mathbf{x} + \mathbf{n}$$

The transmitted signal-to-noise ratio (SNR) can be calculated by multiplying (4.2) by the conjugate transpose of the channel matrix as show below:

$$\begin{bmatrix} h_1^* & -h_2 \\ h_2^* & h_1 \end{bmatrix} \begin{bmatrix} r(t) \\ -r^*(t+1) \end{bmatrix} = \begin{bmatrix} h_1^* & -h_2 \\ h_2^* & h_1 \end{bmatrix} \bullet \begin{bmatrix} h_1 & h_2 \\ -h_2^* & h_1^* \end{bmatrix} \bullet \begin{bmatrix} x_1 \\ x_2 \end{bmatrix} + \begin{bmatrix} h_1^* & -h_2 \\ h_2^* & h_1 \end{bmatrix} \bullet \begin{bmatrix} \eta_1 \\ -\eta_2^* \end{bmatrix}$$

$$\tilde{x}_1 = h_1^* r(t) + h_2 r^*(t+1) = \left(|h_1|^2 + |h_2|^2\right) \bullet x_1 + h_1^* \eta_1 + h_2 \eta_2^* \tag{4.3}$$

$$\text{SNR} = \frac{\mathrm{E}\left(\left(|h_1|^2 + |h_2|^2\right)^2 \bullet |x_1|^2\right)}{\mathrm{E}\left(\left(h_1^* \eta_1 + h_2 \eta_2^*\right)\left(h_1^* \eta_1 + h_2 \eta_2^*\right)^*\right)} = \frac{\left(|h_1|^2 + |h_2|^2\right) E_s}{2\sigma^2}$$

The single user equation model given in (4.2) can be extended to 2 receive antenna case given by:

$$\begin{bmatrix} \mathbf{r}_1 \\ \mathbf{r}_2 \end{bmatrix} = \begin{bmatrix} \mathbf{H}_1 \\ \mathbf{H}_2 \end{bmatrix} \bullet \begin{bmatrix} \mathbf{x}_1 \\ \mathbf{x}_2 \end{bmatrix} + \begin{bmatrix} \mathbf{n}_1 \\ \mathbf{n}_2 \end{bmatrix} \tag{4.4}$$

where $\mathbf{H}_2$ is the channel coefficient matrix to the second receive antenna and $\mathbf{r}_2$ is what is received by the second receiver.

The equation model in (4.4) can further be extended to (4.5) i.e. a two user scenario where $\mathbf{C}_1$ and $\mathbf{C}_2$ corresponds to the channel coefficient matrix of the second user for receive antenna 1 and receive antenna 2 respectively and $\mathbf{y}_2$ represents the data sequence of the second user.

$$\begin{bmatrix} \mathbf{r}_1 \\ \mathbf{r}_2 \end{bmatrix} = \begin{bmatrix} \mathbf{H}_1 & \mathbf{C}_1 \\ \mathbf{H}_2 & \mathbf{C}_2 \end{bmatrix} \bullet \begin{bmatrix} \mathbf{x}_1 \\ \mathbf{y}_2 \end{bmatrix} + \begin{bmatrix} \mathbf{n}_1 \\ \mathbf{n}_2 \end{bmatrix} \tag{4.5}$$

Equation (4.5) can be generalised into a multiuser scenario with K users each with N_t(=2) transmit antenna and N_r receive antenna to give:

$$\begin{bmatrix} \mathbf{r}_1 \\ \mathbf{r}_2 \\ \mathbf{r}_3 \\ \vdots \\ \mathbf{r}_{N_r} \end{bmatrix} = \begin{bmatrix} \mathbf{H}_1^{(1)} & \mathbf{H}_1^{(2)} & \cdots & \cdots & \mathbf{H}_1^{(k)} \\ \mathbf{H}_2^{(1)} & \mathbf{H}_2^{(2)} & \cdots & \cdots & \mathbf{H}_2^{(k)} \\ \mathbf{H}_3^{(1)} & \mathbf{H}_3^{(2)} & \cdots & \cdots & \mathbf{H}_3^{(k)} \\ \vdots & \vdots & \vdots & \vdots & \vdots \\ \mathbf{H}_{N_r}^{(1)} & \mathbf{H}_{N_r}^{(2)} & \cdots & \cdots & \mathbf{H}_{N_r}^{(k)} \end{bmatrix} \bullet \begin{bmatrix} \mathbf{x}^{(1)} \\ \mathbf{x}^{(2)} \\ \mathbf{x}^{(3)} \\ \vdots \\ \mathbf{x}^{(k)} \end{bmatrix} + \begin{bmatrix} \mathbf{n}_1 \\ \mathbf{n}_2 \\ \mathbf{n}_3 \\ \vdots \\ \mathbf{n}_{N_r} \end{bmatrix} \tag{4.6}$$

where $\mathbf{H}_m^{(k)}$ is the channel coefficient matrix from the k th user to the m th receive antenna and $\mathbf{x}^{(k)} \left(= x_{k1}, x_{k2}\right)$ are the data sequence of the k th user.

4.3 Zero-forcing Interference Cancellation

In this section an interference cancellation scheme for a two user space-time block coding scheme as defined in (4.5) and the use of zero-forcing in decoupling the two user signals will be considered. Later the signal-to-noise ratio of the decoupled signal will be calculated.

In the zero-forcing solution [42], the interference between the two space-time co-channel users is removed, without any regard to noise enhancement, by using a matrix linear combiner $\mathbf{D}$ as shown:

$$\mathbf{D}\bullet\begin{bmatrix}\mathbf{r}_1\\ \mathbf{r}_2\end{bmatrix}=\begin{bmatrix}\tilde{\mathbf{r}}_1\\ \tilde{\mathbf{r}}_2\end{bmatrix}=\begin{bmatrix}\tilde{\mathbf{H}} & 0\\ 0 & \tilde{\mathbf{C}}\end{bmatrix}\begin{bmatrix}\mathbf{x}_1\\ \mathbf{y}_2\end{bmatrix}+\begin{bmatrix}\tilde{\mathbf{n}}_1\\ \tilde{\mathbf{n}}_2\end{bmatrix} \tag{4.7}$$

Let $\mathbf{D}$ be defined by a matrix given by $\begin{bmatrix}\mathbf{q} & \mathbf{s}\\ \mathbf{f} & \mathbf{p}\end{bmatrix}$, so

$$\begin{bmatrix}\mathbf{q} & \mathbf{s}\\ \mathbf{f} & \mathbf{p}\end{bmatrix}\bullet\begin{bmatrix}\mathbf{H}_1 & \mathbf{C}_1\\ \mathbf{H}_2 & \mathbf{C}_2\end{bmatrix}=\begin{bmatrix}\tilde{\mathbf{H}} & 0\\ 0 & \tilde{\mathbf{C}}\end{bmatrix} \tag{4.8}$$

From (4.8), $\mathbf{qC}_1=-\mathbf{sC}_2$; $\mathbf{s}=-\mathbf{qC}_1\mathbf{C}_2^{-1}$ and $\mathbf{fH}_1=-\mathbf{pH}_2$; $\mathbf{f}=-\mathbf{pH}_2\mathbf{H}_1^{-1}$. Let $\mathbf{q}=\mathbf{p}=\mathbf{I}_{N_t}$, the solution for $\mathbf{D}$ is therefore given by:

$$\mathbf{D}=\begin{bmatrix}\mathbf{I}_{N_t} & -\mathbf{C}_1\mathbf{C}_2^{-1}\\ -\mathbf{H}_2\mathbf{H}_1^{-1} & \mathbf{I}_{N_t}\end{bmatrix} \tag{4.9}$$

Substituting (4.9) into (4.7) we obtain the decoupled signal matrix as given by

$$\mathbf{D}\bullet\begin{bmatrix}\mathbf{r}_1\\ \mathbf{r}_2\end{bmatrix}=\begin{bmatrix}\tilde{\mathbf{r}}_1\\ \tilde{\mathbf{r}}_2\end{bmatrix}=\begin{bmatrix}\mathbf{I}_{N_t} & -\mathbf{C}_1\mathbf{C}_2^{-1}\\ -\mathbf{H}_2\mathbf{H}_1^{-1} & \mathbf{I}_{N_t}\end{bmatrix}\begin{bmatrix}\mathbf{H}_1 & \mathbf{C}_1\\ \mathbf{H}_2 & \mathbf{C}_2\end{bmatrix}\begin{bmatrix}\mathbf{x}_1\\ \mathbf{y}_2\end{bmatrix}=\begin{bmatrix}\tilde{\mathbf{H}} & 0\\ 0 & \tilde{\mathbf{C}}\end{bmatrix}\begin{bmatrix}\mathbf{x}_1\\ \mathbf{y}_2\end{bmatrix}+\begin{bmatrix}\tilde{\mathbf{n}}_1\\ \tilde{\mathbf{n}}_2\end{bmatrix} \tag{4.10}$$

The received equation of the decoupled signals are then given by

$$\begin{aligned}\tilde{\mathbf{r}}_1&=\tilde{\mathbf{H}}\bullet\mathbf{x}_1+\tilde{\mathbf{n}}_1\\ \tilde{\mathbf{r}}_2&=\tilde{\mathbf{C}}\bullet\mathbf{y}_2+\tilde{\mathbf{n}}_2\end{aligned} \tag{4.11}$$

where $\tilde{\mathbf{H}}=\mathbf{H}_1-\mathbf{C}_1\mathbf{C}_2^{-1}\mathbf{H}_2$, $\tilde{\mathbf{C}}=\mathbf{C}_2-\mathbf{H}_2\mathbf{H}_1^{-1}\mathbf{C}_1$, $\tilde{\mathbf{n}}_1=\mathbf{I}_{N_t}\boldsymbol{\eta}_1-\mathbf{C}_1\mathbf{C}_2^{-1}\boldsymbol{\eta}_2$, $\mathbf{x}_1=(x_{11},x_{12})$, $\mathbf{y}_2=(y_{21},y_{22})$ and $\tilde{\mathbf{n}}_2=\mathbf{I}_{N_t}\boldsymbol{\eta}_2-\mathbf{H}_2\mathbf{H}_1^{-1}\boldsymbol{\eta}_1$.

For a desired decoupled user equation e.g. $\tilde{\mathbf{r}}_1=\tilde{\mathbf{H}}\bullet\mathbf{x}_1+\tilde{\mathbf{n}}_1$, the signal-to-noise ratio expression can be obtained by expanding the matrix element of the received signal. The expansion of $\tilde{\mathbf{H}}$ and $\tilde{\mathbf{n}}_1$ are given by

$$\tilde{\mathbf{H}}=\left[\begin{bmatrix} h_{11} & h_{12} \\ -h_{12}^* & h_{11}^* \end{bmatrix}-\begin{bmatrix} c_{11} & c_{12} \\ -c_{12}^* & c_{11}^* \end{bmatrix}\bullet\begin{bmatrix} c_{21} & c_{22} \\ -c_{22}^* & c_{21}^* \end{bmatrix}^{-1}\bullet\begin{bmatrix} h_{21} & h_{22} \\ -h_{22}^* & h_{21}^* \end{bmatrix}\right]$$

$$\tilde{\mathbf{n}}_1=\left[\begin{bmatrix} 1 & 0 \\ 0 & 1 \end{bmatrix}\bullet\begin{bmatrix} \eta_{11} \\ -\eta_{12}^* \end{bmatrix}-\begin{bmatrix} c_{11} & c_{12} \\ -c_{12}^* & c_{11}^* \end{bmatrix}\bullet\begin{bmatrix} c_{21} & c_{22} \\ -c_{22}^* & c_{21}^* \end{bmatrix}^{-1}\begin{bmatrix} \eta_{21} \\ -\eta_{22}^* \end{bmatrix}\right] \quad (4.12)$$

respectively, where h_{ji} is the channel coefficient of user 1 from the i^{th} transmit antenna to the j^{th} receive antenna, c_{ji} is also defined as the channel coefficient of user 2 from the i^{th} transmit antenna to the j^{th} receive antenna and η_{ij} are the noise samples from the i^{th} user to the j^{th} receive antenna and they are zero mean complex Gaussian noise which are independent and identically distributed.

Further expansion of $\tilde{\mathbf{H}}$ in (4.12) is given by

$$\mathbf{C}_1\mathbf{C}_2^{-1}\mathbf{H}_2=\frac{1}{b}\begin{bmatrix} h_{21}\left(c_{11}c_{21}^*+c_{12}c_{22}^*\right)-h_{22}^*\left(c_{12}c_{21}-c_{11}c_{22}\right) & h_{22}\left(c_{11}c_{21}^*+c_{12}c_{22}^*\right)-h_{21}^*\left(c_{12}c_{21}-c_{11}c_{22}\right) \\ h_{21}\left(c_{11}^*c_{22}^*-c_{12}^*c_{21}^*\right)-h_{22}^*\left(c_{22}c_{12}^*-c_{11}^*c_{21}\right) & h_{22}\left(c_{11}^*c_{22}^*-c_{12}^*c_{21}^*\right)+h_{21}^*\left(c_{22}c_{12}^*-c_{11}^*c_{21}\right) \end{bmatrix}$$

$$\mathbf{C}_1\mathbf{C}_2^{-1}\mathbf{H}_2=\begin{bmatrix} R & S \\ -S^* & R^* \end{bmatrix},\ \text{where } b=\left(|c_{21}|^2+|c_{22}|^2\right) \quad (4.13)$$

$$\text{Therefore, } \tilde{\mathbf{H}}=\mathbf{H}_1-\mathbf{C}_1\mathbf{C}_2^{-1}\mathbf{H}_2=\begin{bmatrix} h_{11}-R & h_{12}-S \\ -h_{12}^*+S^* & h_{11}^*-R^* \end{bmatrix}$$

$$=\begin{bmatrix} M & N \\ -N^* & M^* \end{bmatrix}$$

N.B: $\tilde{\mathbf{H}}$ has the same structure as the channel coefficient matrix $\mathbf{H}$ in (4.2).

Further expansion of $\tilde{\mathbf{n}}_1$ in (4.12) is also given by

$$\tilde{\mathbf{n}}_1=\left[\begin{bmatrix} \eta_{11} \\ -\eta_{12}^* \end{bmatrix}-\frac{1}{b}\bullet\begin{bmatrix} c_{11}c_{21}^*+c_{12}c_{22}^* & c_{12}c_{21}-c_{11}c_{22} \\ c_{11}^*c_{22}^*-c_{12}^*c_{21}^* & c_{22}c_{12}^*-c_{11}^*c_{21} \end{bmatrix}\bullet\begin{bmatrix} \eta_{21} \\ -\eta_{22}^* \end{bmatrix}\right]$$

$$\tilde{\mathbf{n}}_1=\left[\begin{bmatrix} \eta_{11} \\ -\eta_{12}^* \end{bmatrix}-\begin{bmatrix} P & Q \\ -Q^* & P^* \end{bmatrix}\bullet\begin{bmatrix} \eta_{21} \\ -\eta_{22}^* \end{bmatrix}\right] \quad (4.14)$$

$$\tilde{\mathbf{n}}_1=\begin{bmatrix} \eta_{11}-P\eta_{21}+Q\eta_{22}^* \\ -\eta_{12}^*+Q^*\eta_{21}+P^*\eta_{22}^* \end{bmatrix}.$$

The receiver equation of the desired decoupled signal can now be written as:

$$\tilde{\mathbf{r}}_1 = \begin{bmatrix} M & N \\ -N^* & M^* \end{bmatrix} \bullet \begin{bmatrix} x_{11} \\ x_{12} \end{bmatrix} + \begin{bmatrix} \eta_{11} - P\eta_{21} + Q\eta_{22}^* \\ -\eta_{12}^* + Q^*\eta_{21} + P^*\eta_{22}^* \end{bmatrix} \tag{4.15}$$

From (4.15) the expression for the signal-to-noise ratio of the decoupled signal can be obtained by multiplying it by the conjugate transpose of $\tilde{\mathbf{H}}$ as shown below;

$$\begin{bmatrix} M^* & -N \\ N^* & M \end{bmatrix} \begin{bmatrix} \tilde{r}_1(t) \\ -\tilde{r}_1^*(t+1) \end{bmatrix} = \begin{bmatrix} M^* & -N \\ N^* & M \end{bmatrix} \bullet \begin{bmatrix} M & N \\ -N^* & M^* \end{bmatrix} \bullet \begin{bmatrix} x_{11} \\ x_{12} \end{bmatrix} + \begin{bmatrix} M^* & -N \\ N^* & M \end{bmatrix} \bullet \begin{bmatrix} \eta_{11} - P\eta_{21} + Q\eta_{22}^* \\ -\eta_{12}^* + Q^*\eta_{21} + P^*\eta_{22}^* \end{bmatrix}. \tag{4.16}$$

Applying the same procedure that was used in (4.3) to calculate the SNR to (4.16), we obtain

$$\text{SNR} = \frac{\left(|M|^2 + |N|^2\right) E_s}{2\sigma^2 \left(1 + |P|^2 + |Q|^2\right)}. \tag{4.17}$$

Further expansion of (4.17) can be obtained to give the expression in (4.18). Details of the expansion of (4.16) to get (4.17) and subsequently (4.18) are shown in Appendix 1.

$$\text{SNR} = \frac{\left(|h_{11}|^2 + |h_{12}|^2\right) E_s}{2\sigma^2} \tag{4.18}$$

The expression of the SNR in (4.18) compared with (4.3) shows that there will be no SNR penalty for a standalone space-time block coding scheme in a multiuser environment when zero-forcing interference cancellation is used to decoupled the two co-channel users.

Since the SNR is the same as if one user was transmitting (with 2 antennas) and the receiver is equipped with one antenna, it can be concluded that the diversity order is the same as that of Alamouti code [3]. Effectively this shows that it is possible to double the capacity (in terms of the number of users) by applying a Zero-forcing

interference cancellation at the receiver without sacrificing space-time diversity gain while the only penalty incurred will be an additional antenna at the receiver side.

4.4 HR-STTCM in a Multiuser Environment

The construction of HR-STTCM in [4] was based on the concatenation of an outer trellis coded modulation (TCM) code with an inner space-time block coding scheme. The idea used in the construction of TCM which was signal set expansion and set partitioning, was used in the construction of HR-STTCM. The Alamouti code in [3] was used as the building block for the HR-STTCM construction and diagonal matrix multiplication was done on the building block to generate other space-time block codes. For the sake of repetition, the following constraints were placed on the single user design of the HR-STTCM to make sure the frame error rate performance of the scheme performs better that the standalone space-time block coding schemes

- Signal orthogonality; this means that the signals transmitted from each antenna must be orthogonal to each other. This constraint is employed to lower the decoding complexity.
- Signal matrix has unequal eigenvalue. This corresponds to the coding gain advantage observed in the performance of HR-STTCM.
- Transitions leaving from (or merging to) each state in the trellis are uniquely labeled with codewords from a full rank block code. This constraint allows the HR-STTCM construction to achieve full diversity.

The construction of the HR-STTCM can be extended to a multiuser environment and Zero-forcing solution applied at the receiver, as enumerated above in the standalone space-time block code scheme, to decouple the space-time user signals.

4.4.1 System Model

Here also a multiuser environment with K synchronous co-channel users where each user is equipped with N_t (= 2; full rate complex design) transmit antennas and each

uses HR-STTCM encoder will be considered. We limit the signal set from each user to element from the matrices **A** and **B** given by

$$\mathbf{A}=\begin{bmatrix} x_1 & x_2 \\ -x_2^* & x_1^* \end{bmatrix},$$
$$\mathbf{B}=\mathbf{A}\bullet\mathrm{diag}[1,-1]=\begin{bmatrix} x_1 & -x_2 \\ -x_2^* & -x_1^* \end{bmatrix}. \tag{4.19}$$

At the receiver of a desired user, there will be $K\times N_t$ interfering signal and an interference suppression technique can be used to suppress signals from the $K-1$ co-channel space-time user and achieve the desired diversity order which is N_t. The Figure 4.2 below illustrates the schematic diagram of the HR-STTCM in a multiuser environment. The channel coefficients are assumed to undergo quasi-static and flat Rayleigh fading.

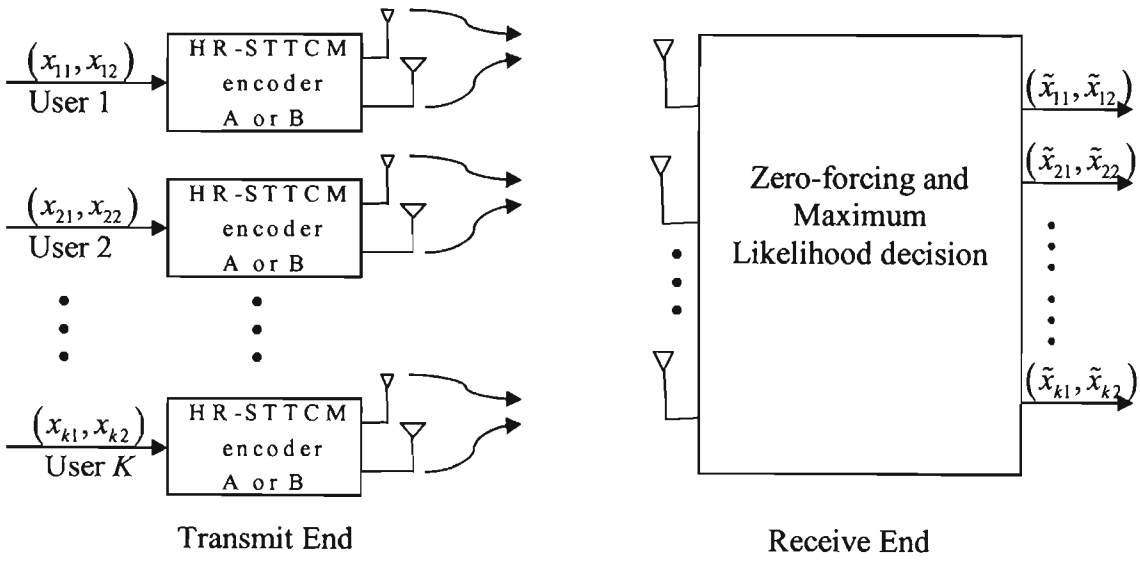

Figure 4.2: Multiuser transmission system with HR-STTCM

For our analysis a 2-user case with each user using an HR-STTCM encoder will be considered. For the 2-user scenario, there are four possible combinations of transmitted data;

- Case 1: User 1 transmits using **A** and user 2 transmits using **A**
- Case 2: User 1 transmits using **A** and user 2 transmits using **B**
- Case 3: User 1 transmits using **B** and user 2 transmits using **A**
- Case 4: User 1 transmits using **B** and user 2 transmits using **B**

Case 1: This has been discussed in the previous section. Since both users transmit using Alamouti matrix.

Case 2: The received signal from the first antenna and the second antenna can be expressed using the equation model in (4.5) to give (4.20) where $\mathbf{G}_1=(g_{11},g_{12})$ and $\mathbf{G}_2=(g_{21},g_{22})$ are the channel coefficient matrix of the second user for receive antenna $1\left(=r_1(t),-\tilde{r}_1^*(t+1)\right)$ and receive antenna 2 $\left(=r_2(t),-\tilde{r}_2^*(t+1)\right)$ respectively. $\mathbf{H}_1=(h_{11},h_{12})$ and $\mathbf{H}_2=(h_{21},h_{22})$ are the channel coefficient matrix of user 1 for receive antenna 1 and receive antenna 2 respectively.

$$
\begin{aligned}
r_1(t) &= x_{11}h_{11}+x_{12}h_{12}+x_{21}g_{11}-x_{22}g_{12}+\eta_{11}(t)\\
-r_1^*(t+1) &= -x_{11}h_{12}^*+x_{12}h_{11}^*+x_{21}g_{12}^*+x_{22}g_{11}^*-\eta_{12}^*(t+1)\\
r_2(t) &= x_{11}h_{21}+x_{12}h_{22}+x_{21}g_{21}-x_{22}g_{22}+\eta_{21}(t)\\
-r_2^*(t+1) &= -x_{11}h_{22}^*+x_{12}h_{21}^*+x_{21}g_{22}^*+x_{22}g_{21}^*-\eta_{22}^*(t+1)
\end{aligned}
$$

$$
\begin{bmatrix} r_1(t)\\ -r_1^*(t+1)\\ \hline r_2(t)\\ -r_2^*(t+1)\end{bmatrix}=\left[\begin{array}{cccc} h_{11} & h_{12} & g_{11} & -g_{12}\\ -h_{12}^* & h_{11}^* & g_{12}^* & g_{11}^*\\ \hline h_{21} & h_{22} & g_{21} & -g_{22}\\ -h_{22}^* & h_{21}^* & g_{22}^* & g_{21}^*\end{array}\right]\cdot\begin{bmatrix} x_{11}\\ x_{12}\\ \hline x_{21}\\ x_{22}\end{bmatrix}+\begin{bmatrix} \eta_{11}(t)\\ -\eta_{12}^*(t+1)\\ \hline \eta_{21}(t)\\ -\eta_{22}^*(t+1)\end{bmatrix} \tag{4.20}
$$

$$
\begin{bmatrix}\mathbf{r}_1\\ \mathbf{r}_2\end{bmatrix}=\begin{bmatrix}\mathbf{H}_1 & \mathbf{G}_1\\ \mathbf{H}_2 & \mathbf{G}_2\end{bmatrix}\cdot\begin{bmatrix}\mathbf{x}_1\\ \mathbf{x}_2\end{bmatrix}+\begin{bmatrix}\mathbf{n}_1\\ \mathbf{n}_2\end{bmatrix}
$$

Note that the structure of matrix element of $\mathbf{G}_1$ and $\mathbf{G}_2$ is not the same as the channel coefficient matrix element of $\mathbf{H}_1$ and $\mathbf{H}_2$.

Case 3: Using the approach used in (4.20) we can obtain the receiver equation as shown in (4.21) below.

$$r_1(t) = x_{11}h_{11} - x_{12}h_{12} + x_{21}g_{11} + x_{22}g_{12} + \eta_{11}(t)$$

$$-r_1^*(t+1) = x_{11}h_{12}^* + x_{12}h_{11}^* - x_{21}g_{12}^* + x_{22}g_{11}^* - \eta_{12}^*(t+1)$$

$$r_2(t) = x_{11}h_{21} - x_{12}h_{22} + x_{21}g_{21} + x_{22}g_{22} + \eta_{21}(t)$$

$$-r_2^*(t+1) = x_{11}h_{22}^* + x_{12}h_{21}^* - x_{21}g_{22}^* + x_{22}g_{21}^* - \eta_{22}^*(t+1)$$

$$\begin{bmatrix} r_1(t) \\ -r_1^*(t+1) \\ r_2(t) \\ -r_2^*(t+1) \end{bmatrix} = \begin{bmatrix} h_{11} & -h_{12} & g_{11} & g_{12} \\ h_{12}^* & h_{11}^* & -g_{12}^* & g_{11}^* \\ h_{21} & -h_{22} & g_{21} & g_{22} \\ h_{22}^* & h_{21}^* & -g_{22}^* & g_{21}^* \end{bmatrix} \cdot \begin{bmatrix} x_{11} \\ x_{12} \\ x_{21} \\ x_{22} \end{bmatrix} + \begin{bmatrix} \eta_{11}(t) \\ -\eta_{12}^*(t+1) \\ n_{21}(t) \\ -\eta_{22}^*(t+1) \end{bmatrix} \tag{4.21}$$

$$\begin{bmatrix} \mathbf{r}_1 \\ \mathbf{r}_2 \end{bmatrix} = \begin{bmatrix} \mathbf{H}_1 & \mathbf{G}_1 \\ \mathbf{H}_2 & \mathbf{G}_2 \end{bmatrix} \cdot \begin{bmatrix} \mathbf{x}_1 \\ \mathbf{x}_2 \end{bmatrix} + \begin{bmatrix} \mathbf{n}_1 \\ \mathbf{n}_2 \end{bmatrix}$$

Note also that the structure of matrix element of $\mathbf{G}_1$ and $\mathbf{G}_2$ is not the same as the channel coefficient matrix element of $\mathbf{H}_1$ and $\mathbf{H}_2$.

Case 4: Using the same approach as enumerated above, the receiver equation is shown in (4.22) as

$$r_1(t) = x_{11}h_{11} - x_{12}h_{12} + x_{21}g_{11} - x_{22}g_{12} + \eta_{11}(t)$$

$$-r_1^*(t+1) = x_{11}h_{12}^* + x_{12}h_{11}^* + x_{21}g_{12}^* + x_{22}g_{11}^* - \eta_{12}^*(t+1)$$

$$r_2(t) = x_{11}h_{21} - x_{12}h_{22} + x_{21}g_{21} - x_{22}g_{22} + \eta_{21}(t)$$

$$-r_2^*(t+1) = x_{11}h_{22}^* + x_{12}h_{21}^* + x_{21}g_{22}^* + x_{22}g_{21}^* - \eta_{22}^*(t+1)$$

$$\begin{bmatrix} r_1(t) \\ -r_1^*(t+1) \\ r_2(t) \\ -r_2^*(t+1) \end{bmatrix} = \begin{bmatrix} h_{11} & -h_{12} & g_{11} & -g_{12} \\ h_{12}^* & h_{11}^* & g_{12}^* & g_{11}^* \\ h_{21} & -h_{22} & g_{21} & -g_{22} \\ h_{22}^* & h_{21}^* & g_{22}^* & g_{21}^* \end{bmatrix} \cdot \begin{bmatrix} x_{11} \\ x_{12} \\ x_{21} \\ x_{22} \end{bmatrix} + \begin{bmatrix} \eta_{11}(t) \\ -\eta_{12}^*(t+1) \\ \eta_{21}(t) \\ -\eta_{22}^*(t+1) \end{bmatrix} \tag{4.22}$$

$$\begin{bmatrix} \mathbf{r}_1 \\ \mathbf{r}_2 \end{bmatrix} = \begin{bmatrix} \mathbf{H}_1 & \mathbf{G}_1 \\ \mathbf{H}_2 & \mathbf{G}_2 \end{bmatrix} \cdot \begin{bmatrix} \mathbf{x}_1 \\ \mathbf{x}_2 \end{bmatrix} + \begin{bmatrix} \mathbf{n}_1 \\ \mathbf{n}_2 \end{bmatrix}$$

Note also that the structure of matrix element of $\mathbf{G}_1$ and $\mathbf{G}_2$ is the same as the channel coefficient matrix element of $\mathbf{H}_1$ and $\mathbf{H}_2$ but different from the structure of $\mathbf{H}$ in (4.2).

It is noted that although, the structure of the channel coefficients matrix obtained as a result of using the expanded Alamouti code matrix i.e. **B** differs from the one obtained in (4.2), the channel coefficient matrix are still orthogonal to each other i.e.

$$\begin{bmatrix} g_1 & -g_2 \\ g_2^* & g_1^* \end{bmatrix} \times \left(\begin{bmatrix} g_1 & -g_2 \\ g_2^* & g_1^* \end{bmatrix} \right)^H = (|g_1|^2 + |g_2|^2)\mathbf{I}_2, \tag{4.23}$$

where $(\bullet)^H$ represents the conjugate transpose of the matrix element and $\mathbf{I}_2$ is a 2×2 identity matrix.

4.5 Decoder Structure for a 4-PSK 2-User Scheme

Here it is assumed that the channel state information is perfectly known at the receiver and the optimum Maximum Likelihood decoding rule can be applied to the decoupled signals in (4.11) as shown below:

$$\begin{aligned} \tilde{\mathbf{x}}_1 &= \arg \min_{\mathbf{x}_1 \in \Re} \left\| \tilde{\mathbf{r}}_1 - \tilde{\mathbf{H}}\mathbf{x}_1 \right\|^2, \\ \tilde{\mathbf{y}}_2 &= \arg \min_{\mathbf{y}_2 \in \Re} \left\| \tilde{\mathbf{r}}_2 - \tilde{\mathbf{C}}\mathbf{y}_2 \right\|^2. \end{aligned} \tag{4.24}$$

The decoder structure for, a 2-state per user and a 4-state per user, 2-User HR-STTCM scheme will be considered. Equivalent trellises of the super trellises are drawn for the two examples, i.e. 2-state per user and 4-state per user. The equivalent trellises are drawn based on the fact that some of the branch metrics for the super trellises are equal.

4.5.1 Decoder of a 2-State HR-STTCM Scheme

At the receiver of the HR-STTCM scheme, we can apply Zero-forcing solution to decouple the two space-time user signals using the approach enumerated above for the standalone space-time block coding scheme. The Zero-forcing solution is applied on the super trellis structure obtained by combining the two users as shown in Figure 4.3 using the look-up table, i.e. Table 4.1.

In the Figure 4.3 and the look-up table 4.1 $A_{i\,(i=0or1)}$ and $B_{j\,(j=0or1)}$ represent the transmitted space-time block code as shown in (4.20) and the subscript represent the partition in which the transmitted symbols belong as explained in chapter 3 (Section 3.2).

Assuming that the channel conditions are known at the receiver, the branch metric of the trellis shown in Figure 4.3 can be calculated using the ML argument in (4.24). The branch metric calculation $\arg\min_{\mathbf{x}_0\in\Re_0}\left\|\tilde{\mathbf{r}}_{1A}-\tilde{\mathbf{H}}_{1A}\mathbf{x}_0\right\|^2$ is used when A_0A_0 and A_0A_1 are given as outputs. The same applies for the following branch metric calculations:

$\arg\min_{\mathbf{x}_1\in\Re_1}\left\|\tilde{\mathbf{r}}_{1A}-\tilde{\mathbf{H}}_{1A}\mathbf{x}_1\right\|^2$ when A_1A_0 and A_1A_1 are outputs,

$\arg\min_{\mathbf{x}_1\in\Re_1}\left\|\tilde{\mathbf{r}}_{1B}-\tilde{\mathbf{H}}_{1B}\mathbf{x}_1\right\|^2$ when A_1B_0 and A_1B_1 are outputs,

$\arg\min_{\mathbf{x}_0\in\Re_0}\left\|\tilde{\mathbf{r}}_{1B}-\tilde{\mathbf{H}}_{1B}\mathbf{x}_0\right\|^2$ when A_0B_0 and A_0B_1 are outputs,

$\arg\min_{\mathbf{x}_1\in\Re_1}\left\|\tilde{\mathbf{r}}_{1A}-\tilde{\mathbf{H}}_{2A}\mathbf{x}_1\right\|^2$ when B_1A_0 and B_1A_1 are outputs,

$\arg\min_{\mathbf{x}_0\in\Re_0}\left\|\tilde{\mathbf{r}}_{1A}-\tilde{\mathbf{H}}_{2A}\mathbf{x}_0\right\|^2$ when B_0A_0 and B_0A_1 are outputs,

$\arg\min_{\mathbf{x}_1\in\Re_1}\left\|\tilde{\mathbf{r}}_{1B}-\tilde{\mathbf{H}}_{2B}\mathbf{x}_1\right\|^2$ when B_1B_0 and B_1B_1 are outputs,

and for $\arg\min_{\mathbf{x}_0\in\Re_0}\left\|\tilde{\mathbf{r}}_{1B}-\tilde{\mathbf{H}}_{2B}\mathbf{x}_0\right\|^2$ when B_0B_0 and B_0B_1 are outputs.

Looking at the 4-state super trellis carefully, we can draw an equivalent 2-state trellis using the branch metric. Since each of the branches (each branch contains 8 parallel transitions) in the 4-state super trellis has one other branch that uses the same branch metric with it, an equivalent 2-state trellis can be drawn with 32 incoming or outgoing transitions per state. The 32 incoming or outgoing transitions are divided into two 16 parallel decoding branches. The equivalent 2-state trellis is given in Figure 4.4. In the equivalent trellises $m\{X_iY_j\}$ is defined as the branch metric when user 1 transmit using X_i block code and user 2 transmits using Y_j.

The parameters used in the branch metric calculation are defined in (4.25). Once the branch metrics are computed, the Viterbi Algorithm [10] is applied to search for the path with the least accumulated metric.

Table 4-1: Look- up Table for the Super Trellis of the 2-State per User 4-PSK HR-STTCM Scheme

Present State		Input		Next State		Output
User1	User2	User1	User2	User1	User2	
0	0	A_0	A_0	0	0	$A_0 A_0$
0	0	A_1	A_0	1	0	$A_1 A_0$
0	0	A_0	A_1	0	1	$A_0 A_1$
0	0	A_1	A_1	1	1	$A_1 A_1$
0	1	A_0	B_0	0	1	$A_0 B_0$
0	1	A_0	B_1	0	0	$A_0 B_1$
0	1	A_1	B_0	1	1	$A_1 B_0$
0	1	A_1	B_1	1	0	$A_1 B_1$
1	0	B_0	A_0	1	0	$B_0 A_0$
1	0	B_0	A_1	1	1	$B_0 A_1$
1	0	B_1	A_0	0	0	$B_1 A_0$
1	0	B_1	A_1	0	1	$B_1 A_1$
1	1	B_0	B_0	1	1	$B_0 B_0$
1	1	B_0	B_1	1	0	$B_0 B_1$
1	1	B_1	B_0	0	1	$B_1 B_0$
1	1	B_1	B_1	0	0	$B_1 B_1$

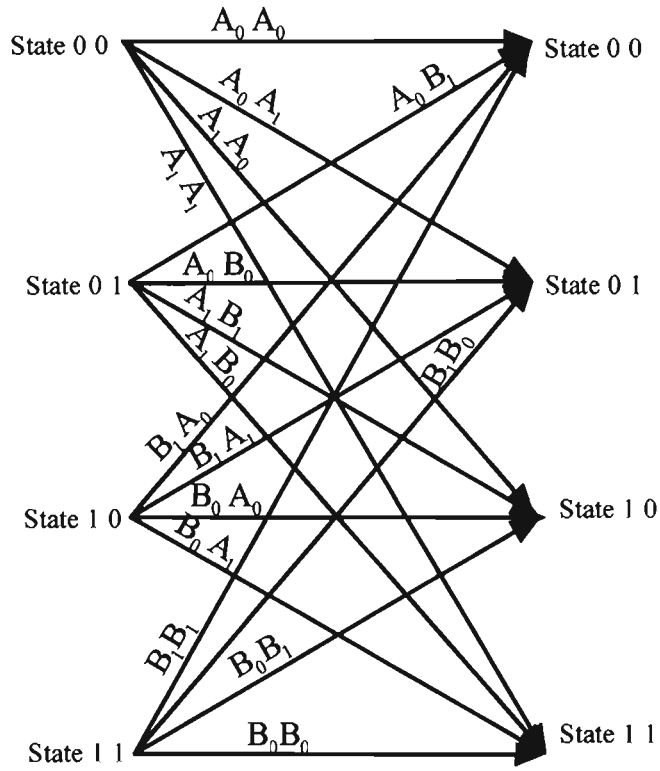

Figure 4.3: Super Trellis for a 2-State per User HR-STTCM 2-User Scheme.

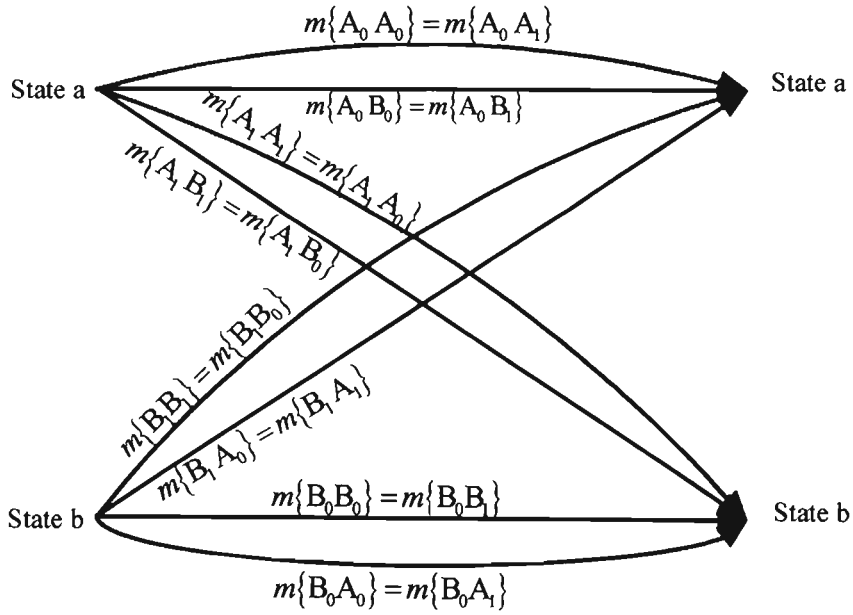

Figure 4.4: Equivalent trellis 2-State HR-STTCM 2-User Scheme

$$\tilde{\mathbf{H}}_{1A} = \mathbf{H}_{1A} - \mathbf{G}_{1A}\mathbf{G}_{2A}^{-1}\mathbf{H}_{2A} \qquad \tilde{\mathbf{H}}_{1B} = \mathbf{H}_{1A} - \mathbf{G}_{1B}\mathbf{G}_{2B}^{-1}\mathbf{H}_{2A}$$

$$\tilde{\mathbf{H}}_{2A} = \mathbf{H}_{1B} - \mathbf{G}_{1A}\mathbf{G}_{2A}^{-1}\mathbf{H}_{2B} \qquad \tilde{\mathbf{H}}_{2B} = \mathbf{H}_{1B} - \mathbf{G}_{1B}\mathbf{G}_{2B}^{-1}\mathbf{H}_{2B}$$

$$\tilde{\mathbf{r}}_{1A} = \mathbf{r}_1 - \mathbf{G}_{1A}\mathbf{G}_{2A}^{-1}\mathbf{r}_2 \qquad \tilde{\mathbf{r}}_{1B} = \mathbf{r}_1 - \mathbf{G}_{1B}\mathbf{G}_{2B}^{-1}\mathbf{r}_2$$

$$\Re_0 = \{(\pm 1, \pm 1), (\pm j, \pm j)\} \qquad \Re_1 = \{(\pm 1, \pm j), (\pm j, \pm 1)\}$$

$$\mathbf{H}_{1A} = \begin{bmatrix} h_{11} & h_{12} \\ -h_{12}^* & h_{11}^* \end{bmatrix} \quad \mathbf{H}_{1B} = \begin{bmatrix} h_{11} & -h_{12} \\ h_{12}^* & h_{11}^* \end{bmatrix} \quad \mathbf{G}_{1A} = \begin{bmatrix} g_{11} & g_{12} \\ -g_{12}^* & g_{11}^* \end{bmatrix} \tag{4.25}$$

$$\mathbf{G}_{1B} = \begin{bmatrix} g_{11} & -g_{12} \\ g_{12}^* & g_{11}^* \end{bmatrix} \quad \mathbf{H}_{2A} = \begin{bmatrix} h_{21} & h_{22} \\ -h_{22}^* & h_{21}^* \end{bmatrix} \quad \mathbf{H}_{2B} = \begin{bmatrix} h_{21} & -h_{22} \\ h_{22}^* & h_{21}^* \end{bmatrix}$$

$$\mathbf{G}_{2A} = \begin{bmatrix} g_{21} & g_{22} \\ -g_{22}^* & g_{21}^* \end{bmatrix} \quad \mathbf{G}_{2B} = \begin{bmatrix} g_{21} & -g_{22} \\ g_{22}^* & g_{21}^* \end{bmatrix}$$

4.5.2 Decoder of a 4-State per user HR-STTCM 2-User Scheme

For a 4-State per user scheme, the look-up table is shown in Table 4.2. The super trellis for the decoder of this scheme will contain a 16-state trellis which is computationally complex and therefore necessitates drawing an equivalent trellis.

Using the approach shown for the 2-state per user scheme, a 4-state equivalent trellis can be drawn as show in Figure 4.5.

Table 4-2: Look- up Table for the Super Trellis of the 4-State per User 4-PSK HR-STTCM Scheme

Present State		Input		Next State		Output
User1	User2	User1	User2	User1	User2	
0	0	A_0	A_0	0	0	$A_0 A_0$
0	0	A_0	A_1	0	1	$A_0 A_1$
0	0	A_1	A_0	1	0	$A_1 A_0$
0	0	A_1	A_1	1	1	$A_1 A_1$
0	1	A_0	B_0	0	3	$A_0 B_0$
0	1	A_1	B_0	1	3	$A_1 B_0$
0	1	A_0	B_1	0	2	$A_0 B_1$

0	1	A_1	B_1	1	2	$A_1 B_1$
0	2	A_0	A_0	0	1	$A_0 A_0$
0	2	A_0	A_1	0	0	$A_0 A_1$
0	2	A_1	A_0	1	1	$A_1 A_0$
0	2	A_1	A_1	1	0	$A_1 A_1$
0	3	A_0	B_0	0	2	$A_0 B_0$
0	3	A_1	B_1	1	2	$A_1 B_0$
0	3	A_0	B_1	0	3	$A_0 B_1$
0	3	A_1	B_1	1	3	$A_1 B_1$
1	0	B_1	A_0	2	0	$B_1 A_0$
1	0	B_1	A_1	2	1	$B_1 A_1$
1	0	B_0	A_0	3	0	$B_0 A_0$
1	0	B_0	A_1	3	1	$B_0 A_1$
1	1	B_0	B_0	3	3	B_0B_0
1	1	B_0	B_1	3	2	B_0B_1
1	1	B_1	B_0	2	3	B_1B_0
1	1	B_1	B_1	2	2	B_1B_1
1	2	B_1	A_0	2	1	$B_1 A_0$
1	2	B_1	A_1	2	0	$B_1 A_0$
1	2	B_0	A_0	3	1	$B_1 A_1$
1	2	B_0	A_1	3	0	B_0A_1
1	3	B_0	B_0	3	2	B_0B_0
1	3	B_0	B_1	3	3	B_0B_1
1	3	B_1	B_0	2	2	B_1B_0
1	3	B_1	B_1	2	3	B_1B_1
2	0	A_0	A_0	1	0	$A_0 A_0$

2	0	A_0	A_1	1	1	$A_0 A_1$
2	0	A_1	A_0	0	0	$A_1 A_0$
2	0	A_1	A_1	0	1	$A_1 A_1$
2	1	A_0	B_0	1	3	$A_0 B_0$
2	1	A_1	B_0	0	3	$A_1 B_0$
2	1	A_0	B_1	1	2	$A_0 B_1$
2	1	A_1	B_1	0	2	$A_1 B_1$
2	2	A_0	A_0	1	1	$A_0 A_0$
2	2	A_0	A_1	1	0	$A_0 A_1$
2	2	A_1	A_0	0	1	$A_1 A_0$
2	2	A_1	A_1	0	0	$A_1 A_1$
2	3	A_0	B_0	1	2	$A_0 B_0$
2	3	A_1	B_0	0	2	$A_1 B_0$
2	3	A_0	B_1	1	3	$A_0 B_1$
2	3	A_1	B_1	0	3	$A_1 B_1$
3	0	B_1	A_0	3	0	$B_1 A_0$
3	0	B_1	A_1	3	1	$B_1 A_1$
3	0	B_0	A_0	2	0	$B_0 A_0$
3	0	B_0	A_1	2	1	$B_0 A_1$
3	1	B_0	B_0	2	3	B_0B_0
3	1	B_0	B_1	2	3	B_0B_1
3	1	B_1	B_0	3	3	B_1B_0
3	1	B_1	B_1	3	2	B_1B_1
3	2	B_1	A_0	3	1	$B_1 A_0$
3	2	B_1	A_1	3	0	$B_1 A_1$
3	2	B_0	A_0	2	1	$B_0 A_0$

3	2	B_0	A_1	2	0	$B_0 A_1$
3	3	B_0	B_0	2	2	B_0B_0
3	3	B_0	B_1	2	3	B_0B_1
3	3	B_1	B_0	3	2	B_1B_0
3	3	B_1	B_1	3	3	B_1B_1

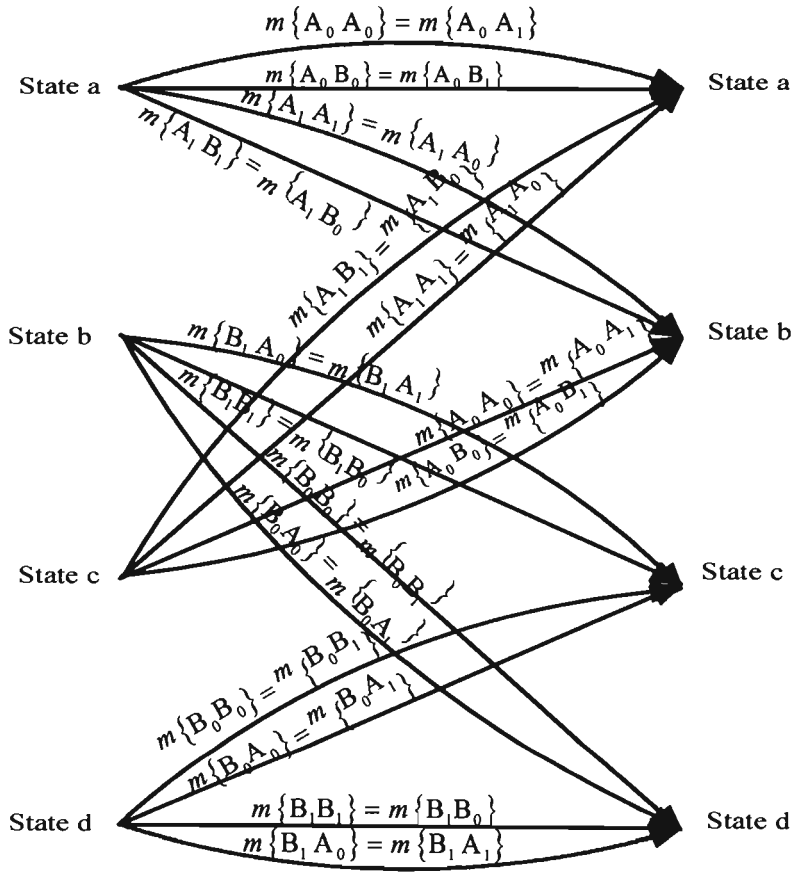

Figure 4.5: Equivalent 4-State HR-STTCM 2-User Scheme

The parameters used in the branch metric calculation are also defined in (4.25). Once the branch metrics are computed, the Viterbi Algorithm [10] is applied to search for the path with the least accumulated metric.

4.6 Simulation Result and Discussion

Monte Carlo simulation results are provided in this section to demonstrate the performance of the standalone space-time block code and the 2-user HR-STTCM schemes for both single user and a 2-user scenario.

QPSK modulation is used throughout the simulation and each of the frames transmitted per user consists of 256 bits. The channel between the transmit and the receive antennas are assumed to undergo quasi-static and flat Rayleigh fading for the simulations. Figure 4.6 and Figure 4.7 show the performance of a 2-state and a 4-State HR-STTCM in both single and 2-user environment respectively.

In the signal-to-noise ratio calculation in (4.18) it is concluded that there is no signal-to-noise ratio penalty when Zero-forcing solution is used to decouple two users with each user employing a space-time block code scheme. In observation of the simulation result of both the 2-state and 4-state HR-STTCM scheme in a two user scenario about 2dB performance degradation in the frame error rate of such scheme is observed.

To justify the simulation results i.e. Figure 4.6 and Figure 4.7, the single user and 2-user trellis is used as given in Figure 4.8.

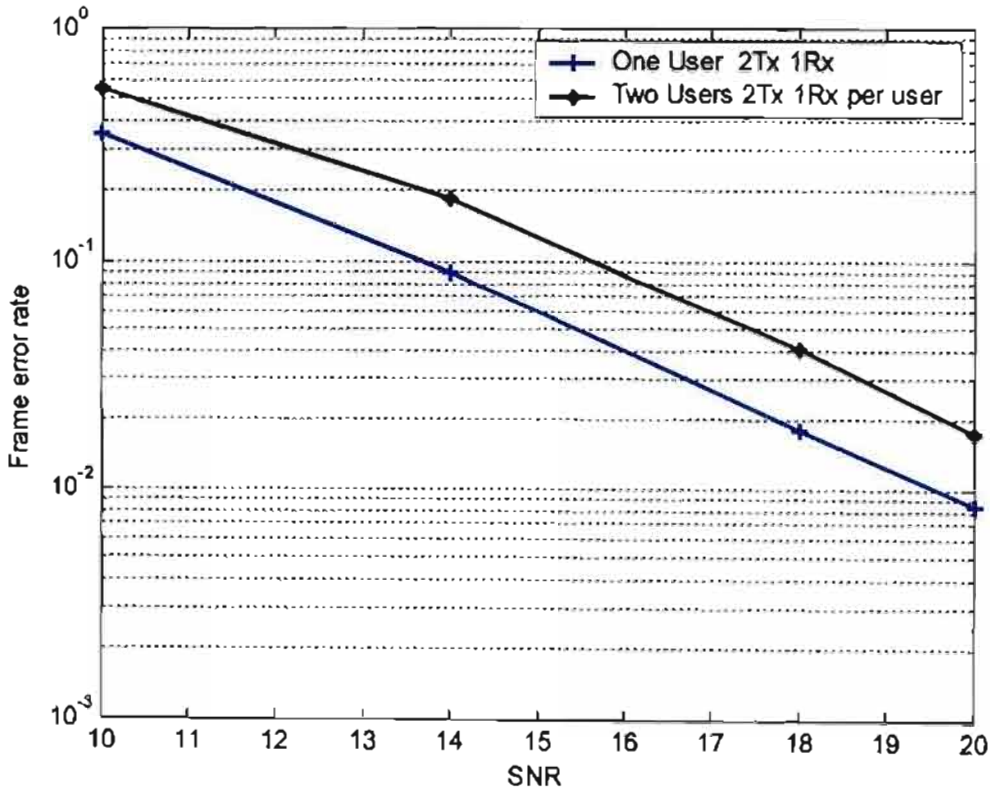

Figure 4.6: Performance of 2-State HR-STTCM in single and 2-User Environment

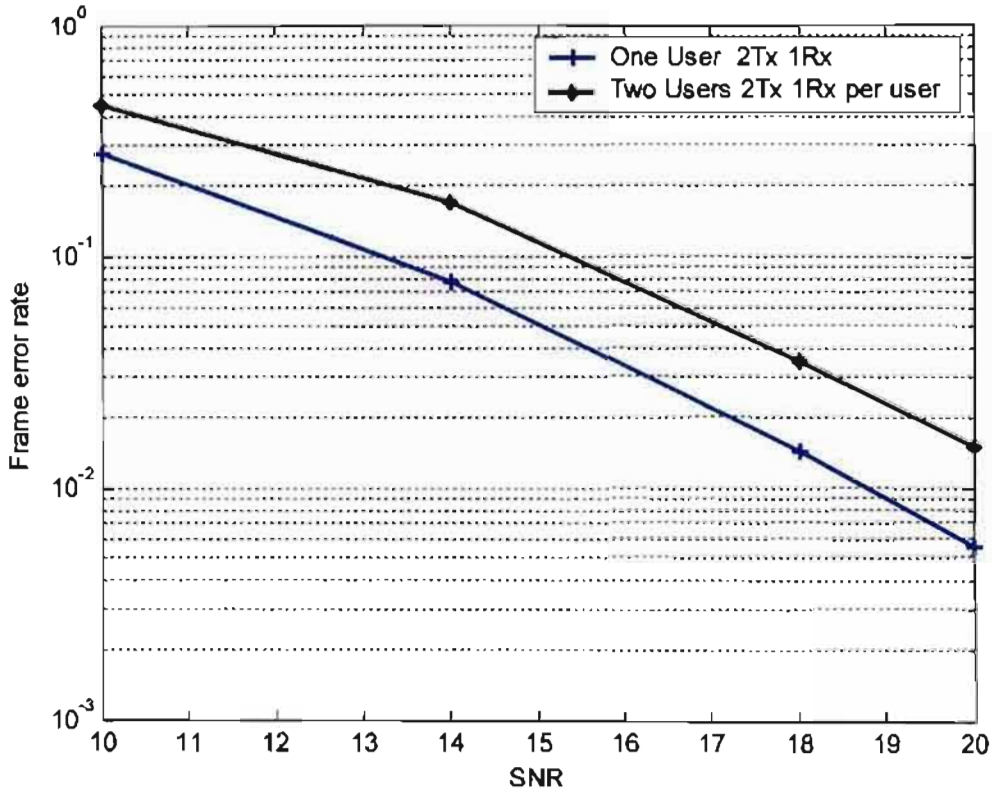

Figure 4.7: Performance of 4-State HR-STTCM in single and 2-User Environment

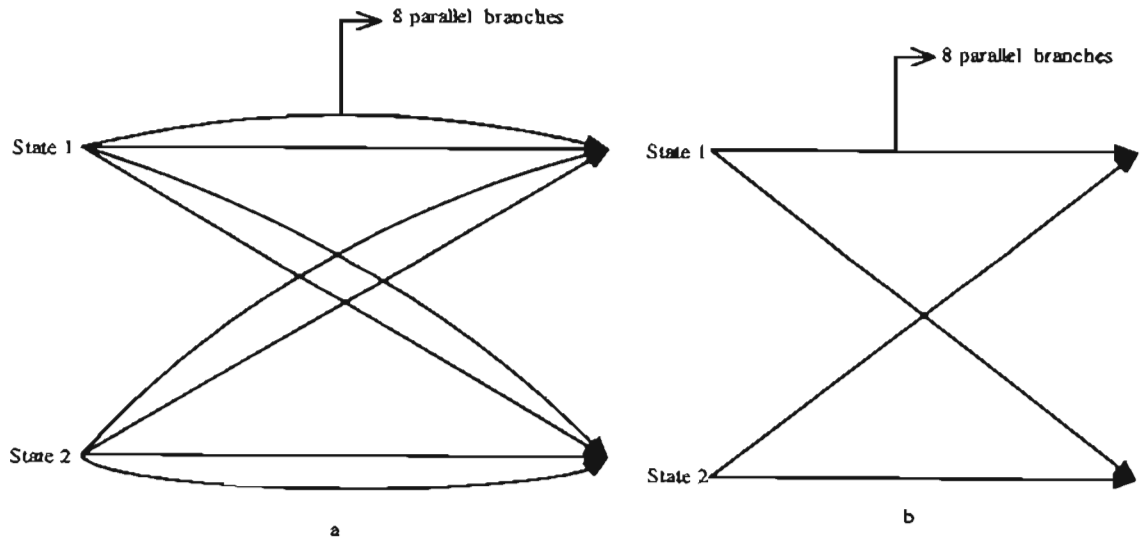

Figure 4.8: a) Trellis of 2-State 2 User HR-STTCM Scheme b) Trellis of a 2-State HR-STTCM Single User

In Figure 4.8(a), the decoding trellis of the 2-State 2-User HR-STTCM scheme consists of 32 outgoing and incoming transitions per state and if we assume that all the

transition per branch are equally likely to be decoded, the probability of decoding correctly a transmitted codeword per state and at a decoding interval equals $1/16 \times 1/16 = 1/256$. The probability for decoding a transmitted codeword in the single user trellis is $1/8 \times 1/8 = 1/64$. Comparing these two values, it can be concluded that since a lower probability value is obtained for the 2-user trellis as compared with the single user trellis, the probability of decoding correctly is reduced in the 2-user case and this account for the performance loss obtained in the simulation result. The same explanation goes for a 4-state HR-STTCM scheme.

In Figure 4.9, the two schemes i.e. 2-state and 4-state HR-STTCM, with a standalone STBC are combined. Unlike HR-STTCM schemes, there is no performance lost between a single user and for STBC schemes.

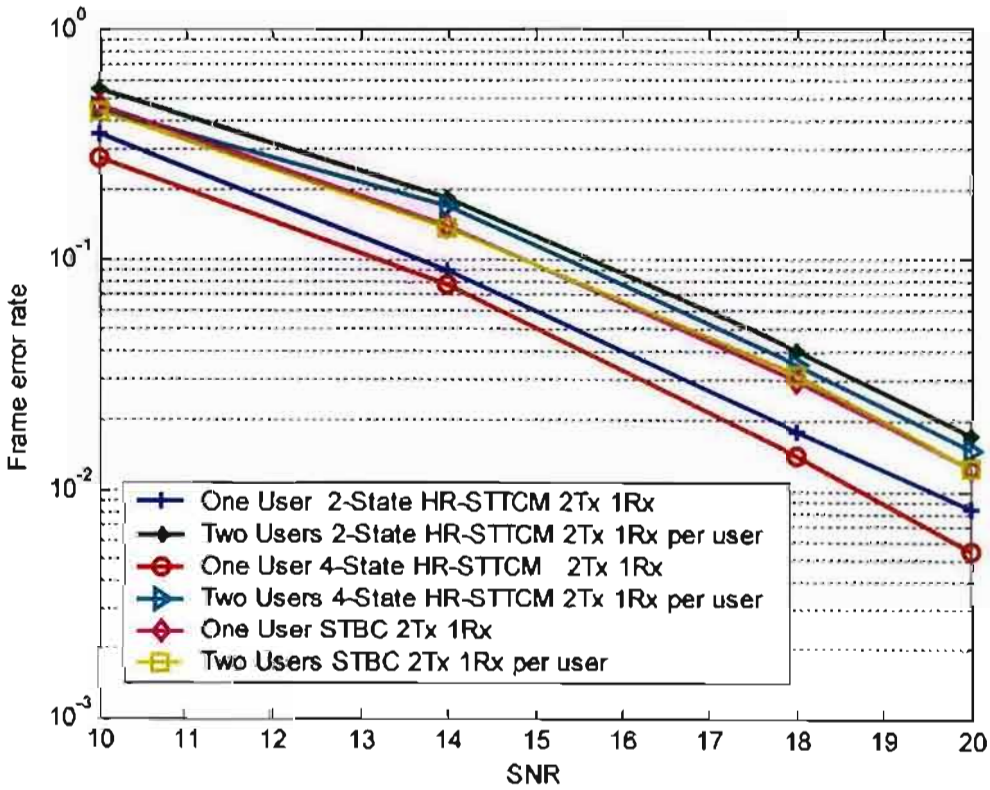

Figure 4.9: Performance of HR-STTCM Schemes and STBC in Single and 2-User Environments

4.7 Summary

In this chapter, by calculating the signal-to-noise ratio for a standalone space-time block code, the performance of the code in a multiuser environment was enumerated.

The Zero-forcing interference cancellation exploits the orthogonality of such code in decoupling signals from different users at the receiver before applying a maximum likelihood decoder. The same idea was applied in decoupling users of high rate-space-time trellis coded modulation schemes.

It was explained from analytical point of view the simulation results that it is not possible to obtain a single user performance for a decoupled HR-STTCM scheme unlike what is obtained for a standalone space-time block code.

CHAPTER 5

PERFORMANCE ANALYSIS OF HIGH RATE SPACE-TIME TRELLIS CODED MODULATION

5.1 Introduction

In [4] High Rate Space-time Trellis Coded Modulation (HR-STTCM) design was introduced as a space-time coding scheme that has higher coding advantage when compared with the earlier design of space-time trellis coded modulation [7], [12] and [14]. The main advantage of the construction in [4] is that the standard technique for designing good trellis coded modulation codes [11], such as the classic set partitioning concept, can be adopted to realize the high rate space-time coded modulation design with large coding gain.

A parameterized class of space-time code, called super orthogonal space-time trellis code (SOSTTC), was later introduced in [21]. SOSTTC gives a systematic approach in the design of high rate space-time trellis coded modulation codes. SOSTTC not only provides a scheme that is an improvement in the coding gain when compared with the original space-time trellis coded modulations, but it also answers the question of a systematic design for any rate, number of states and the maximization of coding gain. The matrix expansion in HR-STTCM, i.e. [4] corresponds to the angle multiplication in the SOSTTC. This means that the identity matrix multiplication with

the original Alamouti code [3] corresponds to the angular multiplication in the SOSTTC.

For example, the multiplication of $diag[1,-1]$ with the Alamouti code in [4] corresponds to $\theta = \pi$ in the orthogonal transmission matrix of the SOSTTC shown in (5.1) below. When $\theta = 0$, (5.1) becomes the Alamouti code in [3]. For an M-PSK modulation with constellation signal represented by $e^{j\frac{2\pi a}{M}}$, $a = 0,1,\cdots M-1$, one can pick $\theta = 2\pi a^{'} / M$, where $a^{'} = 0,1,\cdots M-1$.

$$A(x_1, x_2, \theta) = \begin{pmatrix} x_1 e^{j\theta} & x_2 \\ -x_2^{*} e^{j\theta} & x_1^{*} \end{pmatrix} \tag{5.1}$$

where $(*)$ stands for conjugate, $x_i \in e^{j\frac{2\pi a}{M}}$, $i = 1,2$.

The focus of interest in this chapter is in the pairwise error probability (PEP) and the average bit error probability (BEP) in both quasi-static and rapid fading channels of the HR-STTCM using the orthogonal transmission matrix shown in (5.1). For a quasi-static fading case, the channel coefficients are assumed to be constant over a frame duration but varying from frame to frame, while in a rapid fading case, the channel coefficients are assumed to vary from one transmitted space-time block code in a frame to another.

In [7], performance criteria for space-time codes were derived based on an upper bound on the PEP in both quasi-static and fast fading channels. Although the upper bound derived in [7] allows us to consider all possible error events and to give a final expression for the average error probability term, it is loose for most signal-to-noise ratios.

The looseness of the pioneering work in [7] has generated a large number of research papers [20, 23, 26] with the aim of obtaining a tighter bound for most space-time codes using various methods.

The closed-form expression, i.e. exact expression of the PEP for space-time trellis codes was derived in [23] based on the residual method using characteristic function [28, 29], which has been used previously in the performance analysis of trellis coded

modulation (TCM). Based on this expression, an analytical estimate for the bit error probability was computed, taking into account dominant error events.
The derivation in [23] shows that the exact PEP is the upper bound derived in [7] modified by a correcting factor given by the second product term whose value depends on the poles of the characteristic function [24] of the quadratic form of the complex Gaussian random variable.

In [26], the moment generating function previously used for the analysis of uncoded and coded digital communication over fading channels using only a single transmitter is applied to provide a closed-form expression of the PEP for space-time-coded systems with multiple antennas. The method used in [26] has the additional advantage of allowing for direct evaluation of the transfer function upper bound on the average bit error probability. In [25], the moment generating function based method was extended in analyzing the PEP of the SOSTTC. It was shown that for both slow and fast fading channels it is possible to obtain a closed-form expression for the PEP in terms of the elements of the error signal difference matrix that characterized the super-orthogonal space-time block code.

A different approach to finding the exact expression of the PEP with less computational difficulty is presented in this chapter. This approach is based on the Gauss-Chebysev quadrature technique. This technique has been previously used in the performance analysis of trellis coded modulation (TCM) [27]. This method combines both simplicity and accuracy in finding the closed-form expression of the PEP.
Later in the chapter an estimate of the bit error probability is obtained using the PEP's closed-form expressions taking into account error events up to a finite length.

5.2 System Model and Derivation of the Closed-form Expression of the PEP

A transmission system of N_t transmit antennas and N_r receive antennas will be considered. The binary data stream is first modulated and mapped to a sequence of complex modulation symbols. The complex modulated symbols x_i $\left(i = 1, 2, ..., N_t\right)$ are then fed into an inner space-time block encoder to generate the orthogonal transmitted code matrix defined in (5.1).

$x_{n_t}^{(n)}$ is defined as the complex valued modulated symbol transmitted from the n_tth transmit antenna in the nth signaling interval and $h_{ij}^{(n)}$ as the channel coefficient from the ith transmit antenna to the jth receive antenna at the same signaling interval $i \in \{1,2,...,N_t\}, j \in \{1,2,...,N_r\}$.

Assuming that the channel state information is perfectly known at the receiver, the corresponding set of successive signal samples at the receiver at the nth signaling interval are given by;

$$\begin{aligned} r_l^{(n)} &= h_{l1}^{(n)} x_1^{(n)} e^{j\theta^{(n)}} + h_{l2}^{(n)} x_2^{(n)} + \eta_l^{(n)} \\ r_{l+N_r}^{(n)} &= h_{l1}^{(n)} \left(-x_2^{(n)}\right)^* e^{j\theta^{(n)}} + h_{l2}^{(n)} \left(x_1^{(n)}\right)^* + \eta_{l+N_r}^{(n)}, \end{aligned} \tag{5.2}$$

where $l = 1,2,\cdots,N_r$ and $\eta_j^{(n)}$ are independently identically distributed complex zero mean Gaussian noise samples, each sample with variance $\sigma^2/2$ per dimension. It is assumed that the channel undergoes Rayleigh fading throughout the derivation.

To evaluate the PEP, i.e., the probability of choosing the codeword $\tilde{\mathrm{X}}=\left(\tilde{x}_1^{(1)},\tilde{x}_2^{(1)},...,\tilde{x}_{N_t}^{(1)}\ \tilde{x}_1^{(2)},\tilde{x}_2^{(2)},...,\tilde{x}_{N_t}^{(2)}....\ \tilde{x}_1^{(N)},\tilde{x}_2^{(N)},...,\tilde{x}_{N_t}^{(N)}\right)$ when in fact the codeword $\mathrm{X}=\left(x_1^{(1)},x_2^{(1)},...,x_{N_t}^{(1)}\ x_1^{(2)},x_2^{(2)},...,x_{N_t}^{(2)}....\ x_1^{(N)},x_2^{(N)},...,x_{N_t}^{(N)}\right)$ was transmitted, the maximum likelihood metric corresponding to the correct and the incorrect path will be used. The metric corresponding to the correct path is given by:

$$\begin{aligned} m(r,\mathrm{X}) = \sum_{n=1}^{N}\sum_{l=1}^{N_r}\Bigg[&\left| r_l^{(n)} - \left(h_{l1}^{(n)} x_1^{(n)} e^{j\theta^{(n)}} + h_{l2}^{(n)} x_2^{(n)} \right) \right|^2 \\ &+ \left| r_{l+N_r}^{(n)} - \left(h_{l1}^{(n)} \left(-x_2^{(n)}\right)^* e^{j\theta^{(n)}} + h_{l2}^{(n)} \left(x_1^{(n)}\right)^* \right) \right|^2 \Bigg] \end{aligned} \tag{5.3}$$

The above is based on an observation of N blocks ($2N$ symbols), where each block is described by (5.2).

For the incorrect path, the corresponding metric is given by (5.3) with $x_i^{(n)}, i = 1,2$ and $\theta^{(n)}$ replaced by $\tilde{x}_i^{(n)}, i = 1,2$ and $\tilde{\theta}^{(n)}$ respectively.

The realization of the PEP over the entire frame length and for a given channel coefficient (i.e. H) is given by:

$$\begin{aligned} \mathrm{P}\left(\mathrm{X} \to \tilde{\mathrm{X}} \middle| \mathrm{H}\right) &= \Pr\left\{m(r,\mathrm{X}) \;>\; m\left(r,\tilde{\mathrm{X}}\right)\right\} \\ &= \Pr\left\{m(r,\mathrm{X}) - m\left(r,\tilde{\mathrm{X}}\right) > 0\right\} \end{aligned} \tag{5.4}$$

Substituting (5.3) and the corresponding expression for $m\left(r,\tilde{\mathrm{X}}\right)$ into (5.4) and simplifying gives:

$$\begin{aligned} \mathrm{P}\left(\mathrm{X} \to \tilde{\mathrm{X}} \middle| \mathrm{H}\right) &= \Pr\left\{\sum_{n=1}^{N}\sum_{l=1}^{N_r}\left[|\mathrm{A}|^2 + |\mathrm{B}|^2\right] > 0\right\} \\ &= \Pr\left\{\sum_{n=1}^{N}\sum_{l=1}^{N_r}\left\|\mathrm{H}_l^{(n)}\Delta_n\right\|^2 > 0\right\} \end{aligned} \tag{5.5}$$

where

$$\mathrm{A} = h_{l1}^{(n)}\left(\tilde{x}_1^{(n)}e^{j\tilde{\theta}^{(n)}} - x_1^{(n)}e^{j\theta^{(n)}}\right) + h_{l2}^{(n)}\left(\tilde{x}_2^{(n)} - x_2^{(n)}\right)$$

$$\mathrm{B} = -h_{l1}^{(n)}\left(\tilde{x}_2^{(n)}e^{-j\tilde{\theta}^{(n)}} - x_2^{(n)}e^{-j\theta^{(n)}}\right)^* + h_{l2}^{(n)}\left(\tilde{x}_1^{(n)} - x_1^{(n)}\right)^*$$

and Δ_n is given as the codeword matrix that characterizes the HR-STTCM . The expression of Δ_n is shown in (5.6) below

$$\Delta_n = \begin{bmatrix} x_1^{(n)}e^{j\theta^{(n)}} - \tilde{x}_1^{(n)}e^{j\tilde{\theta}^{(n)}} & \left(-x_2^{(n)}\right)^* e^{j\theta^{(n)}} - \left(-\tilde{x}_2^{(n)}\right)^* e^{j\tilde{\theta}^{(n)}} \\ x_2^{(n)} - \tilde{x}_2^{(n)} & \left(x_1^{(n)}\right)^* - \left(\tilde{x}_1^{(n)}\right)^* \end{bmatrix} \tag{5.6}$$

and $\mathrm{H}_l^{(n)} = \begin{bmatrix} h_{l1}^{(n)} & h_{l2}^{(n)} \end{bmatrix}$. $\|\bullet\|$ stands for the norm of the matrix element.

The conditional PEP given in (5.5) can be expressed in terms of the complementary error function [27] as:

$$\mathrm{P}\left(\mathrm{X} \to \tilde{\mathrm{X}} \middle| \mathrm{H}\right) = \frac{1}{2}\mathrm{erfc}\left(\sqrt{\frac{E_s}{4N_0}\sum_{l=1}^{N_r}\mathrm{H}_l\,\Delta\Delta^H\,\mathrm{H}_l^H}\right). \tag{5.7}$$

The function $\mathbf{\Delta\Delta}^H$ is a diagonal matrix of the form shown in (5.8) below. This represents the codeword matrix for a frame of N blocks. $(\bullet)^H$ represent the conjugate transpose of the matrix element and E_s/N_0 stands for the symbol signal-to-noise ratio.

$$\mathbf{\Delta\Delta}^H = \begin{bmatrix} \Delta_1\Delta_1^H & 0 & \cdots & \cdots & 0 \\ 0 & \Delta_2\Delta_2^H & 0 & \vdots & 0 \\ 0 & 0 & \ddots & \vdots & \vdots \\ \vdots & \vdots & \vdots & \Delta_{N-1}\Delta_{N-1}^H & 0 \\ 0 & 0 & \cdots & 0 & \Delta_N\Delta_N^H \end{bmatrix} \tag{5.8}$$

Complementary error functions, as defined integrally in [22, 7.4.11] is given by;

$$\operatorname{erfc}(b) = \frac{2}{\pi}\int_0^\infty \frac{e^{-b^2\left(t^2+1\right)}}{t^2+1}\,dt \tag{5.9}$$

Combining (5.7) and (5.9) the conditional PEP can be expressed as an integral. Thus, with $E(x)$ denoting the average of x, one gets

$$\mathrm{P}\left(\mathrm{X}\to\tilde{\mathrm{X}}\right) = \frac{1}{\pi}E\left[\int_0^\infty \frac{\exp\left[-\left(t^2+1\right)\frac{E_s}{4N_0}\sum_{l=1}^{N_r}\mathrm{H}_l\,\mathbf{\Delta\Delta}^H\,\mathrm{H}_l^H\right]}{t^2+1}dt\right] \tag{5.10}$$

The above expression (5.10) can be simplified further using the results in [24]. For a complex circularly distributed Gaussian random row vector z with mean μ and covariance matrix $\sigma_z{}^2 = E[zz^*] - \mu\mu^*$, and a Hermitian matrix $\mathbf{M}$, we have;

$$E_z\left[\exp\left(-z\mathbf{M}(z^*)^T\right)\right] = \frac{\exp\left[-\mu\mathbf{M}\left(\mathbf{I}+\sigma_z{}^2\mathbf{M}\right)^{-1}(\mu^*)^T\right]}{\det\left(\mathbf{I}+\sigma_z{}^2\mathbf{M}\right)}, \tag{5.11}$$

where $\mathbf{I}$ is an identity matrix. Applying (5.11) in solving (5.10), (5.12) is obtained. Since $z = \mathrm{H}_l$, $\mathbf{M} = -(t^2+1)\bullet E_s/4N_0 \bullet \mathbf{\Delta\Delta}^H$ ($\mathbf{\Delta\Delta}^H$ is a diagonal matrix and $(t^2+1)\bullet E_s/4N_0$ is constant for a given SNR, thus $\mathbf{M}=\mathbf{M}^{\mathrm{T}}$ i.e. $\mathbf{M}$ is an Hermitian matrix), $\mu = 0$ (H_l has Rayleigh distribution) and $\sigma_z{}^2 = \sigma_{\mathrm{H}_l}{}^2 = \mathbf{I}_{N_t}$.

$$P(X \to \tilde{X}) = \frac{1}{\pi}\int_0^{\infty} \frac{1}{t^2+1} \prod_{l=1}^{N_r} \frac{1}{\det\left[\mathbf{I}_{N_t} + \frac{E_s}{4N_0}\Delta\Delta^H\left(t^2+1\right)\right]_l} dt \tag{5.12}$$

To solve (5.12), an integral equation given by:

$$I = \frac{1}{\pi}\int_0^{\infty} \frac{1}{t^2+1} f\left(t^2+1\right) dt \tag{5.13}$$

is considered, where $f\left(t^2+1\right) = \prod_{l=1}^{N_r} \frac{1}{\det\left[\mathrm{I}_{N_t} + \frac{E_s}{4N_0}\Delta\Delta^H\left(t^2+1\right)\right]_l}$.

Substituting $y = 1/t^2+1$ into (5.13), (5.13) becomes:

$$I = \frac{1}{2\pi}\int_0^{1} \frac{1}{\sqrt{y(1-y)}} f\left(1/y\right) dy \tag{5.14}$$

The above equation (5.14) is in an orthogonal polynomial form [22, 25.4.38] and Gauss-Chebyshev quadrature formula of first kind can be used to solve it.

$$\begin{aligned} \int_{-1}^{1} \frac{f(u)}{\sqrt{1-u^2}} du &= \sum_{i=1}^{m} w_i f\left(u_i\right) + R_m \\ u_i &= \cos\frac{(2i-1)\pi}{2m} \\ w_i &= \frac{\pi}{m} \\ R_m &\le \max_{-1<u<+1} \frac{\pi}{(2m)!2^{2m-1}} \left|f^{2m}(u)\right| \end{aligned} \tag{5.15}$$

The expression in (5.14) can be reduced to (5.15) if $2y-1=u$, then

$$\begin{aligned} 2y-1 &= \cos\frac{(2i-1)\pi}{2m} \\ 2y &= \cos\frac{(2i-1)\pi}{2m} + 1 \end{aligned} \tag{5.16}$$

Using the trigonometric functions

$$\cos v = \cos\left(\frac{v}{2}+\frac{v}{2}\right) = \cos^2\frac{v}{2} - \sin^2\frac{v}{2}, \qquad \sin^2 v + \cos^2 v = 1, \tag{5.17}$$

(5.16) can be expressed as

$$y = \cos^2\frac{(2i-1)\pi}{4m}, \qquad 1/y = \sec^2\frac{(2i-1)\pi}{4m}. \tag{5.18}$$

Therefore

$$I = \sum_{i=1}^{m} w_i \, \mathrm{f}(u_i) + \mathrm{R}_m = \frac{1}{2m}\sum_{i=1}^{m} \mathrm{f}\left(\sec^2\frac{(2i-1)\pi}{4m}\right) + \mathrm{R}_m \tag{5.19}$$

The closed-form expression of the PEP for HR-STTCM using the Gauss-Chebyshev Quadrature formula as enumerated above is now given by:

$$\mathrm{P}\left(\mathrm{X}\to\tilde{\mathrm{X}}\right) = \frac{1}{2m}\sum_{i=1}^{m}\prod_{l=1}^{N_r}\frac{1}{\det\left[\mathbf{I}_{N_T} + \frac{E_s}{4N_0}\mathbf{\Delta}\mathbf{\Delta}^H \sec^2\frac{(2i-1)\pi}{4m}\right]_l} + \mathrm{R}_m \tag{5.20}$$

As m (which is the order of the polynomial i.e. $\mathrm{f}(u_i)$ and also function of degree of precision $\equiv 2m$-1) increases the remainder term R_m becomes negligible.
For quasi-static case, the channel coefficients are assumed constant for entire frame duration, but can vary from frame to frame. Therefore (5.20) results in

$$\mathrm{P}\left(\mathrm{X}\to\tilde{\mathrm{X}}\right) = \frac{1}{2m}\sum_{i=1}^{m}\prod_{l=1}^{N_r}\frac{1}{\det\left[\mathbf{I}_{N_T} + \frac{E_s}{4N_0}\sum_{n=1}^{N}\Delta_n\Delta_n^H \sec^2\frac{(2i-1)\pi}{4m}\right]_l} + \mathrm{R}_m \tag{5.21}$$

For the rapid fading case, the channel coefficients are kept constant for one codeword matrix i.e. one transmission block, and then it varies from block to block in a random manner. Based on this unconditional PEP expression (5.10) can now be written as;

$$P(X \to \tilde{X}) = \frac{1}{\pi} E\left[\int_0^{\infty} \frac{\exp\left[-(t^2+1)\frac{E_s}{4N_0} \sum_{l=1}^{N_r} \sum_{n=1}^{N} H_l^n \Delta_n \Delta_n^H \left(H_l^n\right)^H \right]}{t^2+1} dt \right] \tag{5.22}$$

Following the same procedure as enumerated above for the quasi-static fading case, (5.22) will result in:

$$P(X \to \tilde{X}) = \frac{1}{2m} \sum_{i=1}^{m} \prod_{l=1}^{N_r} \prod_{n=1}^{N} \frac{1}{\det\left[I_{N_r} + \frac{E_s}{4N_0} \Delta_n \Delta_n^H \sec^2 \frac{(2i-1)\pi}{4m} \right]_l} + R_m \tag{5.23}$$

5.3 Numerical Examples

As an example, the rate $r = 1$ BPSK 2-state code [25, Fig 1], whose trellis diagram is illustrated in Figure 5.1 will be considered. The trellis in Figure 5.1 is constructed using the same concept of set partitioning as explained in chapter 3. In this example two sets, each containing two pairs of BPSK symbols are assigned to each state, i.e. there is a pair of parallel path between each pair of states. The labelling $(s,l)/\mathrm{A}(x_i, x_j, \theta)$ along each branch of the trellis refers to the pair of input BPSK symbols (s,l) and the corresponding output symbol function $\mathrm{A}(x_i, x_j, \theta)$ using (5.1) to generate the orthogonal matrix.

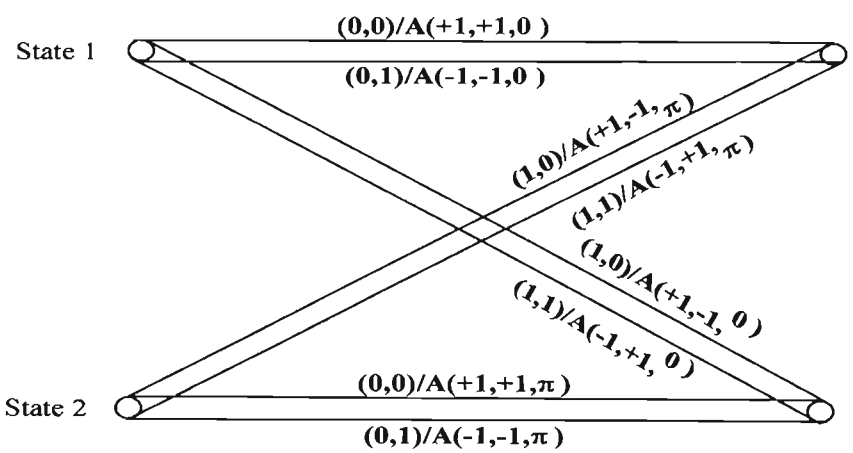

Figure 5.1: Trellis diagram for rate 1, 2-state BPSK HR-STTCM.

First the parallel paths i.e. $N=1$ are considered. Evaluating (5.6) and substituting it into (5.21) and (5.23) shows that the PEP for the error event is the same for both quasi-static and fast fading channels. The codeword matrix is given by:

$$\Delta_1 = \begin{bmatrix} 2 & -2 \\ 2 & 2 \end{bmatrix}, \quad \Delta_1 \Delta_1^H = \begin{bmatrix} 8 & 0 \\ 0 & 8 \end{bmatrix}. \tag{5.24}$$

Also an error event path of length $N=2$ with respect to the all zero path as the correct one, as shown in the trellis diagram in Figure 5.2 is considered. From the trellis diagram we have $x_1^{(1)} = x_2^{(1)} = x_1^{(2)} = x_2^{(2)} = +1$, $\tilde{x}_1^{(1)} = \tilde{x}_2^{(2)} = +1$, $\tilde{x}_2^{(1)} = \tilde{x}_1^{(2)} = -1$, $\theta^{(1)} = \tilde{\theta}^{(1)} = \theta^{(2)} = 0$ and $\tilde{\theta}^{(2)} = \pi$.

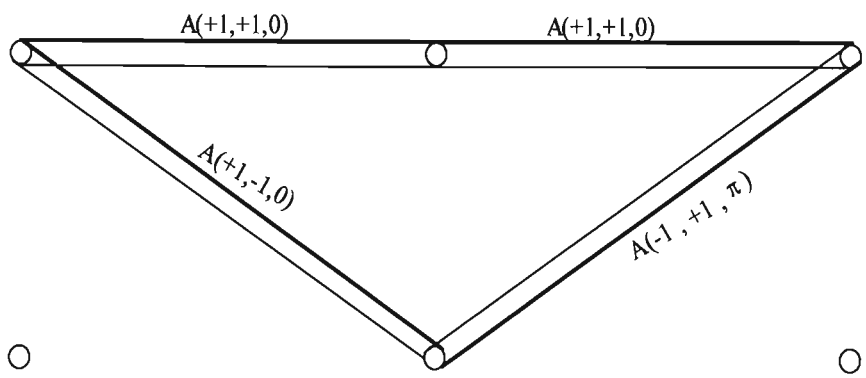

Figure 5.2: *N*=2, 2-state BPSK HR-STTCM

Evaluating the element of the matrix in (5.6) Δ_1 and Δ_2 give;

$$\Delta_1 = \begin{bmatrix} 0 & -2 \\ 2 & 0 \end{bmatrix}, \quad \Delta_1 \Delta_1^H = \begin{bmatrix} 4 & 0 \\ 0 & 4 \end{bmatrix}$$
$$\Delta_2 = \begin{bmatrix} 0 & -2 \\ 0 & 2 \end{bmatrix}, \quad \Delta_2 \Delta_2^H = \begin{bmatrix} 4 & -4 \\ -4 & 4 \end{bmatrix} \tag{5.25}$$

For a quasi-static fading assumption with $m=2$, $N_r=1$ and $N_t=2$, the closed for expression in (5.21) becomes;

$$P\left(X \to \tilde{X}\right) \simeq \frac{1}{4}\left(\frac{1}{\det\left[\mathbf{I}_2 + k_1 \bullet \begin{bmatrix} 8 & -4 \\ -4 & 8 \end{bmatrix}\right]} + \frac{1}{\det\left[\mathbf{I}_2 + k_2 \bullet \begin{bmatrix} 8 & -4 \\ -4 & 8 \end{bmatrix}\right]}\right) \tag{5.26}$$

$$k_1 = \frac{E_s}{4N_0}\sec^2 \pi/8$$

$$k_2 = \frac{E_s}{4N_0}\sec^2 3\pi/8$$

The remainder value R_m in (5.21) is neglected in the computation of $P\left(X \to \tilde{X}\right)$.

For a rapid fading channel with $m = 2$, $N_r = 1$ and $N_t = 2$, the closed-form expression in (5.23) gives;

$$P\left(X \to \tilde{X}\right) \simeq \frac{1}{4}\left(\frac{1}{G} + \frac{1}{R}\right)$$

$$G = \det\left\{\mathbf{I}_2 + k_1 \begin{bmatrix} 4 & 0 \\ 0 & 4 \end{bmatrix}\right\} \bullet \det\left\{\mathbf{I}_2 + k_1 \begin{bmatrix} 4 & -4 \\ -4 & 4 \end{bmatrix}\right\} \tag{5.27}$$

$$R = \det\left\{\mathbf{I}_2 + k_2 \begin{bmatrix} 4 & 0 \\ 0 & 4 \end{bmatrix}\right\} \bullet \det\left\{\mathbf{I}_2 + k_2 \begin{bmatrix} 4 & -4 \\ -4 & 4 \end{bmatrix}\right\}$$

Also an error event of length 3 with respect to the all zero path as the correct one is considered, as shown in the trellis diagram below. From the trellis diagram in Figure 5.3 we have;

$x_1^{(1)} = x_2^{(1)} = x_1^{(2)} = x_2^{(2)} = x_1^{(3)} = x_2^{(3)} = \hat{x}_1^{(1)} = \hat{x}_2^{(3)} = +1$, $\tilde{x}_2^{(1)} = \tilde{x}_1^{(2)} = \tilde{x}_2^{(2)} = \tilde{x}_1^{(3)} = -1$,
$\theta^{(1)} = \tilde{\theta}^{(1)} = \theta^{(2)} = \theta^{(3)} = 0$ and $\tilde{\theta}^{(2)} = \tilde{\theta}^{(3)} = \pi$.

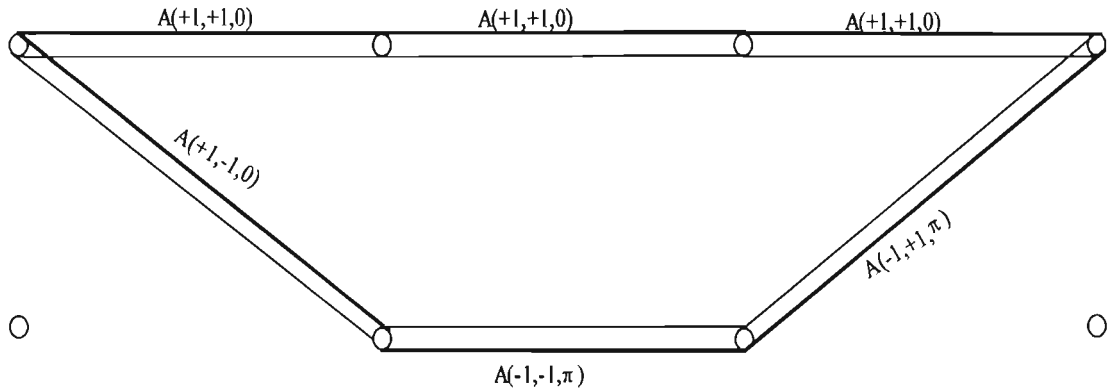

Figure 5. 3: *N*=3 2-State BPSK HR-STTCM

Evaluating the element of the matrix in (5.6) Δ_1, Δ_2 and Δ_3 gives

$$\Delta_1 = \begin{bmatrix} 0 & -2 \\ 2 & 0 \end{bmatrix}, \quad \Delta_1 \Delta_1^H = \begin{bmatrix} 4 & 0 \\ 0 & 4 \end{bmatrix}$$

$$\Delta_2 = \begin{bmatrix} 0 & 0 \\ 2 & 2 \end{bmatrix}, \quad \Delta_2 \Delta_2^H = \begin{bmatrix} 0 & 0 \\ 0 & 8 \end{bmatrix} \tag{5.28}$$

$$\Delta_3 = \begin{bmatrix} 0 & -2 \\ 0 & 2 \end{bmatrix}, \quad \Delta_3 \Delta_3^H = \begin{bmatrix} 4 & -4 \\ -4 & 4 \end{bmatrix}$$

For a quasi-static fading assumption with $m = 2, N_r = 1$ and $N_t = 2$, the closed for expression in (5.21) becomes;

$$\mathrm{P}\left(\mathrm{X} \to \tilde{\mathrm{X}}\right) \simeq \frac{1}{4}\left(\frac{1}{\det\left[\mathbf{I}_2 + k_1 \bullet \begin{bmatrix} 8 & -4 \\ -4 & 16 \end{bmatrix}\right]} + \frac{1}{\det\left[\mathbf{I}_2 + k_2 \bullet \begin{bmatrix} 8 & -4 \\ -4 & 16 \end{bmatrix}\right]} \right) \tag{5.29}$$

$$k_1 = \frac{E_s}{4N_0} \sec^2 \pi/8$$

$$k_2 = \frac{E_s}{4N_0} \sec^2 3\pi/8$$

The remainder value R_m in (5.21) is neglected in the computation of $\mathrm{P}\left(\mathrm{X} \to \tilde{\mathrm{X}}\right)$.

For a rapid fading channel with $m = 2, N_r = 1$ and $N_t = 2$, the closed-form expression in (5.23) gives;

$$P\left(X \to \tilde{X}\right) \simeq \frac{1}{4}\left(\frac{1}{Z}+\frac{1}{V}\right)$$

$$Z = \det\left\{\mathbf{I}_2 + k_1\begin{bmatrix}4 & 0\\ 0 & 4\end{bmatrix}\right\}\bullet\det\left\{\mathbf{I}_2 + k_1\begin{bmatrix}0 & 0\\ 0 & 8\end{bmatrix}\right\}\bullet\det\left\{\mathbf{I}_2 + k_1\begin{bmatrix}4 & -4\\ -4 & 4\end{bmatrix}\right\} \tag{5.30}$$

$$V = \det\left\{\mathbf{I}_2 + k_2\begin{bmatrix}4 & 0\\ 0 & 4\end{bmatrix}\right\}\bullet\det\left\{\mathbf{I}_2 + k_2\begin{bmatrix}0 & 0\\ 0 & 8\end{bmatrix}\right\}\bullet\det\left\{\mathbf{I}_2 + k_2\begin{bmatrix}4 & -4\\ -4 & 4\end{bmatrix}\right\}$$

.

5.4 Analytical Results and Discussion

In this section numerical results for the closed-form PEP expression enumerated in the previous section will be provided. The rate=1, m=2, two-state BPSK modulation and a single receive antenna will be considered. Figure 5.4 shows the PEP for quasi-static fading Rayleigh channel for error event of length 1, 2 and 3 (i.e. N=1, 2 and 3) using (5.21). The PEP is also plotted for rapid fading Rayleigh channel for the error event of length 1, 2 and 3 in Figure 5.5 (i.e. N=1, 2 and 3). Comparing the two graphs i.e. Figure 5.4 and Figure 5.5, the PEP is smaller for fast fading channel. The PEP at N=2 is the worst case for slow fading channel whereas for fast fading channel, the PEP at N=1 is the worst case.

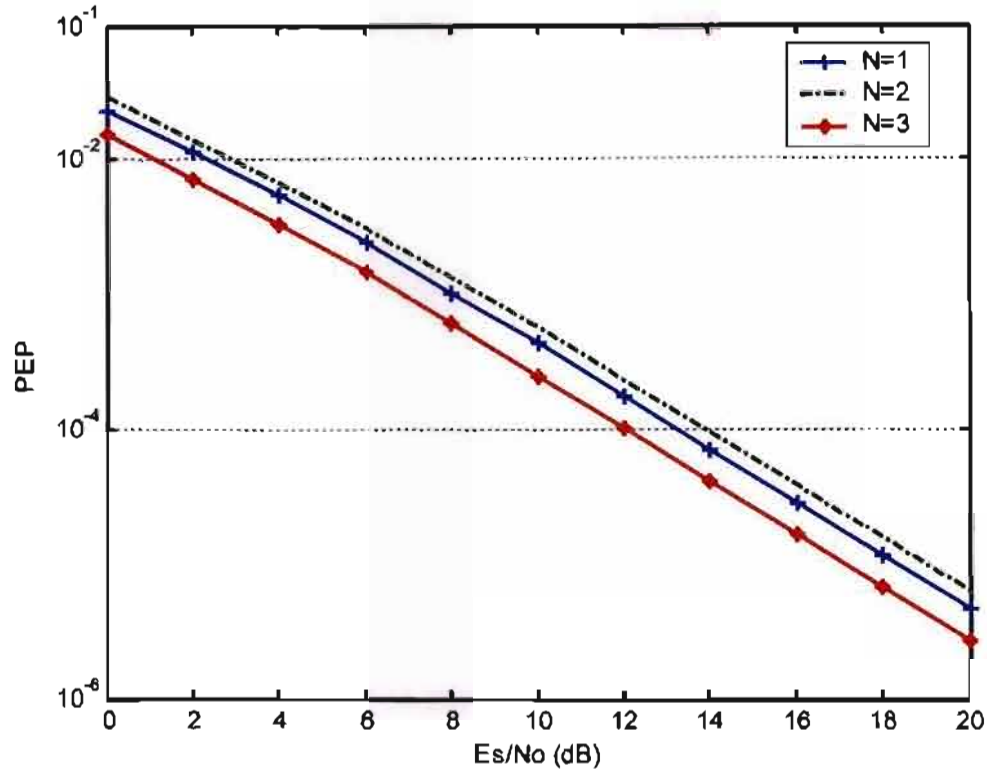

Figure 5.4: PEP performance of rate 1, 2-State BPSK HR-STTCM over quasi-static fading Rayleigh Channel; one receive antenna.

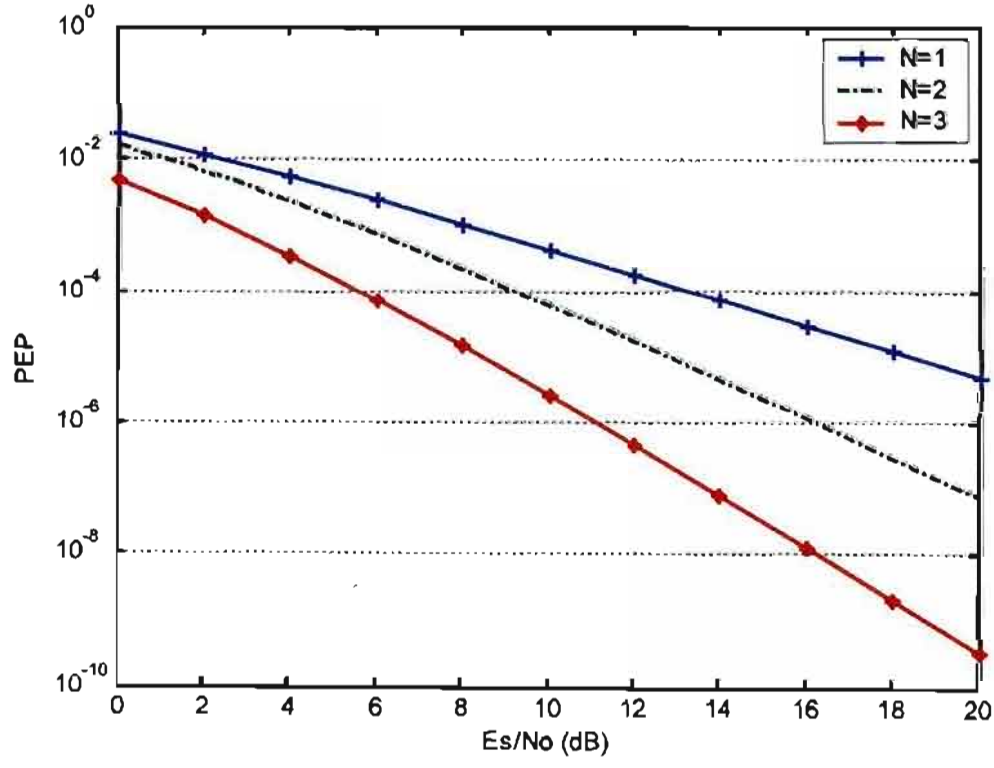

Figure 5.5: PEP performance of rate 1, 2-State BPSK HR-STTCM over Fast fading Rayleigh Channel; one receive antenna

5.5 Approximate Evaluation of the Average Bit Error Probability

In most digital communication systems, the average bit error probability (or frame error probability) is of greater interest than the pairwise error event probability i.e. the PEPs. In the case that the pairwise error probability can be expressed in a product form [7], it is possible to find an upper bound on the bit error probability by using the transfer function approach.

Transfer function method [41] is a technique which makes use of codes' state diagram to obtain the error rate performance of trellis based codes (i.e. convolutional, TCM).

Instead of using the transfer function approach which takes into account the error event of all lengths, an estimation of bit error probability can be obtained through accounting for error event paths of length to a pre-determined specific value using [28];

$$P_b(E) \approx \frac{1}{g} \sum_{X \to \hat{X}} q(X \to \hat{X}) P(X \to \hat{X}), \tag{5.31}$$

where g is the number of input bits per trellis transition and $q\left(X \to \hat{X}\right)$ is the number of bit errors associated with each error event. If the maximum length of error events taken into account is chosen as H, it is sufficient to consider the error event up to H; this represents a truncation of the infinite series used in calculating the union bound on the bit error probability for high SNR values. The choice of H is critical in the sense that most of the dominant error events for the range of SNR of interest should be taken into account by a proper choice while preventing excessive computational complexity (the computational complexity grows exponentially with H).

In this section, the PEP's previously derived will be used to evaluate in closed-form an approximation to the average bit error probability (BEP), $P_b(E)$, based on accounting only for error events of length N less than or equal to H.

If the all zero sequence was transmitted i.e. $\{(0,0)\}$, using the 2-state code in Figure 5.1, there is a single error event path of length 1 i.e. $\{(0,1)\}$ which has a PEP of type PEP_1 and contribute only one bit in error. When accounting for error events of length 2 i.e. $H = 2$ and assuming that the all zero sequence was transmitted

i.e. $\{(0,0)$ and $(0,0)\}$, there are 4 error event paths i.e. $\{(1,0)(1,0)$, $(1,0)(1,1)$, $(1,1)(1,0)$ and $(1,1)(1,1)\}$ which have PEP of type PEP_{II} and they all contribute a total of 12 bits in error.

Also when accounting for error event of length 3 i.e. $H = 3$ and the all zero sequence was transmitted i.e. $\{(0,0)$, $(0,0)$ and $(0,0)\}$, there are 8 error event paths i.e. $\{(1,0)(0,0)(1,0)$, $(1,0)(0,0)(1,1)$, $(1,0)(0,1)(1,0)$, $(1,0)(0,1)(1,1)$, $(1,1)(0,1)(1,0)$, $(1,1)(0,1)(1,1)$, $(1,1)(0,0)(1,0)$, $(1,1)(0,0)(1,1)\}$. All these error event paths have PEP of type PEP_{III} and they contribute in total 28 bits in error. Therefore to approximate the average bit error probability by considering only the error event path of 1, 2 or 3 then we use P_{b1}, P_{b2} and P_{b3} respectively.

$$P_{b1} \simeq \frac{1}{2}(PEP_{I}) \tag{5.32}$$

$$P_{b1} \simeq \frac{1}{2}(PEP_{I} + 12 * PEP_{II}) \tag{5.33}$$

$$P_{b1} \simeq \frac{1}{2}(PEP_{I} + 12 * PEP_{II} + 28 * PEP_{III}) \tag{5.34}$$

The expressions for the PEP types i.e. PEP_{I}, PEP_{II} and PEP_{III} used in the equation above to approximate the average bit error probability depends on the type of fading channel under consideration. For PEP_{I}, its expression is the same for both quasi-static and rapid Rayleigh fading using the codeword matrix (5.24) in (5.21) and (5.23) respectively.

The PEP_{II} expression in quasi-static fading is given by (5.26) while in a rapid fading channel its expression is given by (5.27). Finally, the PEP_{III} expression for both quasi-static and rapid fading is obtained when we use the codeword matrices in (5.28) in both (5.21) and (5.23) to give (5.29) and (5.30), respectively.

5.6 Simulation Results and Discussion

Figures 5.6 and 5.7 show the performance of the bit error probability of 2-state BPSK HR-STTCM for slow i.e. quasi-static and fast (or rapid) fading channels respectively. For a slow fading channel, the result in Figure 5.6 shows, as compared with simulation, that for low SNR, our performance analysis method is loose but asymptotically converges at high SNR. The convergence of the analytical results for small error length is quite fast for rapid fading channels when compared with the performance in quasi-static fading channel. It can inferred that the error length up to 2 is sufficient for the average bit error rate calculation for fast fading channel while longer error lengths are needed to estimate the average bit error rate performance for slow fading channels.

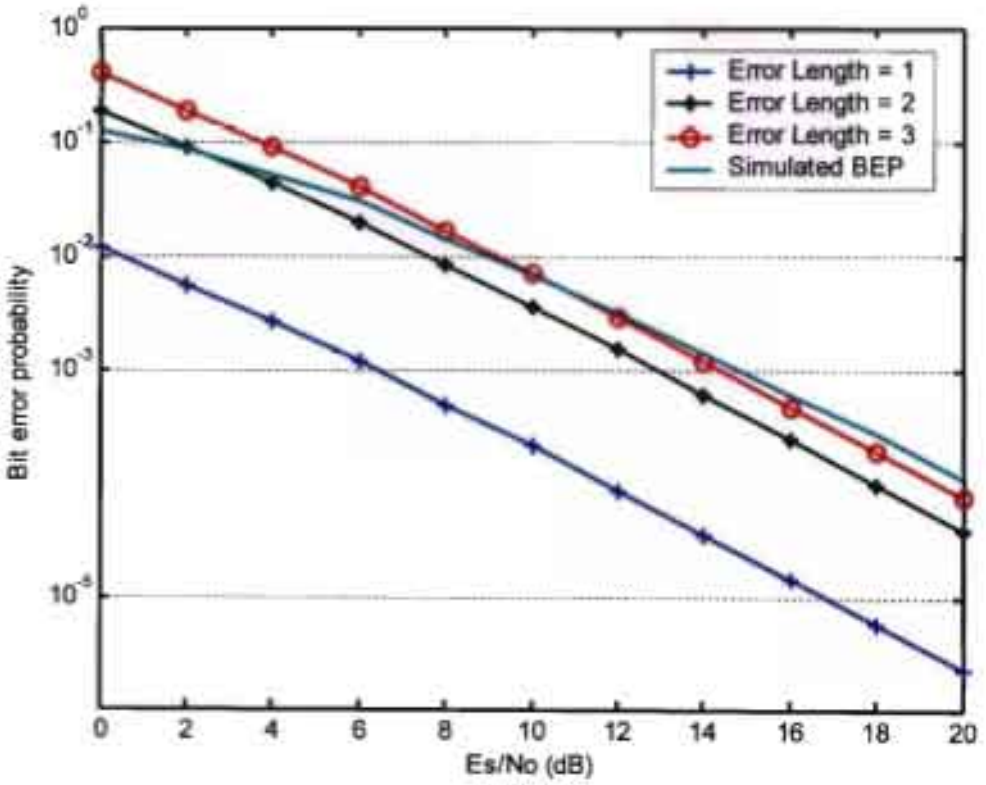

Figure 5.6: Bit error Probability of rate 1, 2-State BPSK HR-STTCM over quasi-static fading Rayleigh Channel with one receive antenna.

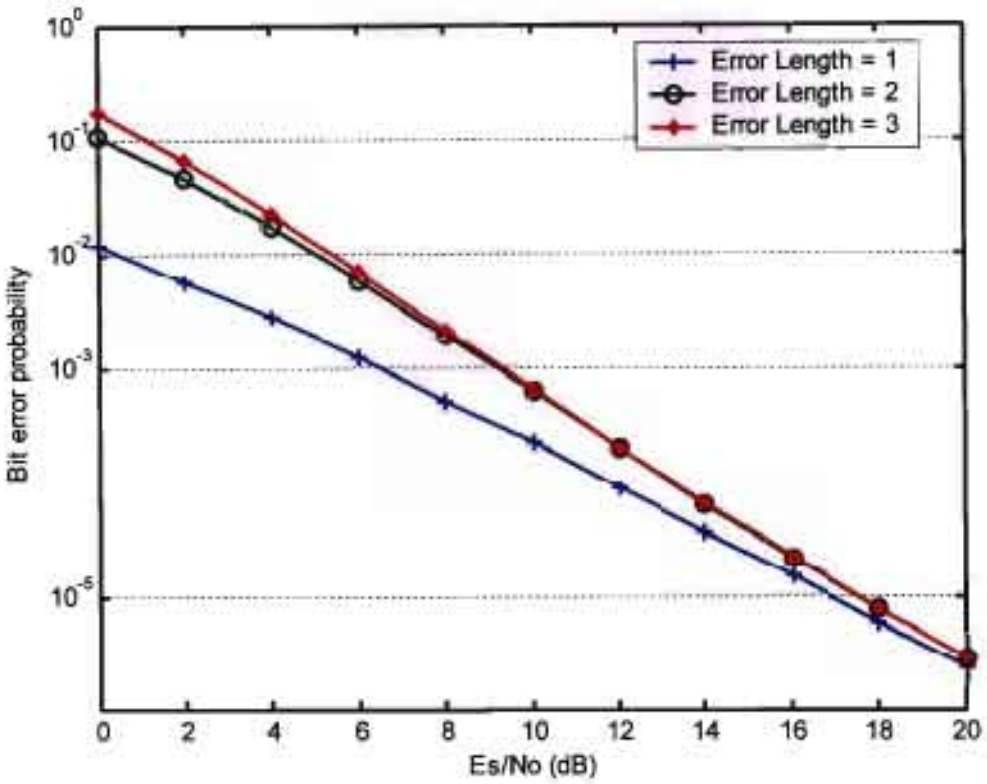

Figure 5.7: Bit error Probability of rate r=1, 2-State BPSK HR-STTCM over fast fading Rayleigh Channel with one receive antenna.

5.7 Summary

In this chapter, the closed-form expression of the pairwise error probability of high rate space-time trellis coded modulation using the orthogonal transmission matrices has been derived. The Gauss-Chebyshev quadrature method used proved to be accurate and made the derivation of the closed-form PEP easily obtainable. The method used here proved to be less computationally complex when compared with the characteristic function technique demonstrated in the literature.

CHAPTER 6

CONCLUSION AND FUTURE WORK

This dissertation focuses on the performance of high rate space-time trellis coded modulation under coherent and non-coherent detection environment. A chapter wise summary and conclusions of the results presented in this dissertation is given below.

In Chapter 1, a brief historical overview of the wireless industry is given and the challenges faced in designing a robust network that can deliver the performance needed to support the emerging trend in the wireless industry. Current literature techniques on various transmit diversity techniques as a way of overcoming some of the challenges faced by signals in wireless network were enumerated. It was established that the capacity obtainable in the wireless network is a function of the diversity technique used and the number of transmit and receive antennas.
Motivation of the research, dissertation overview and original contributions of this dissertation were presented.

In Chapter 2, the concepts of space-time coding were introduced, which are codes that are used to increase the quality of signals in multiple input multiple output systems. The three main primary approaches to space-time coding as discussed in the literature

i.e. layered space-time codes, space-time block code and space-time trellis codes were also discussed. It was concluded that the code design criterion given in this code helps us to determine the performance advantage that is possible for such codes. Space-time block code provides a scheme that has a low decoding complexity due to the orthogonality of the transmitted signals as compared with space-time trellis code for which the decoding complexity increases as the number of antennas increases. In the later part of the chapter, concatenated space-time codes were introduced. This is the use of channel codes e.g. trellis coded modulation, with space-time codes to further improve the performance of the codes in a wireless system.

In chapter 3, an existing form of space-time trellis coded modulation, which is called high rate space-time trellis coded modulation, was presented. The construction of this code is based on the revolutionary idea of Ungerboeck in the design of trellis coded modulation which is signal set expansion and signal set partitioning. It was concluded that the full rate obtained and coding advantage possible in the code was as a result of the signal set expansion and partition. Also the work on this code was extended to a fast fading channel and compared its performance with other space-time codes in such an environment. Simulation results showed that the code outperforms STBC and STTC under both quasi-static and fast fading environments. Later in the chapter, the performance of the code in a non-coherent environment, i.e. when perfect channel state information is not available at the receiver, was presented. The concept of using unitary space-time constellation to estimate channel state information was also applied to estimate the channel state information of the high rate space-time trellis coded system. Simulation results show that some coding gain performance loss is observed for the code under this channel estimation scheme but the code still maintains its diversity gain.

In chapter 4, the multiuser behaviour of both standalone space-time block codes and high rate space-time trellis coded modulation was investigated. The space-time block codes are powerful spatial diversity techniques that provide low decoding. Its low decoding property can be exploited in a multiuser scenario that employs space-time block coding for its transmission. It was demonstrated, by calculating the signal-to-noise ratio at the receiver for a 2-user space-time block code scheme, that the decoupled signal-to-noise ratio is the same as the signal-to-noise ratio for a single user

scheme. Later in this chapter the concept used for space-time block code in a multiuser environment was extended to the high rate space-time trellis coded modulation in such an environment, and it was explained, by using mathematical expressions and simulation that it is not possible to obtain a single user performance, as was the case of a standalone space-time block code, for a decoupled high rate space-time trellis modulation scheme.

In Chapter 5 a simple numerical analysis of the high rate space-time trellis coded modulation using Gauss-Chebyshev quadrature formula was presented. The existing methods in literature for analyzing space-time codes were mentioned and owing to their computation complexity, the Gauss-Chebyshev quadrature method was employed as it provides an easier method of analyzing such codes. The analysis in quasi-static and fast fading spatially uncorrelated channels was considered. Later in the chapter, the analytical bound was compared with simulation results. It was noted that the bound easily converges in fast fading channels for small error lengths but more error events are needed for the bound in quasi-static channel to be tight.

In the analysis it was assumed that there is perfect channel state information at the receiver. In practice, channel estimation is either absent or imperfect. It would be interesting to find a simple numerical analysis method to analyze the high rate space-time trellis coded for imperfect or blind channel estimation.

Appendix 1

CALCULATION OF THE SNR AT THE RECEIVER FOR 2-USER STBC

The equation model for a 2-user standalone space-time block code is given by:

$$\begin{bmatrix} \mathbf{r}_1 \\ \mathbf{r}_2 \end{bmatrix} = \begin{bmatrix} \mathbf{H}_1 & \mathbf{C}_1 \\ \mathbf{H}_2 & \mathbf{C}_2 \end{bmatrix} \bullet \begin{bmatrix} \mathbf{x}_1 \\ \mathbf{y}_2 \end{bmatrix} + \begin{bmatrix} \mathbf{n}_1 \\ \mathbf{n}_2 \end{bmatrix}, \tag{A.1}$$

where all parameters in this appendix is the same as the once enumerated in section 4.3. After zero forcing interference cancellation is applied to (A.1), the decoupled receiver equation for a given terminal is given by;

$$\tilde{\mathbf{r}}_1 = \begin{bmatrix} M & N \\ -N^* & M^* \end{bmatrix} \bullet \begin{bmatrix} x_{11} \\ x_{12} \end{bmatrix} + \begin{bmatrix} \eta_{11} - P\eta_{21} + Q\eta_{22}^* \\ -\eta_{12}^* + Q^*\eta_{21} + P^*\eta_{22}^* \end{bmatrix}. \tag{A.2}$$

Calculating the SNR of (A.2), we multiply it by the transpose conjugate of the channel matrix to give

$$\begin{bmatrix} M^* & -N \\ N^* & M \end{bmatrix} \begin{bmatrix} \tilde{r}_1(t) \\ -\tilde{r}_1^*(t+1) \end{bmatrix} = \begin{bmatrix} M^* & -N \\ N^* & M \end{bmatrix} \bullet \begin{bmatrix} M & N \\ -N^* & M^* \end{bmatrix} \bullet \begin{bmatrix} x_{11} \\ x_{12} \end{bmatrix} + \begin{bmatrix} M^* & -N \\ N^* & M \end{bmatrix} \bullet \begin{bmatrix} \eta_{11} - P\eta_{21} + Q\eta_{22}^* \\ -\eta_{12}^* + Q^*\eta_{21} + P^*\eta_{22}^* \end{bmatrix}$$

$$\begin{bmatrix} M^* & -N \\ N^* & M \end{bmatrix} \begin{bmatrix} \tilde{r}_1(t) \\ -\tilde{r}_1^*(t+1) \end{bmatrix} = \left(|M|^2 + |N|^2\right) \bullet \mathrm{I}_2 \bullet \begin{bmatrix} x_{11} \\ x_{12} \end{bmatrix} + \begin{bmatrix} M^* & -N \\ N^* & M \end{bmatrix} \bullet \begin{bmatrix} \eta_{11} - P\eta_{21} + Q\eta_{22}^* \\ -\eta_{12}^* + Q^*\eta_{21} + P^*\eta_{22}^* \end{bmatrix} \tag{A.3}$$

Therefore the SNR is given by;

$$\mathrm{SNR} = \frac{E\left[\left(|M|^2 + |N|^2\right)^2 \bullet |x|^2\right]}{E\left[\mathrm{B} \bullet \mathrm{B}^*\right]}, \tag{A.4}$$

where $\mathrm{B} = M^*\eta_{11} - M^*P\eta_{21} + M^*Q\eta_{22}^* + N\eta_{12}^* - NQ^*\eta_{21} - NP^*\eta_{22}^*$.
Solving first the denominator of (A.4), we obtain;

$$\begin{aligned}
\mathrm{B} \bullet \mathrm{B}^* = {} & |M|^2|\eta_{11}|^2 - |M|^2 P^*\eta_{11}\eta_{21}^* + |M|^2 Q^*\eta_{11}\eta_{22} + M^*N^*\eta_{11}\eta_{12} - M^*N^*Q\eta_{11}\eta_{21}^* - M^*N^*P\eta_{11}\eta_{22} \\
& - |M|^2 P\eta_{11}^*\eta_{21} + |M|^2|P|^2|\eta_{21}|^2 - |M|^2 PQ^*\eta_{21}\eta_{22} - M^*N^*P\eta_{12}\eta_{21} + M^*N^*PQ|\eta_{21}|^2 \\
& + M^*N^*P^2\eta_{12}\eta_{21} + |M|^2 Q\eta_{11}^*\eta_{22}^* - |M|^2 P^*Q\eta_{21}^*\eta_{22}^* + |M|^2|Q|^2|\eta_{22}|^2 + M^*N^*Q\eta_{12}\eta_{22}^* \\
& - M^*N^*Q^2\eta_{21}^*\eta_{22}^* - M^*N^*PQ|\eta_{22}|^2 + MN\eta_{11}^*\eta_{12}^* - MNP^*\eta_{12}^*\eta_{21}^* + MNQ^*\eta_{12}^*\eta_{22} + |N|^2|\eta_{12}|^2 \\
& - |N|^2 Q\eta_{12}^*\eta_{21}^* - |N|^2 P\eta_{12}^*\eta_{22} - MNQ^*\eta_{11}^*\eta_{21} + MNP^*Q^*|\eta_{21}|^2 - MNQ^{*2}\eta_{21}\eta_{22} - |N|^2 Q^*\eta_{12}\eta_{21} \\
& + |N|^2|Q|^2|\eta_{21}|^2 + |N|^2 PQ^*\eta_{21}\eta_{22} - MNP^*\eta_{11}^*\eta_{22}^* + MNP^{*2}\eta_{21}^*\eta_{22}^* - MNP^*Q^*|\eta_{22}|^2 - |N|^2 P^*\eta_{12}\eta_{22}^* \\
& + |N|^2 P^*Q\eta_{21}^*\eta_{22}^* + |N|^2|P|^2|\eta_{22}|^2
\end{aligned} \tag{A.5}$$

$$
\begin{aligned}
&\Rightarrow \left[|M|^2 |\eta_{11}|^2 + |M|^2 |P|^2 |\eta_{21}|^2 + |M|^2 |Q|^2 |\eta_{22}|^2 + |N|^2 |\eta_{12}|^2 \right. \\
&+ |N|^2 |Q|^2 |\eta_{21}|^2 + |N|^2 |P|^2 |\eta_{22}|^2 - |M|^2 \, 2\,\mathrm{Re}\left(P\eta_{11}^{*}\eta_{21}\right) \\
&+ |M|^2 \, 2\,\mathrm{Re}\left(Q\eta_{11}^{*}\eta_{22}^{*}\right) - |M|^2 \, 2\,\mathrm{Re}\left(PQ\eta_{21}^{*}\eta_{22}^{*}\right) + 2\,\mathrm{Re}\left(MNP^{*}\eta_{11}^{*}\eta_{12}^{*}\right) \\
&- 2\,\mathrm{Re}\left(MNQ^{*}\eta_{11}^{*}\eta_{21}\right) - 2\,\mathrm{Re}\left(MNP^{*}\eta_{11}^{*}\eta_{12}\right) - 2\,\mathrm{Re}\left(MNP^{*}\eta_{12}^{*}\eta_{21}^{*}\right) \\
&+ 2\,\mathrm{Re}\left(M^{*}N^{*}P\eta_{21}\eta_{22}\right) + |\eta_{21}|^2 \, 2\,\mathrm{Re}\left(MNP^{*}Q^{*}\right) - |N|^2 \, 2\,\mathrm{Re}\left(Q\eta_{12}^{*}\eta_{21}^{*}\right) \\
&- 2\,\mathrm{Re}\left(MNQ^{*2}\eta_{21}\eta_{22}\right) - |N|^2 \, 2\,\mathrm{Re}\left(P\eta_{12}^{*}\eta_{22}\right) + |N|^2 \, 2\,\mathrm{Re}\left(PQ^{*}\eta_{21}\eta_{22}\right) \\
&\left. - |\eta_{22}|^2 \, 2\,\mathrm{Re}\left(MNP^{*}Q^{*}\right) + 2\,\mathrm{Re}\left(MNQ^{*}\eta_{12}^{*}\eta_{22}\right) \right]
\end{aligned}
$$

The expectation of the numerator is thus given by:

$$
E\left[\mathrm{B}\bullet\mathrm{B}^{*}\right] = 2\sigma^2\left(|M|^2 + |N|^2\right) + 2\sigma^2|P|^2\left(|M|^2 + |N|^2\right) + 2\sigma^2|Q|^2\left(|M|^2 + |N|^2\right). \tag{A.6}
$$

Substituting (A.6) in (A.4) we obtain

$$
\begin{aligned}
\mathrm{SNR} &= \frac{\left[|M|^2 + |N|^2\right]^2 E_s}{2\sigma^2\left(|M|^2 + |N|^2\right) + 2\sigma^2|P|^2\left(|M|^2 + |N|^2\right) + 2\sigma^2|Q|^2\left(|M|^2 + |N|^2\right)} \\
&= \frac{\left[|M|^2 + |N|^2\right]\bullet E_s}{2\sigma^2\left(1 + |P|^2 + |Q|^2\right)} .
\end{aligned} \tag{A.7}
$$

The elements of (A.7) can further be expanded as follows

$$
\begin{aligned}
&N = h_{12} - S \\
&S = Ph_{22} + Qh_{21}^{*} \quad \therefore \quad N = h_{12} - Ph_{22} - Qh_{21}^{*} \\
&|N|^2 = \left(h_{12} - Ph_{22} - Qh_{21}^{*}\right)\left(h_{12} - Ph_{22} - Qh_{21}^{*}\right)^{*} \\
&= |h_{12}|^2 + |P|^2|h_{22}|^2 + |Q|^2|h_{21}|^2 - 2\,\mathrm{Re}\left\{Ph_{22}h_{12}^{*}\right\} - 2\,\mathrm{Re}\left\{Qh_{21}^{*}h_{12}^{*}\right\} + 2\,\mathrm{Re}\left\{PQ^{*}h_{22}h_{21}\right\}
\end{aligned}
$$

$$
\begin{aligned}
&M = h_{11} - R \\
&R = Ph_{21} - Qh_{22}^{*} \quad \therefore \quad M = h_{11} - Ph_{21} + Qh_{22}^{*} \\
&|M|^2 = \left(h_{11} - Ph_{21} + Qh_{22}^{*}\right)\left(h_{11} - Ph_{21} + Qh_{22}^{*}\right)^{*} \\
&\quad = |h_{11}|^2 + |P|^2|h_{21}|^2 + |Q|^2|h_{22}|^2 - 2\,\mathrm{Re}\left\{Ph_{21}h_{11}^{*}\right\} - 2\,\mathrm{Re}\left\{Q^{*}h_{11}h_{22}\right\} - 2\,\mathrm{Re}\left\{PQ^{*}h_{22}h_{21}\right\}
\end{aligned} \tag{A.8}
$$

$\therefore$

$$
\begin{aligned}
|M|^2 + |N|^2 &= |h_{11}|^2 + |h_{12}|^2 + |P|^2\left(|h_{21}|^2 + |h_{22}|^2\right) + |Q|^2\left(|h_{21}|^2 + |h_{22}|^2\right) \\
&= |h_{11}|^2 + |h_{12}|^2 + \left(|P|^2 + |Q|^2\right)\left(|h_{21}|^2 + |h_{22}|^2\right)
\end{aligned}
$$

The final expression of the signal to noise ratio by further expanding (A.7) is given by

$$\text{SNR} = \frac{|h_{11}|^2 + |h_{12}|^2 + \left(|P|^2 + |Q|^2\right)\left(|h_{21}|^2 + |h_{22}|^2\right).E_s}{2\sigma^2\left(1 + |P|^2 + |Q|^2\right)}. \tag{A.9}$$

Since all channel the channel coefficients i.e. h_{ij} are all modeled as independent distributed Gaussian random variables, (A.9) can then be written as

$$\text{SNR} = \frac{\left(|h_{11}|^2 + |h_{12}|^2\right)E_s}{2\sigma^2}. \tag{A.10}$$

REFERENCES

[1] Telatar I.E., "Capacity of Multi-Antenna Gaussian Channels" *European. Transaction on Telecommunication.* vol 10, no 6, pp. 585-595, Nov./Dec. 1999.

[2] G.J. Foschini and M.J. Gans, "On limits of wireless communications in a fading environment when using multiple antennas," *IEEE Wireless Communication Magazine*, vol. 6, pp. 311-335, Mar. 1998.

[3] S. Alamouti, "Space-time block coding: A simple transmitter diversity technique for wireless communications," *IEEE Journal on Selected Areas in Communication,* vol. 16, pp. 1451-1458, Oct 1998.

[4] S. Siwamogsatham and P. Fitz. "Improved high –rate space time codes via orthogonality and set partitioning,"*IEEE Wireless Communication and Network Conference (WCNC)*, March 2002.

[5] V. Tarokh, H. Jafarkhani, and A. R. Calderbank, "Space-time block codes from orthogonal designs," *IEEE Transaction on Information Theory*, vol. 45, pp. 1456-1467, July 1999.

[6] V. Tarokh, H. Jafarkhani, and A. R. Calderbank,"Space time block code for high data rates wireless communications: Performance results," *IEEE Journal on Selected Areas in Communication*, vol.17, pp. 451-460, Mar. 1999.

[7] V. Tarokh, H. Jafarkhani, and A. R. Calderbank, "Space time codes for high data rate wireless communication; Performance analysis and code construction," *IEEE Transaction Information Theory*, vol.44, no.2, pp. 744-765, March 1998

[8] A. Wittneben, "Base station modulation diversity for digital SIMULCAST," *IEEE Vehicular Technology Conference (VTC'91)*", pp.848-853, May 1991.

[9] N. Seshadri and J. H. Winters, "Two signaling schemes for improving the error performance of frequency division duplex (FDD) transmission systems using transmit antenna diversity," *International Journal on Wireless Information Networks*, vol. 1, no. 1, pp. 49-60, Jan. 1994.

[10] A.J. Viterbi, "Error bounds for convolutional codes and an asymptotically optimum decoding algorithm," *IEEE Transaction on Communication*, vol. 13, pp. 260-269, April 1967.

[11] G. Ungerboeck, "Channel Coding with Multilevel/Phase signals," *IEEE Transaction on Information Theory*, vol.28, pp. 55-67, Jan. 1982

[12] S. Baro, G. Bauch, and A. Hansmann, "Improved codes for space-time trellis-coded modulation," *IEEE Communication Letters*, pp. 20-22, January 2000.

[13] A. R. Hammons, Jr. and H. El-Gamal, "On the theory of space time codes for PSK modulation," *IEEE Transaction on Information Theory*, vol. 46, pp. 524-532, March 2000.

[14] Z. Chen, J. Yuan, and B.Vucetic, "An Improved space-time trellis coded modulation scheme on slow Rayleigh fading channels," *IEEE International Conference on Communication*, pp. 1110-1116, Mar. 2001.

[15] B.M. Hochwald and T. L. Marzeta, "Unitary space –time modulation for multiple-antenna communications in Rayleigh flat fading," *IEEE Transaction on Information Theory*, vol.46, pp.543-564, Mar 2000.

[16] B.M. Hochwald, T. L. Marzeta, T.J.Richardson, and W.Sweldens and R. Urbanke, "Systematic design of unitary space-time constellations," *IEEE Transaction on Information Theory*, vol. 46. 1962-1973, Sept. 2000.

[17] D. Agrawal, T.J. Richardson, and R. Urbanke, "Multiple-antenna signal constellations for fading channels," *IEEE Transaction on Information Theory*, vol. 47. 2618-2626, Sept. 2001.

[18] M. L. McCloud, M. Brehler and M.K. Varanasi, "Signal design and convolutional coding for noncoherent space-time communication on the block-Rayleigh-fading channel," *IEEE Transaction Information Theory*, vol. 48. 1186-1194, May 2002.

[19] S. Siwamogsatham, M.P. Fitz, and J.H. Grimm, "A new view of performance analysis of transmit diversity schemes in correlated Rayleigh fading," *IEEE Transaction on Information Theory*, vol. 48, pp. 950-956, April 2002

[20] G. Taricco and E. Biglieri," Exact Pairwise Error Probability of Space–Time Codes," *IEEE Transaction on Information Theory*, Volume: 48, Issue: 2, pp 510 -513, Feb. 2002

[21] H. Jafarkhani and N. Seshadri, "Super-orthogonal space-time trellis codes", *IEEE Transaction on Information Theory*, vol.49, pp. 937-950, April 2003

[22] M. Abramovitz and I.A. Stegun, Handbook of Mathematic Functions. New York: Dover, 1972

[23] M. Uysal and C. N. Geoghiades, "Error performance analysis of space-time codes over Rayleigh fading channels, "*Journal of Communication and Network (JCN)*, vol. 2, no. 4, pp. 351-356, Dec. 2000.

[24] G.L. Turin, "The Characteristic function of Hermetian quadratic forms in complex normal random variables, "Biometrika, pp. 199-201, June 1960.

[25] M.K. Simon and H. Jafarkhani, " Performance evaluation of super-orthogonal space –time trellis codes using a moment generating function-based approach" *IEEE Transaction on Signal Processing*, Volume: 51, No. 11, pp 2739-2751, Feb. 2002

[26] M. K. Simon, "Evaluation of average bit error probability for space-time coding based on a simple exact evaluation of pairwise error probability, "*International Journal on Communication and Networks*, vol. 3, no. 3, pp.257-264, Sept. 2001.

[27] C. Tellambura, "Evaluation of exact union bound for trellis-coded modulation over fading channels," *IEEE Transaction on Communication*, vol. 44, No. 12, pp 1693-1699, Dec. 1996.

[28] J. K. Cavers and P. Ho, "Analysis of the error performance of trellis coded modulation in Rayleigh fading channels", *IEEE Transaction on Communication*, vol. 40, No. 1, pp 74-83, Jan. 1992.

[29] P. Ho and D. K. P. Fung, "Error performance of interleaved trellis coded PSK modulations in correlated Rayleigh fading channels", *IEEE Transaction on Communication*, vol. 40, No. 12, pp 1800-1809, Dec. 1992.

[30] H. Bengt, "On the Capacity of the MIMO channel-A tutorial introduction" , Norwegian University of Science and Technology, Department of Telecommunication O.S. Bragstads plass 2B, N-7491 Trondheim, Norway, bholter@tele.ntnu.no.

[31] G.J. Foschini, "Layered space-time architecture for wireless communication in a fading environment when using multi-element antenna", *Bell Labs Technical Journal*, vol.1, no. 2, pp 41-59, Autumn 1996.

[32] D. Shiu and J. Kahn, "Layered space time codes for wireless communication using multiple transmit antennas", *Proc. of IEEE ICC' 99*, Vancouver, BC, June 6-10, 1999.

[33] W.Su and X.-G. Xia, "Two generalized complex orthogonal space time block code of rates 7/11 and 3/5 for 5 and 6 transmit antennas," *IEEE Transaction on Information Theory*, vol. 49, no. 1, pp. 313-316, Jan. 2003.

[34] W.Su and X.-G. Xia, "A systematic design of High rate complex orthogonal space-time block codes," *IEEE Communication Letters*, vol.8 no.6, pp 380-382, June 2004

[35] A.V. Geramita and J. Seberry, Orthogonal Designs, Quadratic Forms and Hadamard Matrices, Lecture Notes in Pure and Applied Mathematics, vol. 43, Marcel Dekker: New York and Basel, 1979.

[36] J.Grimm, M. P. Fitz and J.V. Krogmeier, "Further results in space time coding for Rayleigh fading," *Proceeding of Annual Allerton. Conference on Communications, Control and Computing*, Monticello, Illinois, pp. 391-400, Sept. 1998.

[37] Q. Yan and R.S. Blum, "Optimum space-time convolutional codes," *IEEE Wireless Communications and Networking Conference*, pp. 1351-1355, Sept. 2000.

[38] Y.Gong, K.Letaief, "Concatenated space-time block coding with trellis coded modulation in fading channels," *IEEE Transaction on Wireless Communication*, vol. 1, no. 4, pp 580-590, October 2002.

[39] Y. Liu and M. P. Fitz, "Space time turbo codes," *Proceeding of Annual Allerton. Conference on Communications, Control and Computing*, Illinois, pp. 897-898, September 1999.

[40] A. Paulraj, R. Nabar and D. Gore, Introduction to space-time wireless communication. Cambridge University Press, May 2003.

[41] J. G. Proakis, Digital Communication, 3rd Ed., Mc Graw-Hill, 1995.

[42] A. Stamoulis, N. Al-Dhahir and A.R. Calderbank, "Further Results on Interference Cancellation for Space-Time Block-Coded Systems" , 35th *Asilomar Conference on Signals, Systems & Computers*, vol.1, pp. 257-261, Nov. 2001.

[43] S. M. Alamouti, V. Tarokh, and P. Poon, "Trellis coded modulation and transmit diversity," *IEEE International Conference on Universal Personal Communications*, pp. 703-707, 1998.

[44] E. Biglier, D. Divsalar, P. J. McLane, and K.K. Simon, Introduction to Trellis Coded Modulation with Application. New York: Macmillan, 1991.

[45] A.Barg and D.N. Yu, "Bounds on Packings of Spheres in the Grassmann Manifold," *IEEE Transaction on Information Theory*, vol. 48, no. 9, pp. 2450-2454, Sept. 2002.